LOW-FLOW ASSESSMENT FOR UNGAUGED SUB-BASIN IN UPPER PING RIVER BASIN, THAILAND

Mr. Sokseyla Man

A Thesis Submitted in Partial Fulfillment of the Requirements
for the Degree of Master of Engineering in Water Resources Engineering
Department of Water Resources Engineering
FACULTY OF ENGINEERING
Chulalongkorn University
Academic Year 2021

การประเมินอัตราการไหลต่ำสุดสำหรับลุ่มน้ำที่ไม่มีสถานีวัดน้ำท่าในลุ่มน้ำปิงตอนบนของประเทศไทย

นายสกไทรลา หมอน

วิทยานิพนธ์นี้เป็นส่วนหนึ่งของการศึกษาตามหลักสูตรปริญญาวิศวกรรมศาสตรมหาบัณฑิต
สาขาวิชาวิศวกรรมแหล่งน้ำ ภาควิชาวิศวกรรมแหล่งน้ำ
คณะวิศวกรรมศาสตร์ จุฬาลงกรณ์มหาวิทยาลัย
ปีการศึกษา 2564

Thesis Title	LOW-FLOW ASSESSMENT FOR UNGAUGED SUB-BASIN IN UPPER PING RIVER BASIN, THAILAND
By	Mr. Sokseyla Man
Field of Study	Water Resources Engineering
Thesis Advisor	Assistant Professor Supattra Visessri, Ph.D.

Accepted by the FACULTY OF ENGINEERING, Chulalongkorn University in Partial Fulfillment of the Requirement for the Master of Engineering

.... Dean of the FACULTY OF ENGINEERING
(Professor SUPOT TEACHAVORASINSKUN, D.Eng.)

THESIS COMMITTEE

.... Chairman
(Assistant Professor Anurak Sriariyawat, Ph.D.)

.... Thesis Advisor
(Assistant Professor Supattra Visessri, Ph.D.)

.... Examiner
(Associate Professor TUANTAN KITPAISALSAKUL, D.Eng.)

.... External Examiner
(Assistant Professor Chaiwat Ekkawatpanit, Ph.D.)

สกไทรลา หมอน : การประเมินอัตราการไหลต่ำสุดสำหรับลุ่มน้ำที่ไม่มีสถานีวัดน้ำท่าในลุ่มน้ำปิงตอนบนของประเทศไทย. (LOW-FLOW ASSESSMENT FOR UNGAUGED SUB-BASIN IN UPPER PING RIVER BASIN, THAILAND) อ.ที่ปรึกษาหลัก : ผศ. ดร.สุภัทรา วิเศษศรี

การขาดแคลนน้ำเป็นปัญหาหนึ่งที่ส่งผลกระทบต่อชีวิตความเป็นอยู่ของประชากรในประเทศไทยอย่างมาก การประเมินอัตราการไหลต่ำจึงอาจมีส่วนช่วยเพิ่มประสิทธิภาพการบริหารจัดการทรัพยากรน้ำและลดความเสี่ยงจากการขาดแคลนน้ำได้ วิธีการประเมินอัตราการไหลต่ำสำหรับลุ่มน้ำที่มีสถานีตรวจวัดนั้นมีขั้นตอนที่ไม่ซับซ้อนเนื่องจากมีข้อมูลที่นำมาใช้คำนวณได้โดยตรง แต่สำหรับลุ่มน้ำที่ไม่มีสถานีตรวจวัดนั้น การประเมินอัตราการไหลต่ำมีความยากเนื่องจากข้อจำกัดด้านข้อมูลที่ไม่มีการตรวจวัด หรือข้อมูลมีอยู่น้อย หรือข้อมูลมีคุณภาพไม่ดี ด้วยความท้าทายเหล่านี้ การศึกษานี้จึงถูกพัฒนาขึ้นโดยมีเป้าหมายเพื่อประเมินความสามารถในการนำไปใช้งานของวิธีการประเมินอัตราการไหลต่ำ 3 รูปแบบ ได้แก่ 1) วิธีการวิเคราะห์การถดถอยแบบขั้นตอน (Stepwise regression method) ซึ่งค่าอัตราการไหลต่ำของลุ่มน้ำที่ไม่มีสถานีตรวจวัดประมาณได้จากสมการความสัมพันธ์ระหว่างดัชนีอัตราการไหลต่ำและลักษณะทางกายภาพของลุ่มน้ำ 2) วิธีการประมาณค่าจากลุ่มน้ำที่มีความคล้ายคลึงกัน (Basin similarity method) ซึ่งค่าอัตราการไหลต่ำของลุ่มน้ำที่ไม่มีสถานีตรวจวัดประมาณได้จากค่าดังกล่าวของลุ่มน้ำที่มีสถานีตรวจวัดที่มีความคล้ายคลึงกัน โดยความคล้ายคลึงนี้จะพิจารณาจากความคล้ายคลึงทางกายภาพและความคล้ายคลึงของบริเวณที่ตั้ง และ 3) วิธีการประมาณค่าโดยคำนึงถึงสภาพภูมิอากาศ (Climate adjustment method) ซึ่งวิธีนี้พิจารณาระยะทางระหว่างลุ่มน้ำที่ไม่มีและมีสถานีตรวจวัด และช่วงการทับซ้อนของข้อมูลในการคำนวณอัตราการไหลต่ำ เป็นหลัก การศึกษานี้ประเมินดัชนีการไหลต่ำ 3 ดัชนีด้วยกัน ได้แก่ 1) อัตราการไหลที่เปอร์เซนต์ไทล์ที่ 95 (Ninety-five-percentile flow: Q95) 2) ดัชนีการไหลพื้นฐาน (Baseflow index: BFI) และ 3) อัตราการไหลในรอบ 7 วันที่มีค่าต่ำสุดในแต่ละปีและมีรอบการเกิดซ้ำ 10 ปี (Annual minimum 7-day moving average streamflow with a 10-year recurrence interval: 7Q10) การศึกษานี้ใช้ลุ่มน้ำปิงตอนบนซึ่งประกอบด้วยลุ่มน้ำย่อย 25 ลุ่มน้ำเป็นพื้นที่ศึกษา และใช้ข้อมูลในการวิเคราะห์ตั้งแต่ พ.ศ.2538-2557 ผลการศึกษาพบว่า วิธีการประเมินอัตราการไหลต่ำทั้ง 3 รูปแบบ มีความสามารถในการประเมินอัตราการไหลสำหรับลุ่มน้ำย่อยที่ไม่มีสถานีตรวจวัดในลุ่มน้ำปิงตอนบนได้แต่ด้วยระดับประสิทธิภาพที่แตกต่างกัน วิธีการประมาณค่าโดยคำนึงถึงสภาพภูมิอากาศมีประสิทธิภาพสูงในการคาดการณ์ 7Q10 และ Q95 แต่คาดการณ์ BFI ได้ไม่ดีนัก ช่วงการทับซ้อนของข้อมูลที่ควรใช้ในการคำนวณด้วยวิธีนี้เพื่อให้ได้ประสิทธิภาพกาคาดการณ์ระดับปานกลาง คือ 5 ปี หากช่วงการทับซ้อนของข้อมูลสั้นกว่า 5 ปี ควรใช้วิธีการวิเคราะห์การถดถอยแบบขั้นตอนในการคาดการณ์ดัชนีการไหลต่ำ

สาขาวิชา	วิศวกรรมแหล่งน้ำ	ลายมือชื่อนิสิต ....
ปีการศึกษา	2564	ลายมือชื่อ อ.ที่ปรึกษาหลัก ....

6170410921 : MAJOR WATER RESOURCES ENGINEERING
KEYWORD: Climate adjustment Low-flow indices Regional regression Regionalization Sub-basin Similarity Upper Ping River Basin

Sokseyla Man : LOW-FLOW ASSESSMENT FOR UNGAUGED SUB-BASIN IN UPPER PING RIVER BASIN, THAILAND. Advisor: Asst. Prof. Supattra Visessri, Ph.D.

Water scarcity has become one of the most remarkable problems in Thailand. An assessment of low-flow may lead to better water resources management and reduce the risk of water scarcity. The assessment of low-flow in gauged basins where the flow time series are available is straightforward. The challenge exists in ungauged or poorly-gauged basins where the flow data are unavailable or of low quality. Due to the studies of low-flow assessment in ungauged basins are of limited, this study aims to address the low-flow assessment in 25 sub-basins in the Upper Ping River basin in Thailand with available data from 1995-2014 by defining an applicable regionalization method for extrapolating beyond the limitations of observed flow data. Three regionalization methods namely regional regression method, sub-basin similarity method, and climate adjustment method are investigated for the selected sub-basins. The regional regression method is based on a stepwise regression procedure as the relationship between low-flow characteristics and basin physical characteristics. The sub-basin similarity method considered the weight of donor basins according to a combination of physical similarity and spatial proximity. The climate adjustment method considered the distance, choice of record augmentation technique, and the length of overlap period between the subject and the donor basins. Ninety-five-percentile flow (Q95), baseflow index (BFI), and the annual minimum 7-day moving average streamflow with a 10-year recurrence interval (7Q10) are selected in representing the low-flow characteristics of the sub-basins. The result indicated that the three regionalization methods are applicable to predict low-flow in the Upper Ping River basin but with a different predictive degree. However, the comparison further indicated that the climate adjustment method performs well in predicting 7Q10 and Q95 while for BFI it yields a moderate performance when there are available flow records of at least 5 years. Alternatively, applying the regional regression method with Q95 is more recommended than the sub-basin similarity method or with 7Q10 and BFI when there is no flow record available or available with a period of fewer than 5 years.

Field of Study:	Water Resources Engineering	Student's Signature ....
Academic Year:	2021	Advisor's Signature ....

ACKNOWLEDGEMENTS

Foremost, I would like to express my sincere gratitude to my advisor Asst. Prof. Supattra Visessri, Ph.D., for the continuous support of my master's research, for her patience, enthusiasm, motivation, and immense knowledge. Her guidance helped me in all the time of research and writing of this thesis. I could not have imagined having a better advisor for my master's study. Besides my advisor, I would like to thank the rest of my thesis committee: Asst. Prof. Anurak Sriariyawat, Ph.D., Assoc. Prof. Tuantan Kitpaisalsakul, D.Eng., and Asst. Prof. Chaiwat Ekkawatpanit, Ph.D., for their valuable time, encouragement, insightful comments, and useful questions.

This research is extensive thanks to the ASEAN or Non-ASEAN Countries Scholarship Program of Chulalongkorn University for providing me a great opportunity to be here for more self-development and gain more profound knowledge. I will use the knowledge that I obtain here to develop in my country.

Furthermore, I would like to acknowledge all lecturers and staff of the Department of Water Resources Engineering for offering the lectures, knowledge, and guidance.

Moreover, I would like to offer my heartfelt gratitude to my father Mr. Samy Morn, my mother Mrs. Sokheang Thor, and my siblings for their endless love and support.

Last but not least, my sincerest thank is extended to seniors, juniors, and friends who always support and inspire me during my study.

Sokseyla Man

TABLE OF CONTENTS

Page

LIST OF TABLES

Page

LIST OF FIGURES

Page

CHAPTER 1
INTRODUCTION

1.1 Background

Water is vital for human living and essential for environmental, economic, and ecological management. In practice, both surface water and groundwater have been extracted and used for many purposes. For instance, water has been taken to supply for agriculture, daily consumptions, industrial uses, electricity production, and maintaining biodiversity. However, a major proportion of water has been extracted from surface water such as rivers, streams, lakes, and reservoirs.

Due to the growth of the global population, the water demand for food production and social development towards better living conditions have also been increasing (Kundzewicz, 1997). Since the amount of water is limited especially in the dry year while the demand has increased higher, this may lead some areas to face the problem of water scarcity. In order to cope with the problem, the management of water resources is essentially required. In recent years, water resources management has become more focused on mid-term and long-term planning for water demand and conservation management, water transfer, and diversion (Karamouz et al., 2003). For riparian countries, the monitoring of flow characteristics in the river basin is the principal for water resources management responding to the problem of water scarcity. One of the most essential indicators which are beneficial for flow characterization is known as "low-flow". In general, low-flow is defined as a seasonal phenomenon that naturally occurs as a vital part of the annual water flow pattern of a basin (Smakhtin, 2001). In some cases, it is also defined as "minimum flow in a river during the dry period" (Laaha and Blöschl, 2007). During low-flow periods, most stream habitats are reduced in area and water quality and may also affect biota. During dry months, the significant increase in water demand for households, agriculture, recreation, and energy generation can worsen the natural conditions of low flow. Low-flow characteristics information provides threshold values for different water-based activities and is required for some water resources management issues such as irrigation, water supply, and water quality and quantity estimations (Eslamian, 2018). The information is also essential for water supply planning and design, water quality management, hydropower design, cooling-plant facility design, reservoir design, sanitary landfill allocation, aquatic conservation, and inter-basin transfers of water and allowable basin withdrawal decision making (Tasker, 1987).

In the Southeast Asia region, several important rivers contribute significantly to the growth and development of riparian countries. Particularly, the most vital and largest river basin in Thailand is the Greater Chao Phraya River basin which is the heart of business and agriculture and has played an important role in the economic development of this country (Vatcharasinthu and Babel, 1999). The Greater Chao Phraya River basin consists of eight river basins including Ping, Wang, Yom, Nan, Chao Phraya, Sakae Krang, Pasak, and Tha Chin. In the dry season, the river flow is found insufficient to meet the demand for both agricultural and non-agricultural sectors which has rapidly increased in recent years and often confronts severe water scarcities (Gupta, 2001). This clearly shows that the water availability in the Greater Chao Phraya River basin must be well managed to sustain the socio-economic development of the country. The Ping River basin is the largest sub-basin among the eight sub-basins and covers about 24 percent of the total average annual runoff that feeds the entire Chao Phraya river system (Sharma et al., 2007). This illustrates that the flow contribution from the Ping River basin is essential for the Chao Phraya River and if the flow in the Ping River basin decreases much, it will cause a significant decrease in the flow in the Chao Phraya River and lead to water scarcity or drought and in turn, obstruct national economy and development.

According to Pratoomchai et al. (2015), Thailand has experienced suffering from water scarcity many times such as in 1986, 1987, 1990, 1998, 2002, 2005, and 2012 resulting in severe damage throughout the country. To respond to the problems of water scarcity in the Ping River basin, it is beneficial to assess the magnitude and frequency of the low flow in the basin. The accuracy of low-flow estimation is mainly dependent on the available records of observed flow data. The flow data can be recorded by flow gauges which are installed along the river. However, many sub-basins in the Ping River basin remain ungauged or with shorter records of data compared to the recommended periods which are at least 20 years for low-flow estimation (Laaha and Blöschl, 2005). A lack of suitable data often means that design or environmental decisions are based on little or no hydrological information (Nathan and McMahon, 1992). While the short records are unlikely to provide adequate information for quantifying the reliable frequency of extreme low-flow events, various techniques for extrapolating beyond the limitations of the observed data and improving the accuracy of low-flow estimation are likely to be necessary. This is because the estimation of low-flow is essential for preventing water scarcity and improving water resources management in the Greater Chao Phraya River basin where Bangkok, the capital city of Thailand, is located.

This study will focus on assessing different techniques for estimating low-flow in ungauged sub-basins using the case study of the Upper Ping River basin instead of the case of the Ping River basin to avoid the strong impacts of anthropogenic activities such as Bhumibol reservoir operation on the mainstream. The low-flow data sets of the Upper Ping River basin used in this study are assumed to sufficiently represent a natural low-flow regime.

1.2 Objectives

The overall purpose of this study is to define the applicable method for low-flow estimation in ungauged sub-basins of the Upper Ping River basin. To achieve the overall purpose, the following objectives are required:

- To develop a low-flow characteristics database for the Upper Ping River basin
- To assess the performance of different methods for low-flow estimations in ungauged sub-basins

1.3 Scopes of Study

- This study is conducted in the Upper Ping River basin which is located in the northwestern part of Thailand.
- The daily rainfall data between 1995 and 2014 from 43 stations obtained from the Royal Irrigation Department (RID) and the Thai Meteorological Department (TMD) are used for low-flow analysis.
- The daily flow data between 1995 and 2014 from 25 stations obtained from RID and the Department of Water Resources (DWR) are used for the analysis.

- The land use and soil type data are obtained from the Land Development Department (LDD) and are assumed to have negligible change over the period of study.
- The Digital Elevation Model (DEM) with a resolution of 30 m downloaded from Earth data - NASA is used for this study.
- A set of relatively informative low-flow indices are selected in representing the low-flow characteristics of the study basin.
- Widely used methods of ungauged predictions, e.g., spatial regionalization and temporal regionalization methods are investigated and compared for low-flow estimation in the study.

1.4 Overall Framework of Study

The overall framework of the study consists of three main steps which are briefly described in the following part and the procedure is illustrated in *Figure 1.1* below. More details are provided in Chapter 4.

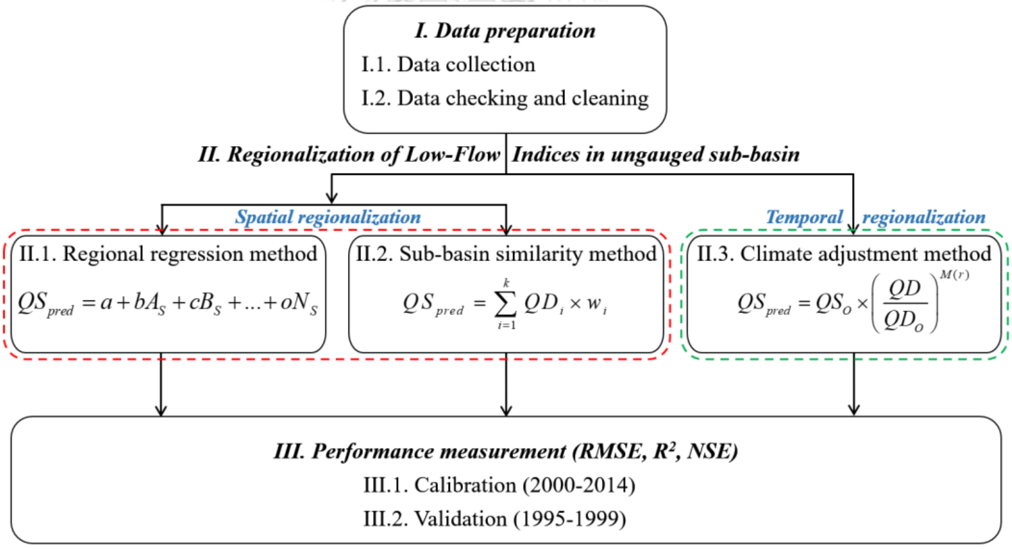

Figure 1.1 Overall framework of the study

➢ <u>Step I: Data preparation</u>

This step aims to prepare all required data to be ready for use in this study.

I.1. *Data collection:* all required data such as daily flow, daily rainfall, and the available basin properties are collected to develop low-flow measures for assessing low-flow characteristics.

I.2. *Data checking and cleaning:* applicable data are then selected from the collected data with filling-in missing data if necessary.

➢ <u>Step II: Regionalization of low-flow indices (LFI) in ungauged sub-basins</u>

This step aims to predict the low-flow indices in ungauged sub-basins by transferring the information from the gauged sub-basins. The computation of low-flow indices including ninety-five-percentile flow (Q95), baseflow index (BFI), and annual minimum 7-day moving average flow with a 10-year recurrence interval (7Q10) for ungauged sub-basins can be quantified based on the low-flow regionalized from the flow data in gauged sub-basins. Two regionalization methods which are spatial regionalization (Regression and Sub-basin similarity methods) and temporal regionalization (Climate adjustment method) were tested in this study.

II.1. *Low-flow assessment for ungauged sub-basins by using the regression method:* the regression equation used in this study is developed from the gauged sub-basins as the relationship between each of the low-flow indices and informative basin characteristics which are chosen based on the stepwise method. The predicted low-flow indices for ungauged sub-basins are then possible to be calculated by substituting their basin characteristics into the developed regression equation.

II.2. *Low-flow assessment for ungauged sub-basins by using the sub-basin similarity method:* in similarity-based regionalization, the low-flow indices are directly transferred from similar sub-basins to the target sub-basin. The integrated similarity-based approach considering both spatial proximity and physical similarity is used since Zhang and Chiew (2009) suggested that it performed relatively better than approaches based on either spatial proximity or physical similarity alone.

II.3. *Low-flow assessment for ungauged sub-basins by using the climate adjustment method:* the prediction of low-flow indices, in this case, is determined by selecting the neighboring gauged sub-basin with the shortest Euclidean distance between their centroids as the donor and adjusting the donor's low-flow index values using record augmentation techniques. In this study, four overlap periods of 1-yr, 5-yr, 10-yr, and 15-yr are tested to compare the prediction performance. The overlap period is referred to the period where the data of the donor and the subject sites are overlapped.

➢ Step III: Performance measurement

This step aims to define the most applicable method among the selected methods. In this study, the most applicable method is selected and discussed based on three statistical indicators such as Nash-Sutcliffe efficiency (NSE), coefficient of determination (R^2), and root-mean-square-error (RMSE) after doing calibration and validation to represent the performance of regionalization methods used in this study. Moreover, the period for calibration is selected later than the validation due to there is a change in land-use data records in the year 2000 and the study would like to assess the method performance when land-use change especially for the regional regression method which is known as the method to develop relationship equations between low-flow indices and basin characteristics. Therefore, the longer period which is from 2000 to 2014 for the calibration and the shorter period from 1995-1999 for the validation are chosen.

1.5 Expected Output

- Low-flow characteristics database of the Upper Ping River basin.
- Suggested methodology for predicting flow in ungauged sub-basins of the Upper Ping River basin.

1.6 Expected Outcome

- Understanding of low-flow regime and its roles in basin hydrology.
- Ability to identify key basin characteristics contributing to low-flow.

1.7 Outline of the Thesis

This thesis consists of six chapters. Chapter 1 describes the importance and rationale behind the research as well as an outline of the main objective of the thesis. Chapter 2 reviews definitions, theories, methodology, and previous studies in the low-flow assessment. Knowledge obtained from the literature review in Chapter 2 will be applied to the selected study site which is the Upper Ping River basin. The description of the Upper Ping River basin is presented in Chapter 3. The methods which are evaluated for estimating low-flow characteristics in the Upper Ping River basin are explained in Chapter 4. Chapter 5 focuses on discussions of the results and chapter 6 is the conclusions and recommendations for further studies.

CHAPTER 2
LITERATURE REVIEW

2.1 Definition of Key Terms

This study focuses on the estimation of the low-flow in ungauged basins of the Upper Ping River basin. Therefore, a better understanding of the two key terms of "Low-flow hydrology" and "Ungauged basin" offers insight to this research.

2.1.1 Low-flow Hydrology

Due to the similarity of definition, there are some confusions in differentiating between "drought" and "low-flow". Various definitions have been defined depending on the contexts and focus of the studies. In 1931, the U. S. Weather Bureau defined the drought as "a lack of rainfall so great and so long continued as to affect injuriously the plant and animal life of a place and to deplete water supplies both for domestic purposes and the operation of power plants, especially in those regions where rainfall is normally sufficient for such purposes" (Havens, 1954). According to Pereira et al. (2009), another term of droughts is defined as "a natural but temporary imbalance of water availability which consists of persistent lower-than-average precipitation, of uncertain frequency, duration and severity, of unpredictable or difficult occurrence, resulting in diminished water resources availability, and reduced carrying of the ecosystem". Another general term of drought from a hydrological point of view is given in Tallaksen and Van Lanen (2004) as "a sustained and regional extensive occurrence of below average natural water availability". Low-flow, on the other hand, is defined by international glossary of hydrology as "flow of water in a stream during prolonged dry weather". However, it seems not yet clearly separated from the drought. So later on, it has been defined as "a seasonal phenomenon, and an integral component of a flow regime of any river" (WMO, 1974). According to Smakhtin (2001), low-flow in some cases is defined as "minimum flow in a river during the dry periods of the year".

Based on Beran and Rodier (1985), a differentiation between droughts and low-flow is made. The main feature of drought is the shortage of water for any specific objective. Normally, low-flow is experienced during a drought, however, it features only one element of the drought, which is the drought magnitude. The study of low-flow is conducted to understand the physical development of flows at a point along a river. In terms of streamflow deficits, hydrological drought has been studied over a season or longer periods and in a regional context (Yevjevich, 1967). Zelenhasić and Salvai (1987), however, clarify that streamflow deficits in the short term (less than a season) can also be defined as droughts.

2.1.2 Ungauged Basin

According to Blöschl (2006), an ungauged basin is shortly defined as a basin where no streamflow data are available. This definition seems mainly focused on quantity without mentioning the quality of data. Sivapalan et al. (2003), on the other hand, defined the meaning of the ungauged basin from a wider point of view. The ungauged basin is then defined as a basin with inadequate records (both in terms of data quantity and quality) of hydrological observations to enable computation of hydrological variables of interest (both water quantity and/or quality) at the appropriate spatial and temporal scales and to the accuracy acceptable for practical applications. An ungauged basin is therefore referred to as both a completely ungauged and a poorly-gauged basin. A lack of suitable data often means that design or decisions are based on little or no hydrological data and have high uncertainty (Nathan and McMahon, 1992).

2.2 Low-flow Assessment in Gauged Basin

There are many low-flow measures to analyze the low-flow regime of a river depending on the type of data available and the type of required output information. The term “low-flow measure” refers to the various methods developed for analyzing the low-flow regime of a river, frequently in graphic form (Smakhtin, 2001). However, the selection of the most appropriate method is the main challenge for the hydrologist (Nathan and McMahon, 1992).

2.2.1 Low-flow Measures

According to Gustard et al. (1992), various low-flow measures describe and quantify different properties of flow regimes and different applications in water use. The low-flow measures with regime property which they describe, the data employed in their calculation and application are summarized in *Table 2.1*. A set of possible low-flow measures and indices used in this study is selected based on this guideline.

Table 2.1 Summary of low-flow measures (Gustard et al., 1992)

Measures	**Property Described**	**Data Employed**
Flow duration curve	Proportion of time a given flow is exceeded	Daily flow or flows averaged over several days, weeks, or months
Baseflow hydrograph	Flow exists in the stream without the contribution of direct runoff from the rainfall	Daily flow or flows averaged over several days, weeks, or months
Low-flow frequency curve (annual minimum)	Proportion of years in which the mean discharge over a given duration is below a given magnitude	Annual minimum flow daily or averaged over several days
Low-flow spells (duration of deficiency periods)	Frequency with which the flow remains continuously below a threshold for a given duration	Periods of low flows extracted from the hydrograph followed by a statistical analysis of duration
Deficiency volumes	Frequency of requirement of a given volume of make-up water to maintain a threshold flow	As for spells except the analysis focuses on the volume below the threshold
Storage yield	Frequency of requirement for a given volume of storage to supply a given yield	Daily flows or flows averaged over several days or monthly flow
Time to accumulate runoff volume	Time to accumulate a given volume of runoff with a given frequency of occurrence	Accumulated runoff volume starting at different points of the year

1) Flow Duration Curve

A flow duration curve that has been widely used in hydrological practice is one of the most informative methods of displaying the complete range of river flows from low to flood flows (Gustard et al., 1992). It is a cumulative frequency curve that demonstrates the percentage of time specified discharges were equaled or exceeded during a given observation period (Searcy, 1959). In other words, it is known as the relationship between the magnitude and frequency of streamflow. The curve is much beneficial and simple tool for indicating the flow characteristic of a stream throughout the range of flow, without concern for the sequence of occurrence (Nathan and McMahon, 1992). However, this measure is sensitive to the length of the streamflow record (Carthaigh, 1987). To construct a flow-duration curve, all complete years of record can be selected; not necessarily to be continuous, but the selected records should be for years in which physical conditions in the basin, such as diversions, artificial storage, or other anthropogenic impacts, were the same. For the partial years of records, they are recommended to be excluded (Searcy, 1959).

Flow durations are determined by arranging the value of daily average flows for the recording period from the highest to the lowest and ranking each value starting from 1 to the highest order. The frequencies of exceedance are then calculated based on the statistical probability of extreme event such as the Weibull formula (Eq. 2.1) to determine the plotting position where P *is* the probability that a given flow is equaled or exceeded; m is the ranking position and n is the number of events for the period of record (Helsel and Hirsch, 1992):

$$P = \frac{m}{n+1} \qquad \textit{Eq. 2.1}$$

2) Baseflow Hydrograph

The total streamflow is technically divided into two important components which are direct flow and baseflow. In general, the baseflow originates from groundwater storage or other delayed sources. It can be characterized by various baseflow separation techniques based on its hydrograph deriving from the total streamflow hydrograph (Smakhtin, 2001). A variety of baseflow separation techniques have been used for separating baseflow from the total streamflow. One of the frequently used separation techniques is called the local-minimum technique. Examples of this technique can be found in White and Sloto (1990) and Sloto and Crouse (1996). In the local-minimum technique, each day in the window of 2N-1 days is checked to determine whether its flow is the lowest in that interval and whether the lowest flow is a local minimum. If the day meets these criteria, it is linked by straight lines to adjacent local minimums. The flow values for each day between local minimums are calculated by using the slope of the connecting line on each day. The technique can be visualized as connecting the lowest points on the hydrograph with straight lines to define the baseflow hydrograph.

3) Low-flow Frequency Curve

A low-flow frequency curve demonstrates the proportion of years when a flow is equaled or exceeded. In another word, it shows the average interval in years (return period or recurrence interval) that the river falls below a given discharge (Smakhtin, 2001). Extreme value frequency analysis is a predictive statistical tool commonly applied in hydrology to make inferences concerning the probability of occurrence of low flows. A series of observed annual flow minima is used in the low-flow frequency analysis. In the analysis, a statistical distribution representing the relationship between the magnitudes of the events and the exceedance probabilities are fitted to the observed low-flow data, and the parameters of the probability distribution are estimated. The commonly used distributions in low-flow frequency analysis are the Pearson Type III, Log-Pearson Type III, Gumbel, Weibull, Log-Normal, and Gamma distributions. The fitted distribution is then able to be used to predict the magnitude associated with a specific non-exceedance probability. The available fitted probability distribution allows extrapolation beyond the range of the probabilities of the observed data series, which is limited by the recorded length (Ouarda et al., 2008). However, the frequency curves produced by the distribution in some cases do not fit the observed data at many stations, the observed data is therefore sometimes fitted using graphical curve-fitting techniques instead (Zalants, 1991).

2.2.2 Low-flow Indices

Low-flow is characterized by indices which are the single numbers describing an aspect of the low-flow behavior at a site or in a region. *Table 2.2* summarizes the low-flow indices, the definitions, and the research in which they were applied.

Table 2.2 Summary of low-flow indices

Low-flow Indices		Definitions	Applied Research
Ninety-five-percentile Flow	Q95	Flow that is equaled or exceeded for 95 percent of the observation period.	(Laaha and Blöschl, 2005)
Baseflow Index	BFI	Non-dimensional proportion which is defined as the baseflow volume divided by the total streamflow volume	(Zhang et al., 2013)
Annual minimum N-day moving average flow (NQy)	7Q10 7Q2	Average flow that can be expected for N-consecutive days, every recurrence interval (year)	(Arihood and Glatfelter, 1991)
Sustained low-flow	SLF	The lowest flow which is not exceeded for 7 consecutive days in any year	(Carthaigh, 1987)

1) Ninety-five-percentile Flow

A ninety-five-percentile flow is known as one of the most practical indices to characterize the low-flow of a river. It represents flow that is equaled or exceeded for 95 percent of the observation period and can be easily determined from the flow duration curve (WMO, 2008). Q95 can be used for establishing low-flow criteria for stream standards in some countries. On the other hand, it can also be used as a reference streamflow level to differentiate streamflow drought flows from nondroughted flows (Zelenhasić and Salvai, 1987).

2) Baseflow Index

The baseflow index is a non-dimensional index which is defined as the baseflow volume divided by the total streamflow volume. The values range between 0 and 1. The high index of baseflow indicates that the river flow can be sustained by the basin during a prolonged dry period. For some approaches of baseflow separation, the baseflow index is sensitive to missing data since one missing day may lead to erasing several days of data from the baseflow separation. Therefore, the missing data should be filled-in before applying baseflow separation techniques (WMO, 2008). BFI can be estimated for every year or the entire observation period. It was recommended to be a good indicator of the effects of geology on low-flow. For that reason, it is widely used in many regional low-flow studies (Gustard et al., 1992).

3) Annual Minimum N-day Average Flow with a Recurrence Interval

Low-flow statistics that describe the magnitude and frequency of low-flow events are presented as minimum average streamflow over some recurrence interval at a flow gauging site. 7Q10 which represents the annual minimum 7-day moving average flow with a 10-year recurrence interval is one of the most common low-flow statistics (Riggs, 1985). Annual minima can be derived from a daily flow series by selecting the lowest flow every year and the average of the minima calculated. The annual minima may be utilized to determine a distribution function for assessing the frequency or recurrence interval of low-flow (WMO, 2008).

2.3 Spatial Regionalization of Low-flow Characteristics in Ungauged Basins

For ungauged basins, the streamflow records are generally not available or available with short periods at the site of interest. When the observed records are unavailable or inadequate for frequency analysis, other approaches must be applied (Ouarda et al., 2008). Prediction in Ungauged Basins (PUB) is an important task for water resources planning and management but remains a fundamental challenge for the hydrological community (Sivapalan et al., 2003). Regionalization refers to a process of transferring hydrological information from gauged to ungauged or poorly gauged basins to estimate the streamflow (Razavi and Coulibaly, 2013). The selection of a donor (gauged) basin is a common technique for predictions in ungauged basins and thus for assessing low-flow characteristics at an ungauged basin. The technique includes subjectivity in the choice of donor basins and how to transfer the low-flow characteristic from the donor to the ungauged basin.

2.3.1 Regional Regression Methods

Multiple regression is a frequently used method to develop a relationship between the low-flow statistic of interest and an optimal set of basin characteristics which is established using stepwise linear regression for homogeneous subregions to predict low-flow characteristics in ungauged basins. If the study area is large or very heterogeneous in terms of the low-flow processes, it is beneficial to separate the region into multiple homogeneous regions. For the various regions, a regression model is fitted independently between specific low-flow statistics and basin characteristics and performing cross-validation (Laaha et al., 2013). The most appropriate classification procedure to define homogeneous regions depends mainly on the climate and physical basin characteristics. The basin characteristics which are most commonly related to low-flow characteristics include basin area, mean annual precipitation, basin slope, stream density, percentage of open water and forests, various soil types, length of the mainstream, basin shape, watershed perimeter, and mean elevation (Engeland and Hisdal, 2009). As stated in Nathan and McMahon (1992), a common form of prediction equations can be simplified as Eq. 2.2 below:

Low-flow characteristics = f (basin characteristics) *Eq. 2.2*

1) Stepwise Regression Procedure

The problem of selecting a subset of independent variables in regression analysis has led to various subset selection procedures. In general, the procedure selects the independent variable that maximizes the squared partial correlation coefficient with the dependent variable (Bendel and Afifi, 1977). Stepwise regression is a popular technique to produce a regression model with satisfactory performance. If a nonsignificant basin characteristic is observed, it will be removed from the model. The application of the stepwise regression does not require selecting the regressive subjectively. Through the method, all the possible influential variables are put into the disposal plan and optimally picked out for the independent variables which have a great influence on the dependent variable. The method offsets the weakness of multiple regression analysis, i.e. the shortcoming of selecting the regression variable manually and obtaining the more ideal forecasting result (Lan and Guo, 2008).

2.3.2 Nearest Basin Method

The nearest basin method consists of transferring parameters from neighboring basins to the ungauged basin. The rationale is that basins that are close to each other should have similar behavior since climate and basin conditions should vary evenly in space. Although this approach depends on the density of the gauged basin network, it is intuitively attractive (Oudin et al., 2008). The method avoids using basin characteristics explicitly and simply focuses on the geographical similarity between the basins. As a geographical proximity approach, the method establishes a model for an ungauged basin by simply using the parameter values from the nearest gauged basin. The use of only geographical locations makes the nearest basin method avoid misspecification of regional models and data uncertainty of basin characteristics (Li et al., 2010). As far as it is known, the nearest basin method is typically limited to the case where some ungauged basins are far away from any gauged basins. It is easily understood that the method is also unable to work efficiently where numerous gauged basins are nearby but share substantially different parameter values. Considerable heterogeneity within a region causes the problem of robustness. The basic assumption of the nearest basin method is that nearby basins share similar hydrological behavior, but it is not necessarily true in a large study region (Post et al., 1998).

2.3.3 Basin Similarity Method

The concept of this method is to transfer hydrological parameters from gauged to ungauged basins based on the similarity of their physiographic basin characteristics. The basic assumption is that hydrological processes are linked to basin physiography, so the flows from similar physiographical basins may experience similar effects of the climatic variable. The obstacle to the donor selection technique is that the information on basin similarity probably consists of numerous basin characteristics and it is not easy to find a similarity measure that uses the most relevant characteristics information. Similar to the regional regression method, the relevant basin characteristics may be selected by applying a stepwise regression analysis between low-flow indices and the basin characteristics and then weighted them depending on the coefficients in the regression model (Laaha and Blöschl, 2005).

According to Razavi and Coulibaly (2013), basins are firstly grouped according to their physical or non-hydrological similarities. Multivariate statistical analysis is normally used to group the basins. It is recommended that one use a ranked proximity technique if basin attributes have different units and ranges. Then, the parameters of gauged basins are computed, and the parameters located in the same group are arranged (e.g., by using the arithmetic mean, to obtain the regional parameter set). That parameter set is then used to generate flow in the ungauged basin which has physical similarities. Zhang and Chiew (2009), on the other hand, indicate that the integrated similarity-based approach considering both spatial proximity and physical similarity performs slightly better than approaches based on either spatial proximity or physical similarity alone.

2.4 Temporal Regionalization of Low-flow Characteristics in Ungauged Basins

Due to the variability of climate conditions and other sources of variability that occur over short time scales, low-flow characteristics estimated from a few years of flow records deviate from the long-term average (Tallaksen and Van Lanen, 2004). An attempt to account for temporal change of low-flow characteristics has been developed using the climate adjustment method which is summarized below.

2.4.1 Climate Adjustment Method

The estimation of low-flow from short streamflow records has become a common problem for hydrologists (Vogel and Kroll, 1991). According to Laaha and Blöschl (2005), the climate adjustment method is one of the applicable methods to deal with the problem of low-flow estimation from a short streamflow record. The method consists of two steps which are the donor site selection and the record augmentation.

1) Donor Site Selection

Donor site selection can be specified into two types which are downstream site, and basin similarity.

a) Downstream Site

Downstream site selection is referred to the technique using the nearest downstream gauged site as the donor. The rationale of this technique is that the donor site and the subject site would have some overlap in the basin area. Therefore, they may have similar characteristics of climate and hydrology. However, considering only one gauge as a donor is the main obstacle to this technique. Hence, the method is maybe less robust than the others using more than one gauge as the donor, especially for basins where the changes of land use or the presence of some constructions have taken place at the stream. The selection procedure comprises only one step which is the selection of adjacent downstream gauge at the same stream as a donor.

b) Basin Similarity

In the basin similarity technique, the donors are selected based on the similarity of physiographic basin characteristics. The basic assumption of this technique is that hydrological processes are linked to basin physiography, so the flows from similar physiographical basins may experience similar effects of the climatic variable.

The procedure for selecting a donor for the basin similarity method is presented in Laaha and Blöschl (2005) and can be described as below:

1. Select all stations within the same seasonality zone as possible donors
2. Perform a stepwise regression between LFI and basin characteristics to determine the most relevant basin characteristics for assessing the similarity
3. Weight the selected basin characteristics by the coefficients of the regression
4. Calculate Euclidean distances between the subject site and all possible donors in the space of weighted basin characteristics
5. Select the most similar site with the shortest Euclidean distance as a donor.

2) Record Augmentation Techniques

Streamflow record augmentation techniques can effectively increase the length of short streamflow records by exploiting the cross-correlation among nearby longer records (Vogel and Kroll, 1991). Once the suitable donor is selected, the predicted LFI at the subject site can be extrapolated by transferring the information from the donor based on two record augmentation techniques. The first technique adjusts the low-flow indices at the subject site by scaling with the ratio of LFI calculated from the entire observations period and LFI calculated from the overlap period (Eq. 2.3).

$$QS_{pred} = QS_o \cdot \left(\frac{QD}{QD_o} \right) \qquad \textit{Eq. 2.3}$$

where:

QS_{pred} : the adjusted value of LFI at the subject site

QS_o : LFI at the subject site determined from the overlap period

QD_o : LFI at the donor site determined from the overlap period

QD : LFI at the donor site determined from the entire observation period.

The second technique applies the same principle but includes a weighting coefficient M(r), which is the function of the length of overlap period in years and the correlation coefficient, to strengthen the correlation between subject and donor sites (Eq. 2.4).

$$QS_{pred} = QS_o \cdot \left(\frac{QD}{QD_o} \right)^{M(r)} \qquad \textit{Eq. 2.4}$$

3) Combination of Adjusted Values from Multiple Donors

In the case of multiple donors, the adjusted values for each of the selected donors can be combined as a single adjusted value. Robson and Reed (1999) recommended using a weighted geometric average which seems to be more reliable to the presence of outliers in the adjusted values than an arithmetic average. The weights (w) are computed from the distance between the donor and subject sites. The formula of the weighted geometric average is as shown in the following Eq. 2.5:

$$QS_{pred} = \prod_{i=1}^{n} \left(QS_{pred}^{(i)} \right)^{w_i / \Sigma w_i} \qquad \textit{Eq. 2.5}$$

2.5 Previous Study of Estimating Low-flow Characteristic in Ungauged Basins

The estimation of low-flow in an ungauged basin is the big challenge in water resources planning and management to respond to the problem of water scarcity. A comparison study of regionalization approaches for the ungauged basin was conducted by Oudin et al. (2008) based on 913 basins in France. Spatial proximity (nearest basin), physical similarity (basin similarity), and regression were the selected regionalization approaches for the study. The comparison demonstrated that in France, where a dense network of gauging stations is available, spatial proximity provides the best regionalization solution while the physical similarity approach and the regression approach are intermediary and the least satisfactory, respectively.

Another comparison of the regionalization approach was studied by Samuel et al. (2011) to estimate continuous streamflow in the ungauged basin across Ontario, Canada. In this study, different regionalization methods including spatial proximity (i.e., kriging, inverse distance weighted (IDW), and mean parameters), physical similarity, and regression-based approaches were applied. The results indicated that spatial proximity (IDW and kriging) produced better model performances than the remaining three.

A study of temporal regionalization was conducted by Laaha and Blöschl (2005) to analyze the relative performance of different climate adjustment methods for assessing low-flow characteristics from short streamflow records. In this study, 132 basins in Austria with basin areas ranging from 9 to 479 km^2 were selected. Q95 which is the flow that is equaled or exceeded on 95% of the observation period was chosen as the low-flow index in the comparison study. The results illustrated that the downstream donor selection method performs the best. The method yields the smallest RMSE, the largest R^2, and the fewest outliers if the adjusted Q95 flow estimates from shortened records are compared to estimates from the full 20-year record. As opposed to the downstream donor method, the method of basin similarity yields larger errors on most statistical indicators. The result also defined that the selection of record augmentation techniques is less important than the donor site.

CHAPTER 3
STUDY AREA

3.1 Location and Topography

The Upper Ping River basin is situated in the northwestern part of Thailand. It stretches from latitude 17°00'N to 19°48'N and from longitude 98°05'E to 99°23'E as shown in *Figure 3.1* and covers the area of 26,674 km^2 (*Table 3.4*).

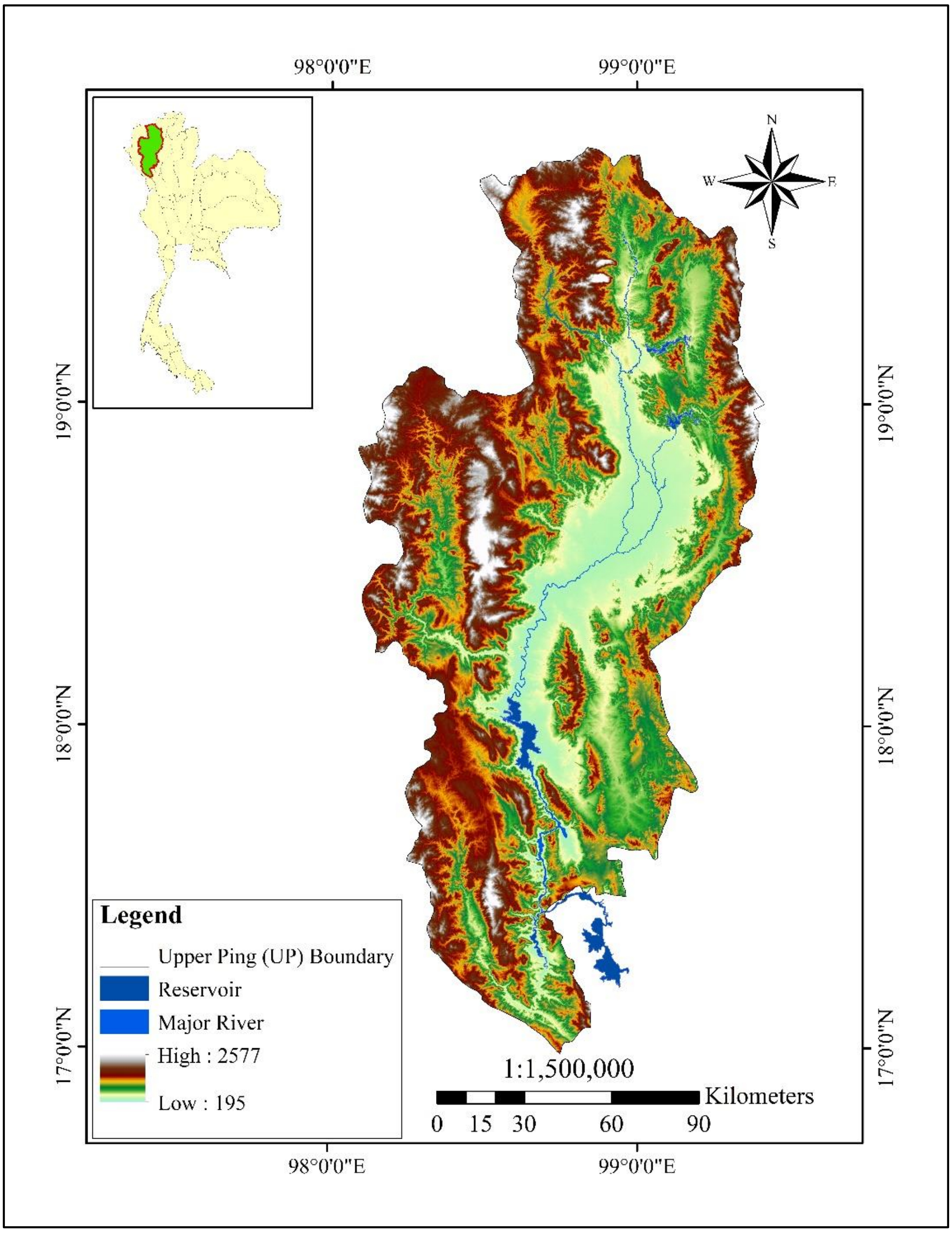

Figure 3.1 Location and elevation of Upper Ping River basin

The basin borders Myanmar at the north, Salawin basin at the west, Wang, and Kok basins at the southeast and the northeast, respectively. The topography of the basin includes hilly and mountains, valleys, and lowland plains (Reda et al., 2015). The elevations range from 195 meters to 2577 meters above the mean sea level (*Figure 3.1*). The Bhumibol dam was built within the north boundaries of Tak province and separated the Upper Ping River basin (Chiang Mai and Lamphun provinces) from the Lower Ping River basin (Kamphaeng Phet and Nakhon Sawan provinces) as shown in *Figure 3.2*.

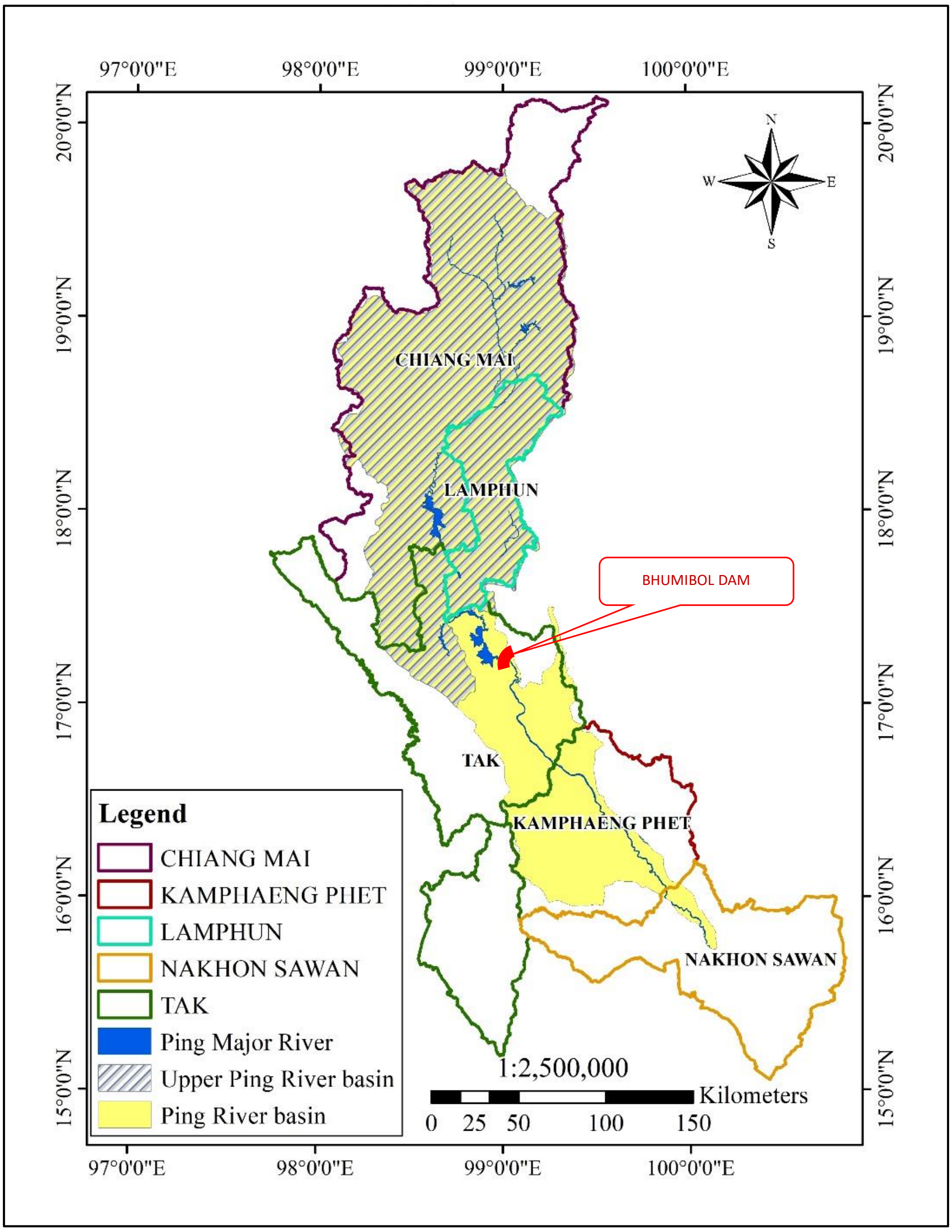

Figure 3.2 Ping River basin provinces

3.2 Streamflow

The number of 25 flow gauged stations with the study period of 20 years between 1995 and 2014 is selected according to the trade-off between the number of gauged stations, record length, and the ratio of missing data to the total periods (*Table 3.1*). This study will use the data from 1995 to 2014 with the highest number of flow stations and missing data not exceeding 20%. *Figure 3.4* summarizes the data availability of the selected 25 stations.

Table 3.1 Number of flow stations with record periods and the ratio of missing data

Periods	**Number of stations with varying ratios of missing data to the total periods**		
	≤ 30%	**≤ 20%**	**≤ 10%**
1995-2013	27	22	20
1995-2014	28	25	19
1995-2015	27	24	6
1995-2016	27	24	6
1995-2017	27	18	6

The information on the location of the flow gauge is as shown in the following *Table 3.2* and *Figure 3.3*.

Table 3.2 Selected flow stations in Upper Ping River basin

No.	**Station**	**Lat.**	**Lon.**	**Source**	**No.**	**Station**	**Lat.**	**Lon.**	**Source**
1	P.1	18.7858	99.0081	RID	14	060403	19.379	98.696	DWR
2	P.4A	19.1208	98.9475	RID	15	060701	18.957	99.239	DWR
3	P.20	19.3525	98.9736	RID	16	060804	18.665	98.632	DWR
4	P.21	18.9247	98.9428	RID	17	060806	18.795	98.725	DWR
5	P.24A	18.4169	98.6747	RID	18	060807	18.652	98.692	DWR
6	P.56A	19.2839	99.1903	RID	19	060808	18.608	98.857	DWR
7	P.67	19.0197	98.9617	RID	20	061001	18.54	98.595	DWR
8	P.73	18.2883	98.6531	RID	21	061004	18.363	98.535	DWR
9	P.75	19.1478	99.0100	RID	22	061006	18.283	98.529	DWR
10	P.77	18.4325	99.0833	RID	23	061301	18.546	98.355	DWR
11	060201	19.3211	98.9344	DWR	24	061302	18.548	98.358	DWR
12	060301	19.4506	99.2178	DWR	25	061501	17.386	98.471	DWR
13	060302	19.3740	99.2490	DWR					

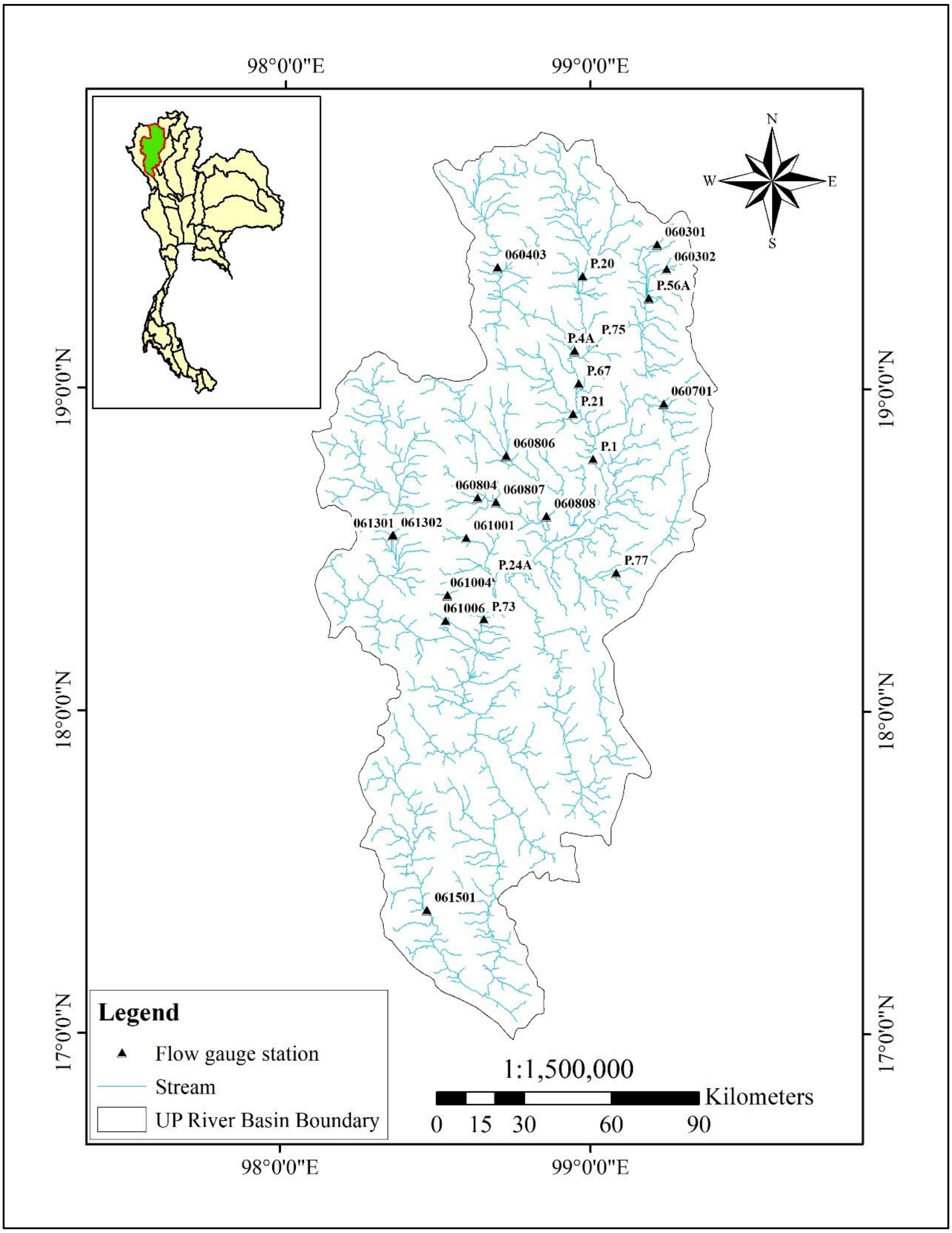

Figure 3.3 Location of the 25 flow stations

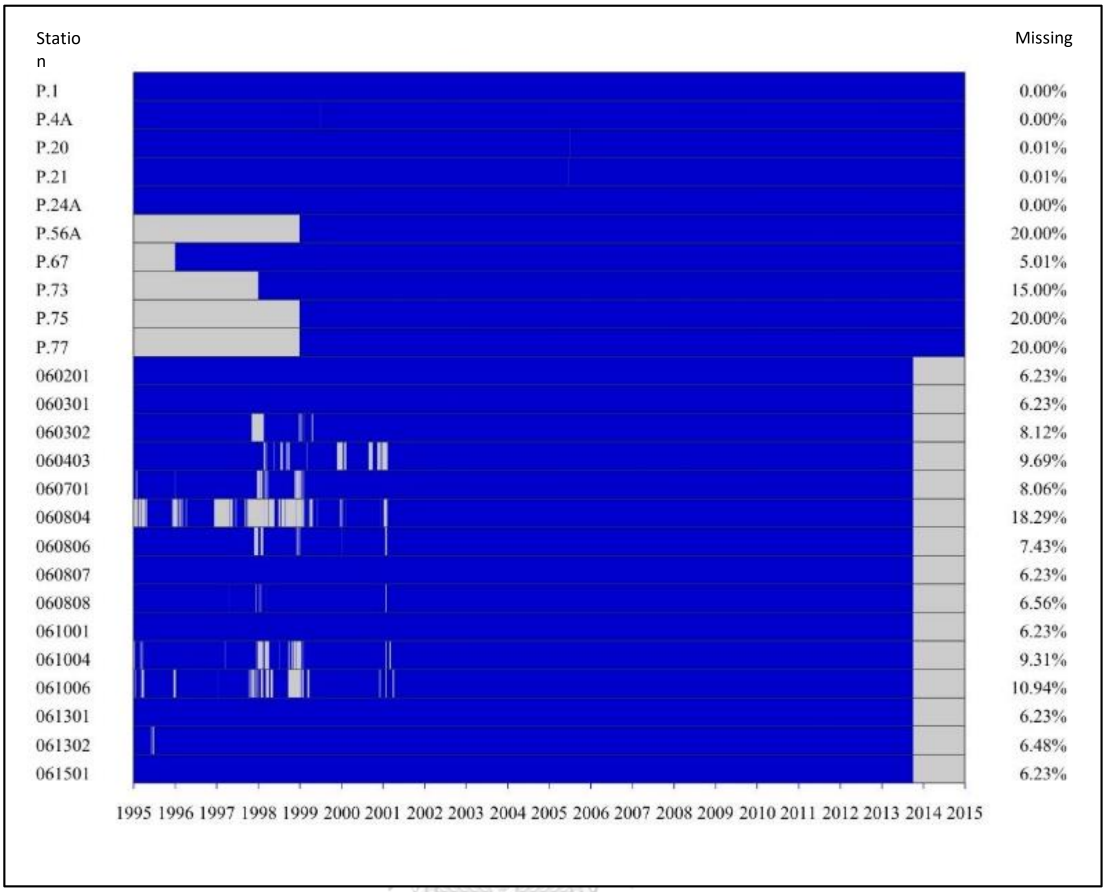

Figure 3.4 Available and missing data of the 25 flow stations from 1995 to 2014 (Blue: Available data, Gray: Missing data)

3.3 Rainfall

The weather in the Upper Ping River basin is mainly affected by the southwest and northeast monsoon. Furthermore, the depression from the South China Sea also influences the basin during July and September which results in abundant rainfall from May to October. The climate is mainly characterized by the average annual rainfall of 1097 mm and the average annual temperature of 26.7^{o}C (Sharma and Babel, 2014).

As corresponding to the selected flow stations, the rainfall data from 43 stations are also selected from 1995 to 2014 with missing data not exceeding 20%. The information indicating the location of stations is as shown in the following *Table 3.3* and *Figure 3.5*. *Figure 3.6* summarizes the availability of data from the selected rainfall stations.

Table 3.3 Selected rainfall stations in Upper Ping River basin

No.	Station	Lat.	Lon.	Source	No.	Station	Lat.	Lon.	Source
1	07013	18.8397	98.9756	RID	23	327004	18.869	99.141	TMD
2	07022	18.7133	99.0414	RID	24	327006	19.363	99.205	TMD
3	07032	18.7442	99.1244	RID	25	327007	18.498	98.365	TMD
4	07042	18.8475	99.0483	RID	26	327008	17.801	98.358	TMD
5	07052	18.8689	99.1394	RID	27	327009	18.846	98.735	TMD
6	07082	18.6269	98.8989	RID	28	327011	18.713	99.041	TMD
7	07122	19.3644	99.2047	RID	29	327012	18.848	99.045	TMD
8	07132	19.3647	98.9667	RID	30	327014	18.628	98.899	TMD
9	07142	18.8478	98.7358	RID	31	327016	19.365	98.968	TMD
10	07152	18.4983	98.365	RID	32	327020	18.806	98.923	TMD
11	07162	17.7958	98.36	RID	33	327021	18.801	98.903	TMD
12	07182	18.4158	98.6797	RID	34	327022	17.933	98.683	TMD
13	07242	18.8028	98.925	RID	35	327024	18.614	98.902	TMD
14	07252	19.2686	98.9756	RID	36	327025	19.095	99.087	TMD
15	07262	18.8067	98.9033	RID	37	327501	18.79	98.977	TMD
16	07282	18.1503	98.3931	RID	38	329002	18.461	99.138	TMD
17	07292	18.6111	98.9006	RID	39	329003	18.524	98.944	TMD
18	07391	18.7892	99.0169	RID	40	329005	18.314	98.821	TMD
19	07472	17.9167	98.6833	RID	41	329006	17.634	98.781	TMD
20	07502	19.0667	99.2167	RID	42	329201	18.567	99.033	TMD
21	07731	17.7836	98.3753	RID	43	376010	17.344	98.657	TMD
22	327003	18.4161	98.68	TMD					

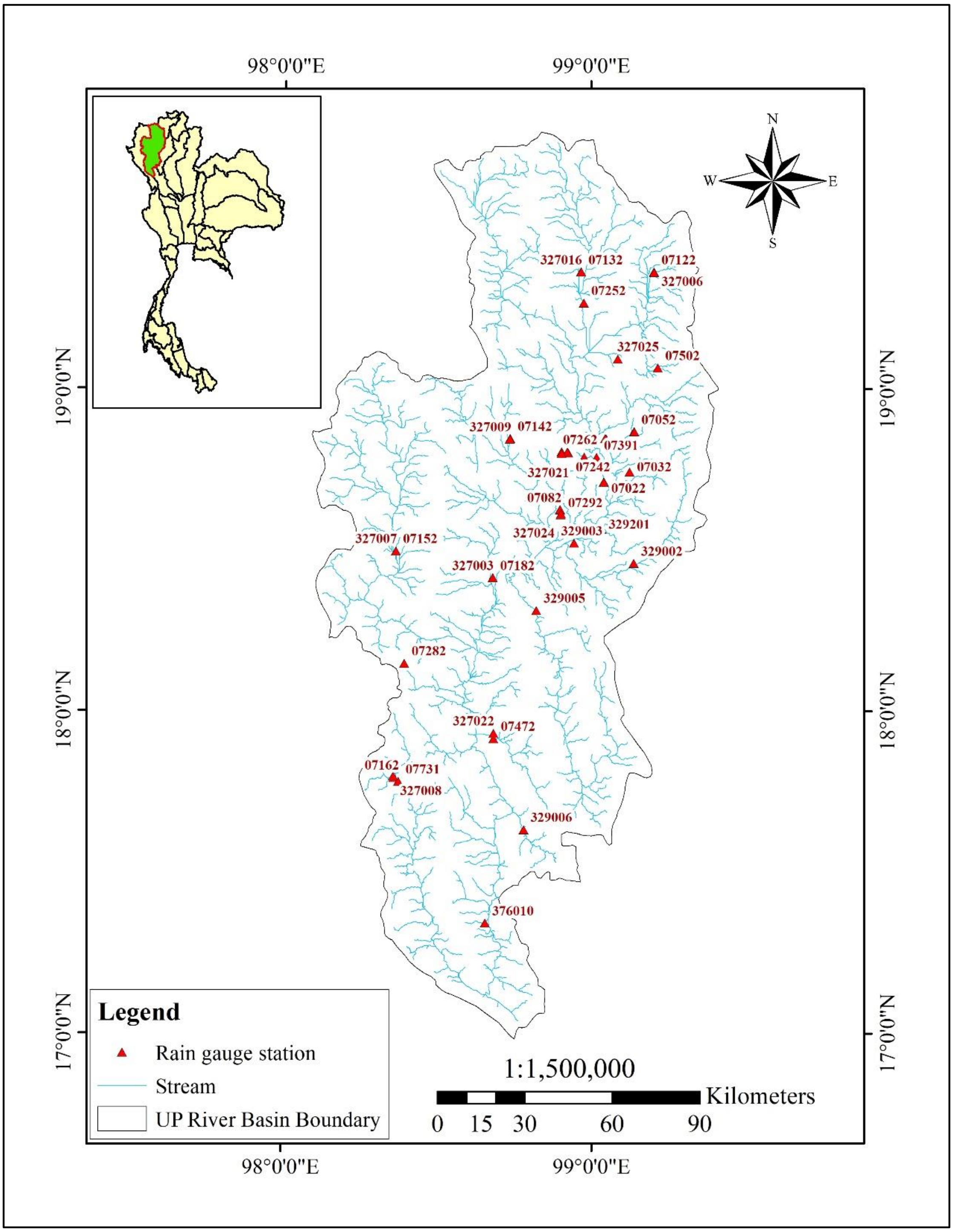

Figure 3.5 Location of the 43 rainfall stations

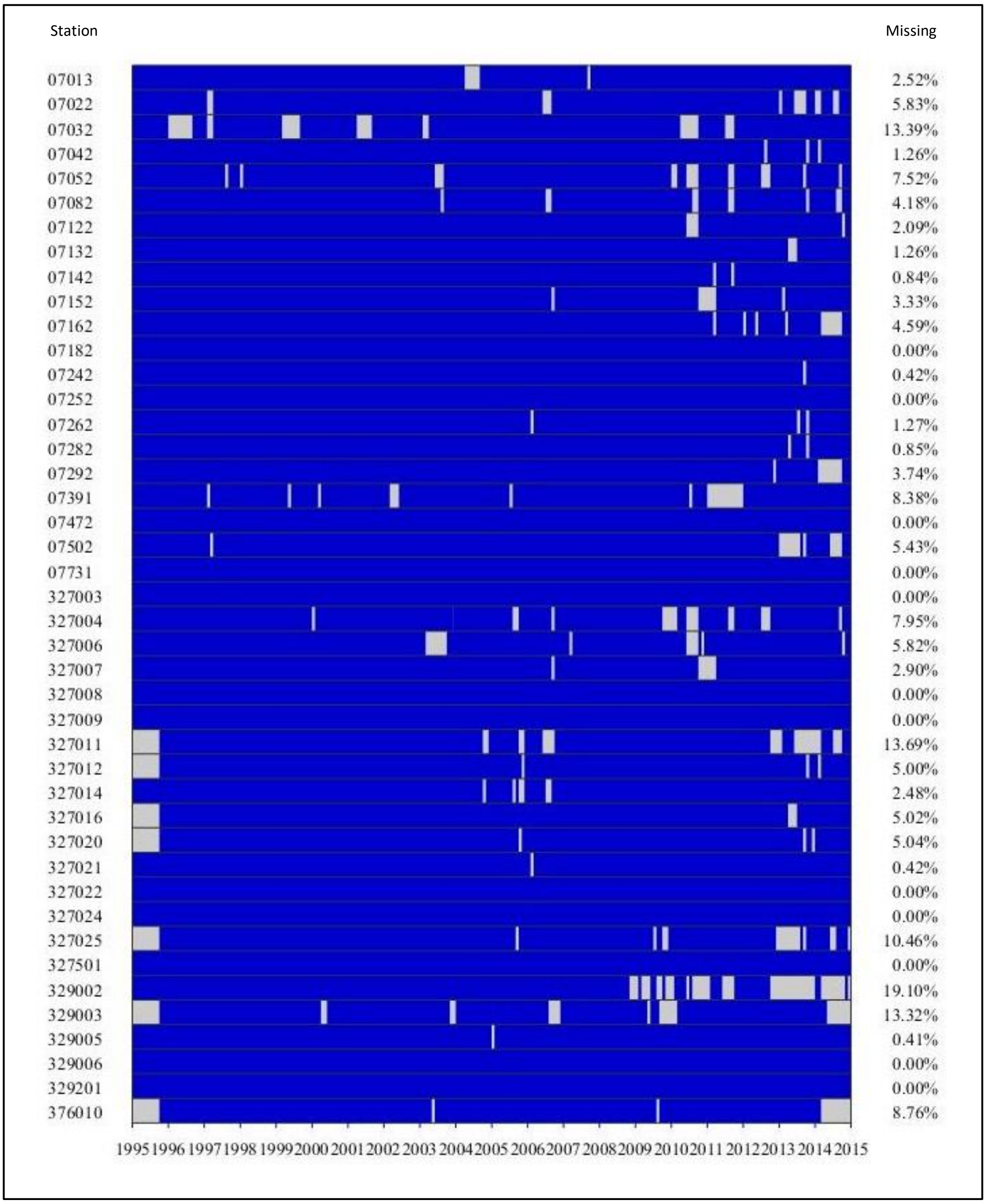

Figure 3.6 Available and missing data of the 43 rainfall stations from 1995 to 2014 (Blue: Available data, Gray: Missing data)

3.3.1 Rainfall Consistency Test

Testing the consistency of the rainfall data over a long period of record is important for further analysis. Double Mass Curve (DMC) is a popular technique to check the consistency of the hydrologic data to ensure that any trends detected depend on the meteorological causes and not to change by other causes such as methods for observation, exposure, or location of gauge.

In this study, the DMC is used to adjust inconsistent rainfall data by comparing data for a single station with that of a pattern composed of the data from surrounding stations. If the data are proportional to each other, these two variables are plotted as a straight line. In contrast, a change in slope of the DMC refers to the inconsistency of the data and the variation of the slope defines the level of change in the relation. In this study, the quality of the 43 observed rainfall stations which are located inside the Upper Ping River basin from 1995 to 2014 is tested.

As shown in *Figure 3.7*, the test result indicated that 42 out of the 43 stations are found to be consistent over the period of records except for station 07391 which captured a significant break in slope from 2006 to 2008 before returning to the earlier trend (*Figure 3.8* (a)). The break from 2006 to 2008 seems to be occurred due to any non-meteorological cause. Therefore, adjusting the slope of the DMC would be beneficial for the reliability and accuracy of further analysis. The break in slope can be adjusted by using Eq 3.1.

$$P_a = \frac{a_1}{a_2} P_o \qquad \textit{Eq. 3.1}$$

where P_a is the adjusted annual rainfall, P_o is the observed annual rainfall, a_1 is the DMC slope for 1995-2006 (before changing in slope), and a_2 is the DMC slope for 2006-2008 (after changing in slope). The change that occurred over the rainfall record length was believed to be caused by temporary change. Therefore, the proportion of a_1 over a_2 was used for adjustment. The result of the adjusted DMC of the inconsistent rainfall station (07391) is shown in *Figure 3.8* (b).

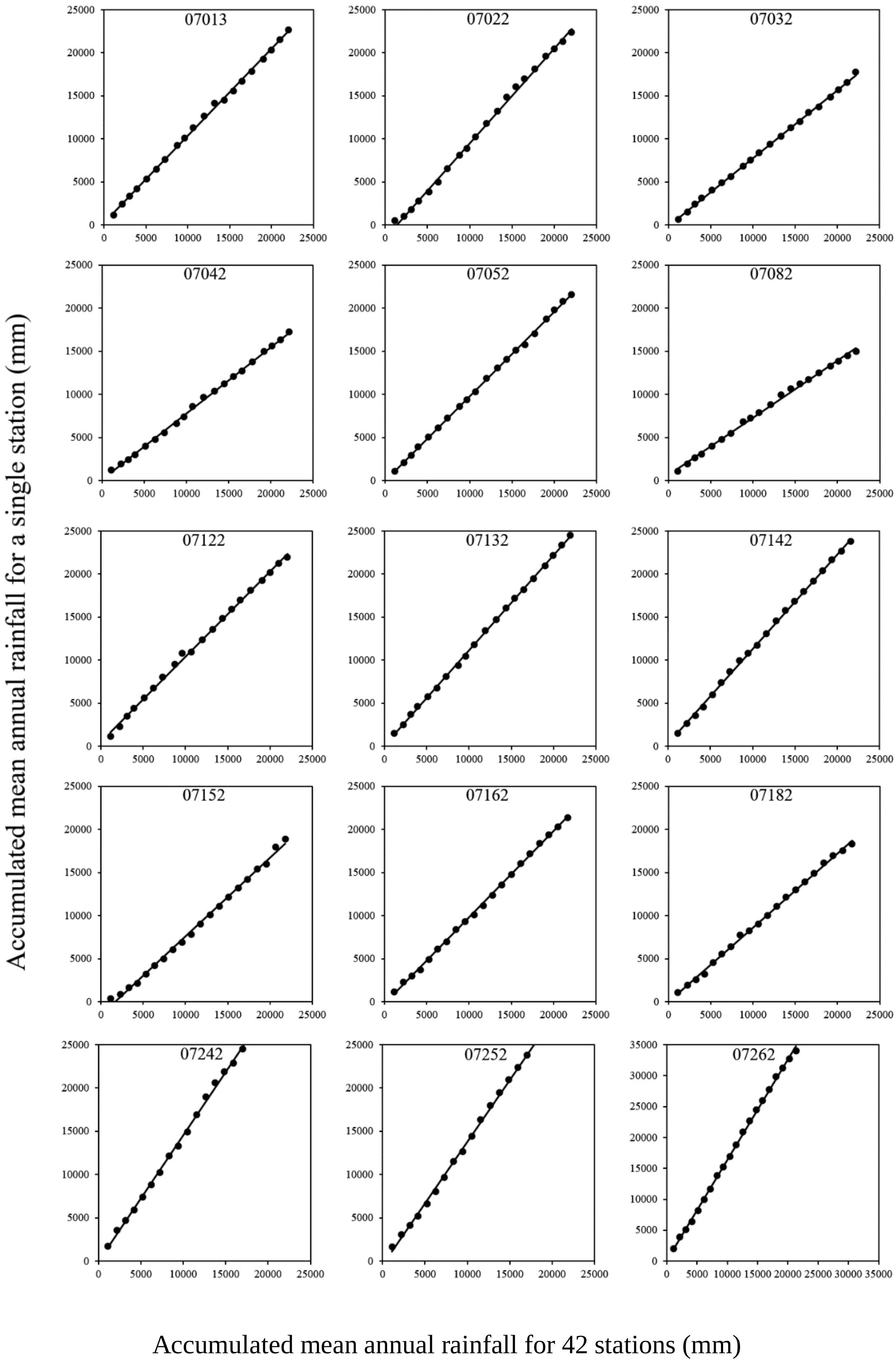
07013
07022
07032
07042
07052
07082
07122
07132
07142
07152
07162
07182
07242
07252
07262
Accumulated mean annual rainfall for a single station (mm)
Accumulated mean annual rainfall for 42 stations (mm)

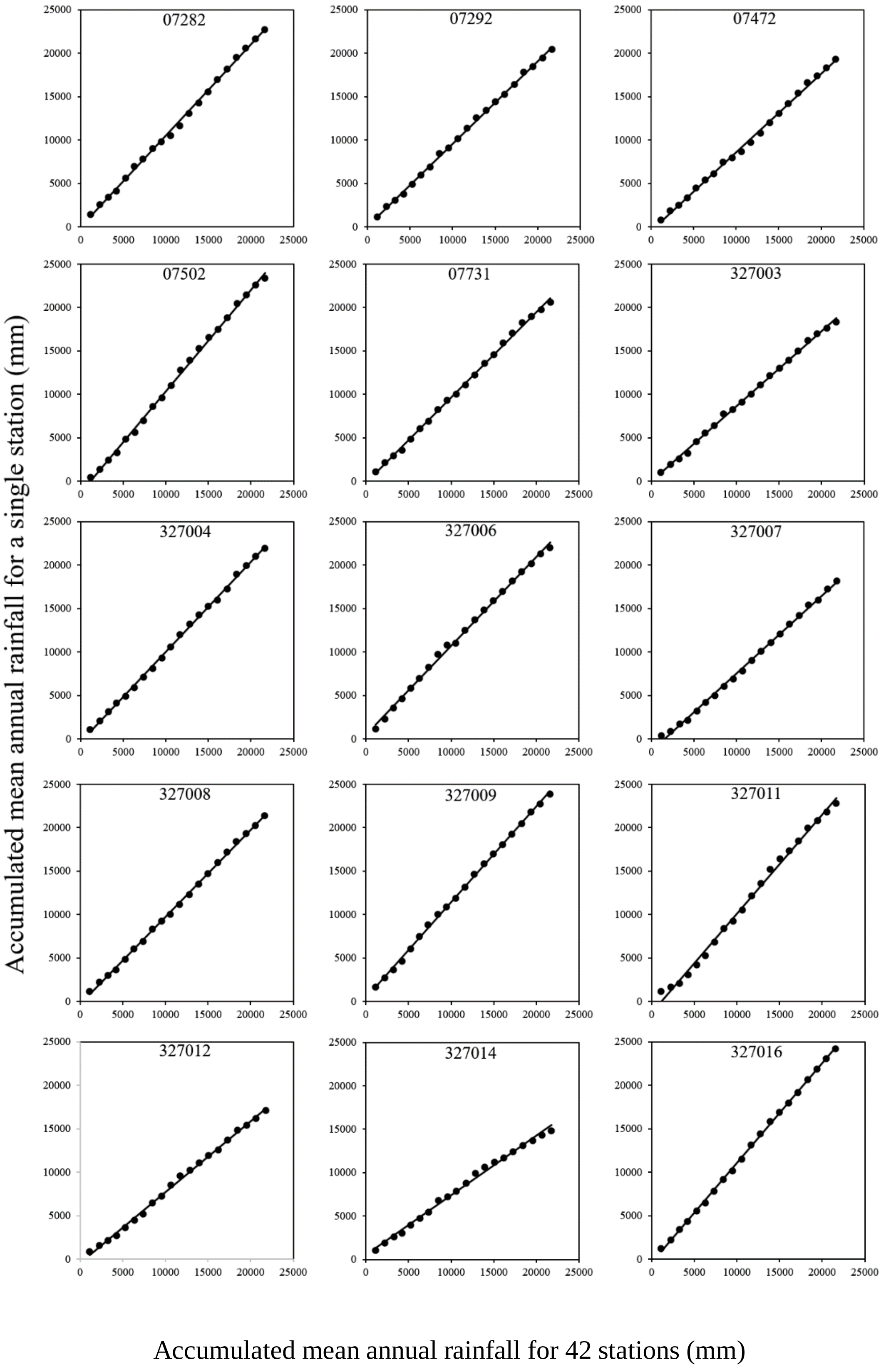
07282
07292
07472
07502
07731
327003
327004
327006
327007
327008
327009
327011
327012
327014
327016
Accumulated mean annual rainfall for a single station (mm)
Accumulated mean annual rainfall for 42 stations (mm)

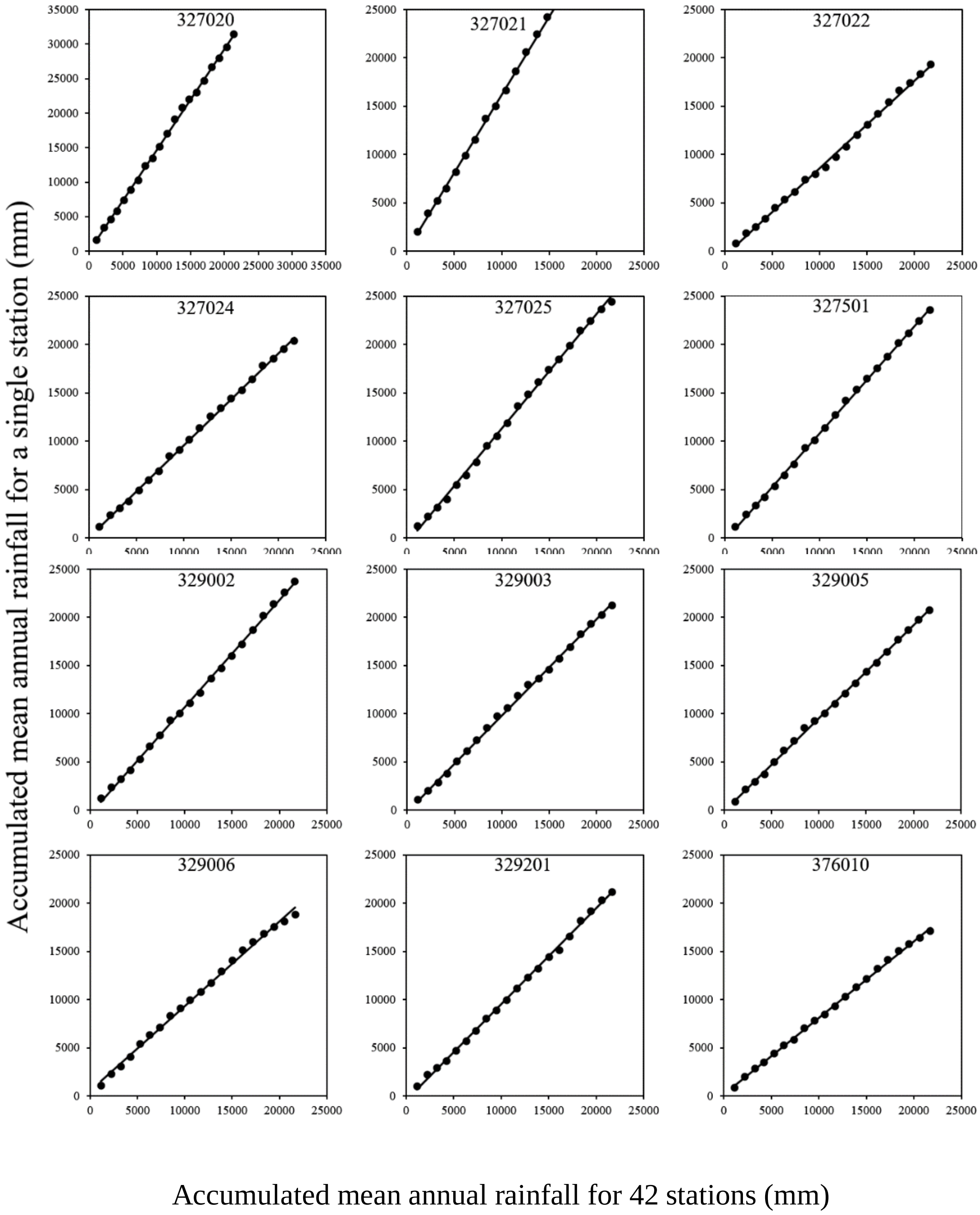

Figure 3.7 Consistency test by the double mass curve of the 42 rainfall stations

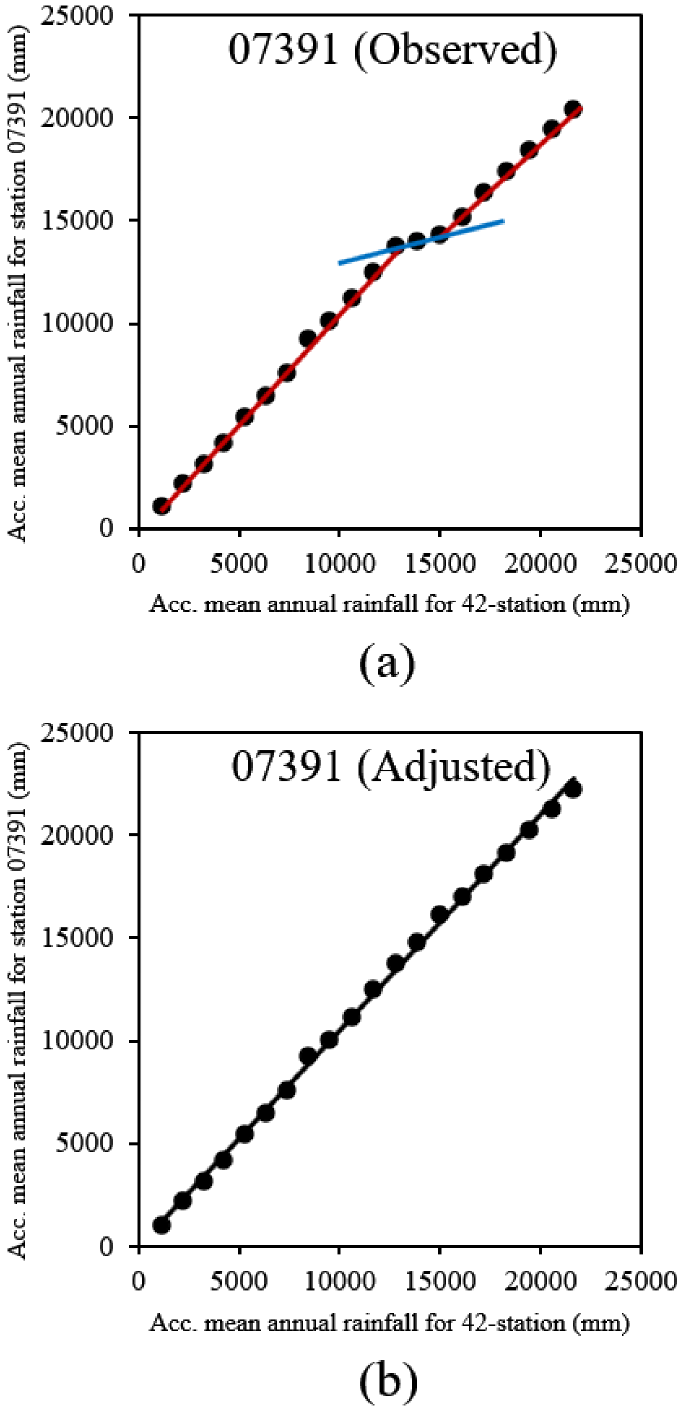

Figure 3.8 DMC of the inconsistent station 07391 before (a) and after adjusting (b)

3.4 Land Use

Figure 3.9 shows the distribution of land-use types in the Upper Ping River basin. Land use can be classified into five main different types, such as Forest (F), Agriculture (A), Urban (U), Open water (W), and Mixed land-use (M). The major land use of the Upper Ping River basin is the forest which covers the area of 21,235 km^2 or equal to 80.1% of the total area. The second majority is known as agriculture which covers another 14.4% of the total area while the Urban, Open water, and Mixed land-use areas show a minor proportion to the total area as also describe in *Table 3.4.*

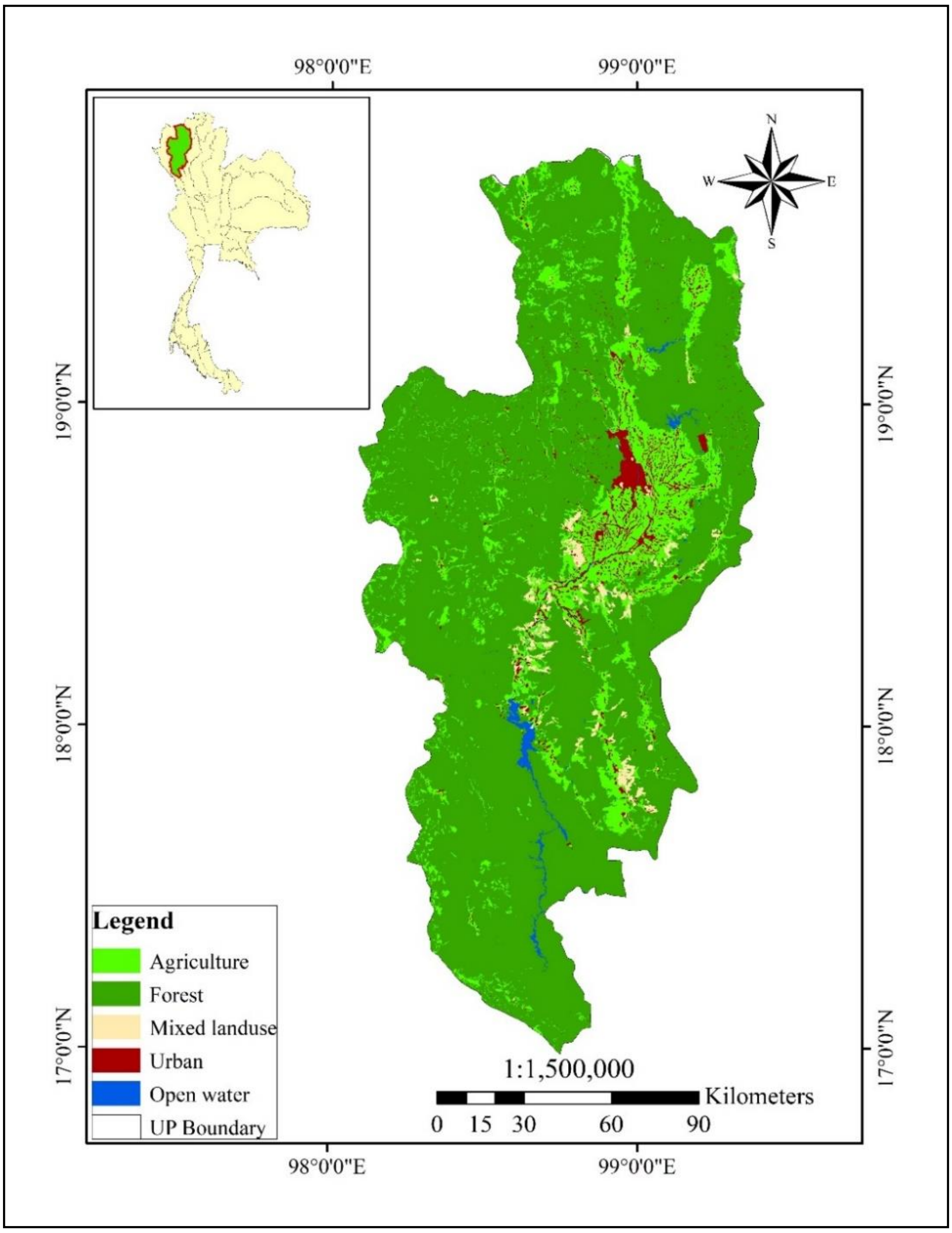

Figure 3.9 Land-use type in the Upper Ping River basin

Table 3.4 Total and percentage area of land-use type in the Upper Ping River basin

Land-use Type		**Area (km^2)**	**Area (%)**
Forest	F	21,235	80.1
Agriculture	A	3,823	14.4
Mixed land-use	M	370	1.4
Urban	U	735	2.8
Open water	W	337	1.3
Total		26,674	100

3.5 Soil Type

Figure 3.10 demonstrates the distribution of soil types in the Upper Ping River basin. There are thirty-six soil types in the area. However, only four types among the total show the major value in terms of proportion to the total area. The first majority is Soil type group 62 which distributes 69.5% and can be found almost everywhere in the basin while the second and third majorities are Soil type group 48 and Soil type group 20 which distribute 9.4% and 3.4% to the basin, respectively. Another majority that distributes about 3.2% to the basin is Soil type group 29. The information of the soil type group is described in *Table 3.5*.

Table 3.5 Description of soil type group in the Upper Ping River basin (LDD, 2014)

Group of Soil	Distinct Characteristics	Area (km^2)	Area (%)
Group 20	Very deep siltstone sandy soil group developed from the distributary sediment, the soil reaction is neutral or base, bad to rather bad drainage, low to moderate fertility	912	3.4
Group 29	Deep to very deep clay soil group developed from the fine mass parent material, good to moderate good drainage, low fertility	854	3.2
Group 48	Shallow soil group to rock fall or rock waste layer and may find rock wall layer within 150 cm. Depth from the ground surface, good drainage, low fertility	2,499	9.4
Group 62	Complex slope area having slope more than 35%, this vicinity area has not been studied, surveyed, and classified because the area is high steep regarded as difficult for management and preservation for agricultural purpose	18,541	69.5
Other Groups	-	3,868	14.5
	Total	26,674	100

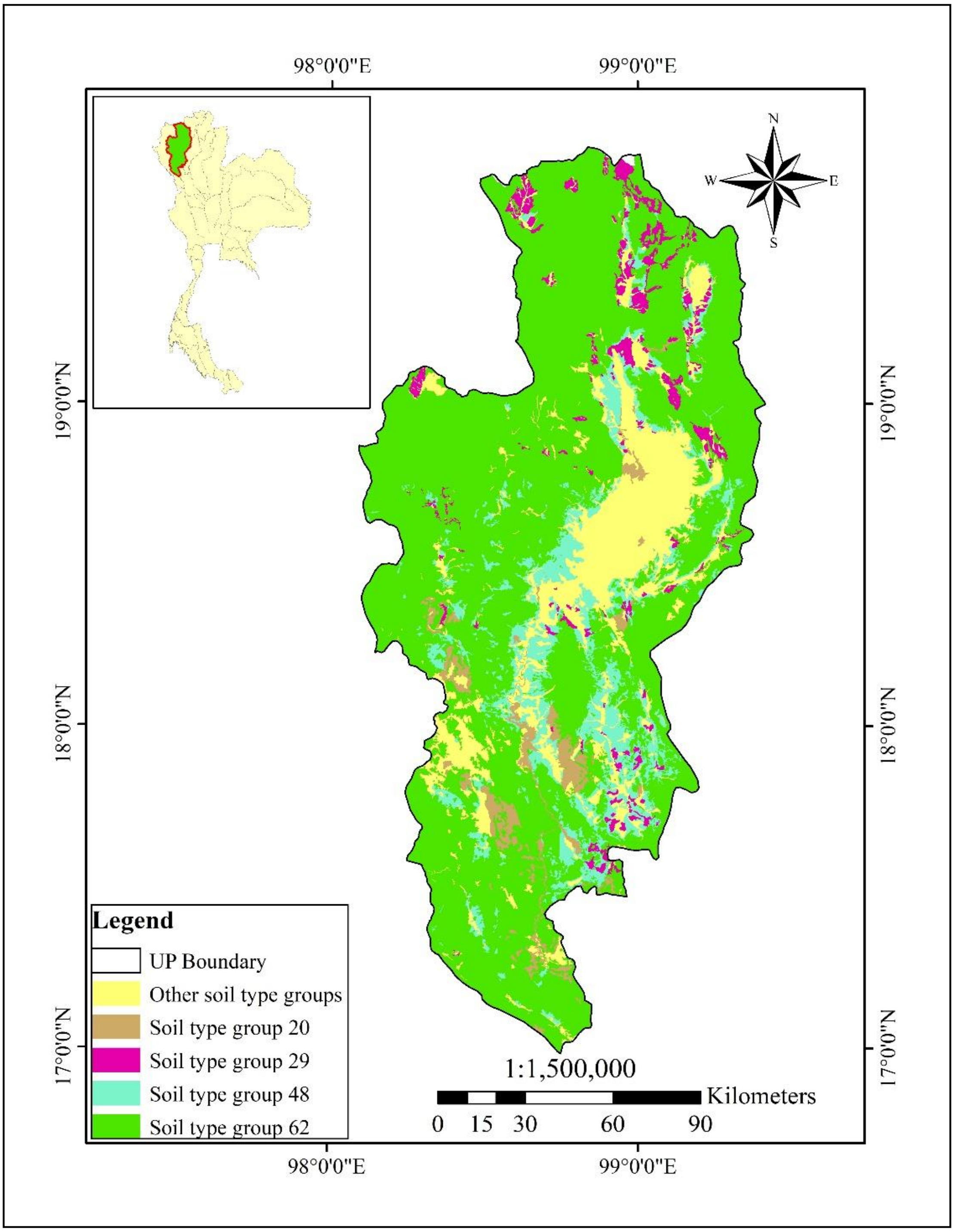

Figure 3.10 Soil type distribution in the Upper Ping River basin

CHAPTER 4
METHODOLOGY

The methodology applied in this research to achieve the overall objectives is presented in this chapter. The overall framework consists of three main steps, including (1) data preparation, (2) regionalization of low-flow indices in ungauged sub-basin, and (3) performance measurement as briefly shown in Section 1.4. The detailed procedure is described in the following sections.

4.1 Data Preparation

4.1.1 Data Collection

The daily rainfall and daily streamflow with a period of 20 years between 1995 and 2014 are obtained from RID, DWR, and TMD. The 20 years is divided into two sub-periods for calibration and validation of the low-flow estimation methods. The calibration period is from 2000-2014 and the validation period is from 1995-1999. There are 43 rainfall and 25 flow stations used in this study. The soil types and land use are obtained from LDD. The Digital Elevation Model (DEM) with a resolution of 30 m, which is an important input to delineate the sub-basins in this study, is obtained from Earth data-NASA.

4.1.2 Data Checking and Cleaning

As mentioned in sections 3.2 and section 3.3, there are some missing data in the streamflow and rainfall records. In general, the missing streamflow data can be filled in by various techniques, for instance, streamflow modeling such as HEC Flow which can generate the flow for filling into the missing records. However, the missing data of both streamflow and rainfall records in this study are filled in by applying the simple average of the records on the same day and month in the years in which the data are available as applied in Kimhuy (2018). The records from gauging stations that are suspicious to have data quality issues were excluded from the analysis.

4.2 Regionalization of Low-flow Indices in Ungauged Sub-basin

For each regionalization method, the value of various record lengths is assessed by using hypothetically shortened records. This represents the case of without record or only short records being available at the subject/ungauged site. However, the full record length for all subject sites is available in this study, so the adjusted low-flow indices for hypothetically shortened records with the observed low-flow indices estimated from the complete records can be compared.

As mentioned in section 1.4, the development of low-flow measures from the flow data in gauged sub-basins is necessary to be done to quantify the selected low-flow indices including ninety-five-percentile flow (Q95), baseflow index (BFI), and the annual minimum 7-day moving average flow with a 10-year recurrence interval (7Q10) before moving forward to the next procedure of regionalizing the low-flow indices for ungauged sub-basins. In this study, the regionalization methods are grouped into two which are the spatial regionalization (Regression and Sub-basin similarity methods) and temporal regionalization (Climate adjustment method).

4.2.1 Low-flow Indices

Based on their importance and data availability, three recommended and widely used low-flow indices, such as Q95, BFI, and 7Q10, mentioned in Pyrce (2004) and Gustard et al. (1992) are selected to represent the low-flow characteristics in this study. The calculation of the selected low-flow indices is performed according to the steps explained in the following sections.

1) Ninety-five-percentile Flow

The ninety-five-percentile flow which is known as the most often used low-flow index in the academic study is defined as the flow equaled or exceeded during 95 percent of the observation period (Pyrce, 2004). It could be noticed that if the value of Q95 is high, the stream seems to have more water most of the time. So, the high value of Q95 represents a lower risk of water scarcity compared to other stations with the lower value of Q95. In contrast for the station with the low value of Q95, the stream is most likely to be dried more often which lead to a higher risk of water scarcity compared to other station with a higher value. Therefore, the station with the low Q95 should be monitored more closely to reduce the severity produced by water scarcity or drought.

Q95 of the 25 selected flow gauged stations in this study is determined from the flow duration curve which is plotted based on the continuous daily streamflow records between 1995 and 2014. The obtained values of Q95 are then assumed to represent the long-term averages of Q95.

In this study, the flow duration curve which illustrates the percentage of time that specified streamflow is equaled or exceeded during a given observation period is plotted between the magnitude of daily streamflow and the exceedance probability based on the procedure as summarized below:

1. Arranging the daily mean flows for the recording period from the highest value to the lowest value
2. Ranking each streamflow value starting from 1 to the largest order.
3. The exceedance probabilities are then determined using the Weibull formula (Eq. 4.1) to compute the plotting position.

$$P = \frac{m}{n+1} \qquad \textit{Eq. 4.1}$$

where:

P : probability that a given flow is equaled or exceeded

m : ranked position

n : number of events for the period of record.

2) Baseflow Index

The baseflow index is known as a non-dimensional index which is defined as the baseflow volume divided by the total streamflow volume (Eq. 4.2). BFI represents the slow or delayed contribution and may be influenced to a significant extent by basin geology. The value of BFI ranges from 0 to 1. If the value is close to 1, it represents the high contribution of groundwater or/and other delayed sources to streamflow and, in contrast, if the value is close to 0, the contribution to the streamflow is low. Hydrology (1980) recommended it to be a good indicator of the effects of geology on low-flow.

$$BFI = \frac{Baseflow\ volume}{Total\ streamflow\ volume} \qquad \text{Eq. 4.2}$$

In this study, the BFI is determined using the method of local minimum as described in White and Sloto (1990) and can be summarized as below:

1. The daily streamflow time series Q_i are grouped using a moving window length of fifteen days and a window overlap of fourteen ($Q_1, Q_2, Q_3, \ldots, Q_{15}$), ($Q_2, Q_3, Q_4, \ldots, Q_{16}$), …, ($Q_{n-14}, Q_{n-13}, Q_{n-12}, \ldots, Q_n$).
2. Local minimum, $QB_1, QB_2, QB_3, \ldots, QB_n$, are identified by selecting the minima of each block obtained from step 1.
3. The QB_i are then connected with the straight lines to define the baseflow hydrograph.
4. The volume under baseflow hydrograph V_B is calculated between the first baseflow QB_1 and the last baseflow QB_n
5. The volume under streamflow hydrograph V_A is calculated for the same QB_i period.
6. The baseflow index is then can be calculated by V_B/V_A

3) Annual Minimum 7-day Moving Average flow with a 10-Year Recurrence Interval

Annual minimum 7-day moving average flow with a 10-year recurrence interval (7Q10) is known as the most commonly used single low-flow indices (Pyrce, 2004). As similar to the Q95, the value of 7Q10 is beneficial for indicating the level of risk which could be caused by water scarcity. 7Q10 can be determined from the annual series of minimum 7-day moving average flows at the selected 25 flow stations. The average flow for each consecutive 7-day period is calculated from the daily records, and the lowest average value for each year represents that year in the annual series. The 7-day minimum average flows are fitted to three distributions namely Normal, Gumbel, and Log-Pearson type III distributions using “L-moment ratio diagram for the goodness of fit test” to define the applicable distribution for determining the annual minimum 7-day average flow with a recurrence interval of 10 years.

The following Eq. 4.3 is used to estimate the 7Q10. Fitting the Log-Pearson type III distribution requires determining the mean, standard deviation, and skewness coefficient of the logarithms.

$$\log Q_T = \overline{X} + KS \qquad \textit{Eq. 4.3}$$

where:

Q_T : annual minimum 7-day moving average flow with a 10-year recurrence interval (7Q10), T = 10 years

$\bar{X}$: logarithms mean of the annual minimum 7-day average streamflow

K : skewness coefficient

S : logarithms standard deviation of the annual minimum 7-day average streamflow.

4.2.2 Regional Regression Method

The regional regression method applied in this study was similar to that has been previously used by Samuel et al. (2011). Firstly, all input data are standardized to eliminate the effects of a different order of magnitude that may exist in the sub-basin characteristics. Next, the regression coefficients were computed using the stepwise regression procedures in which all selected sub-basin characteristics are included in the analysis. Then, out of the selected sub-basin characteristics, only a set of the characteristics that are statistically significant or associated with the largest regression coefficients for each station are selected for predicting streamflow in ungauged sub-basins. The rationale of this selection is that only a large correlation coefficient may be a good indicator of the predictive power of the sub-basin characteristics. A common equation that relates the most significant sub-basin characteristics to the low-flow indices in gauged sub-basin can be written in the form of Eq 4.4:

$$QD = a + bA + cB + ... + oN \qquad \textit{Eq. 4.4}$$

where:

QD : predicted low-flow indices in gauged sub-basin (donor)

a : regression constant

$b, c, ..., o$: regression coefficients

$A, B, ..., N$: gauged sub-basin characteristics

The predicted low-flow indices in ungauged sub-basin are then calculated by substituting the sub-basin characteristics of the ungauged sub-basin into the regression equation deriving from the gauged sub-basins. Therefore, the equation to predict low-flow indices in the ungauged sub-basin can be transformed to the following Eq. 4.5:

$$QS_{pred} = a + bA_S + cB_S + ... + oN_S \quad \text{Eq. 4.5}$$

where:

QS_{pred} : predicted low-flow indices in ungauged sub-basin/subject site

$A_S, B_S, ..., N_S$: ungauged sub-basin characteristics

1) Sub-basin Characteristics

The relationships between low-flow indices and sub-basin characteristics have to be developed based on sub-basins with good quality of data and relatively natural flow regimes (Gustard et al., 1992).

There are 51 available sub-basin characteristics to be considered in this study:

1. Sub-basin area
2. Sub-basin elevation (min, mean, and max)
3. Sub-basin slope (min, mean, and max)
4. Annual rainfall (wet, dry, and total)
5. The proportion of 36 soil type groups of sub-basins
6. The proportion of 5 land-use types of sub-basin.

To avoid redundancy in the regression equation, only the independent sub-basin characteristics which are selected from the 51 basin characteristics mentioned above should be pre-selected for the stepwise regression procedure. In the process of pre-selection, if two basin characteristics within the same group are found to have a high correlation coefficient between each other, one of them will be removed and another one will be kept for stepwise regression.

4.2.3 Sub-basin Similarity Method

Figure 4.1 demonstrates the procedure for assessing the low-flow indices in ungauged sub-basin by the regional regression method.

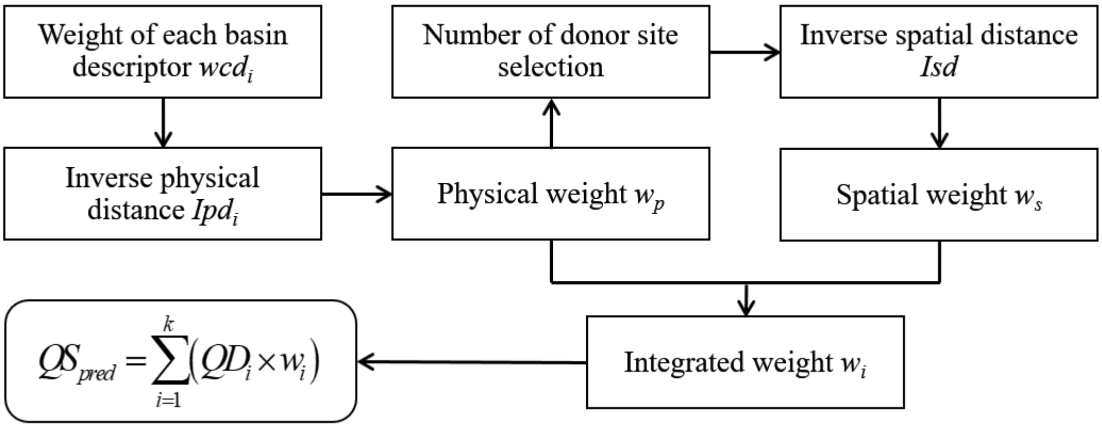

Figure 4.1 Low-flow regionalization by sub-basin similarity method

In this method, the integrated similarity-based approach considering both the spatial proximity and physical similarity as applied in Bao et al. (2012) is used in this study because the literature suggested that it outperformed other methods (Zhang and Chiew, 2009). The method can be summarized as follows:

The weights for donor sub-basins are estimated from a combination of inverse physical distance and inverse spatial distance for each ungauged sub-basin. The inverse physical distance is a function of the sub-basin descriptors of the donor and the subject site while the inverse spatial distance is a function of the distance between the donor site, which is selected according to the physical weight, and the subject site. According to the study of Bao et al. (2012), the most suitable number of donors for regionalization was five. Moreover, our coarse basin network is not suitable for donors of more than five. Therefore, the number of donors from one to five is tested.

In the sub-basin similarity method, the various impacts of sub-basin characteristics or descriptors on the low-flow indices are first considered. The absolute values of the correlation coefficients ($r_{\mathrm{i,j}}$) between sub-basin descriptors and low-flow indices are regarded as the weight (wcd_i) for each sub-basin descriptor. The formula to determine wcd_i is as shown in Eq. 4.6:

$$wcd_i = \frac{\sum_{j=1}^{n} Abs(r_{i,j})}{\sum_{i=1}^{m}\sum_{j=1}^{n} Abs(r_{i,j})} \qquad \textit{Eq. 4.6}$$

where:

m : number of sub-basin descriptors

n : number of low-flow indices

For the physical distance estimation, the fifteen physical descriptors of the sub-basin are all standardized to eliminate the impacts of different units. The physical weight (wp_i) of each donor sub-basin is estimated from the inverse physical distance (Ipd_i) between the donor sub-basins and the ungauged sub-basin for each standardized sub-basin descriptor considering the wcd. The Ipd_i and wp_i can be calculated by using Eq. 4.7 and 4.8, respectively.

$$Ipd_i = \frac{1}{\sum_{j=1}^{m} Abs(c_{i,j} - c_{0,j}) \times wcd_j} \qquad \textit{Eq. 4.7}$$

$$wp_i = \frac{Ipd_i}{\sum_{i=1}^{k} Ipd_i} \qquad \textit{Eq. 4.8}$$

where:

$c_{i,j}$: descriptors of the donor sub-basins

$c_{0,j}$: descriptors of the ungauged sub-basin

k : number of donor sub-basins

The spatial weight (ws_i) of each donor sub-basin is estimated from the inverse spatial distance (Isd) between the donor sub-basins and the ungauged sub-basin and can be calculated by Eq. 4.9:

$$ws_i = \frac{Isd_i}{\sum_{i=1}^{k} Isd_i},\ Isd_i = \frac{1}{s_i} \qquad \textit{Eq. 4.9}$$

where:

s_i : spatial distance between the donor and the ungauged sub-basins

Considering both the physical weight and the spatial weight, the integrated weight (w_i) of each donor sub-basin can be estimated by using Eq. 4.10:

$$w_i = \frac{wp_i + ws_i}{\sum_{i=1}^{k}\left(wp_i + ws_i\right)} \qquad \textit{Eq. 4.10}$$

Next, the low-flow indices in the ungauged sub-basin are transferred from the donor sub-basins with the integrated weights and can be calculated by Eq. 4.11. The streamflow could then be simulated with QS_{pred} in the ungauged sub-basin.

$$QS_{pred} = \sum_{i=1}^{k}\left(QD_i \times w_i\right) \qquad \textit{Eq. 4.11}$$

where:

QS_{pred} : predicted LFI at the subject (ungauged) sub-basin

QD_i : LFI at the donor sub-basin

4.2.4 Climate Adjustment Methods

The climate adjustment method (CAM) which is one of the applicable methods to deal with the problem of estimating low-flow from short streamflow records described in Laaha and Blöschl (2005) is applied in this study.

The approach to this method consists of two steps:

1. Selection of appropriate donors for each subject site.
2. Application of record augmentation techniques to predict the low-flow indices for the subject site from the donor site.

1) Donor Selection

In this study, the donor is selected based on the shortest Euclidean distance between the centroid of the donor (gauged) sub-basin and the centroid of the subject (ungauged) sub-basin.

2) Record Augmentation Techniques

Once the suitable donor has been selected, the predicted low-flow indices at the subject site can be adjusted by transferring the information from the donor based on two record augmentation techniques. In the first technique, the low-flow characteristic is adjusted at the subject site by scaling with the ratio of low-flow indices calculated from the entire observations period and low-flow indices calculated from the overlap period of the donor. In this study, four overlap periods of 1-yr, 5-yr, 10-yr, and 15-yr are selected to test the predictive performance. The predicted low-flow indices at the subject site can be extrapolated using the following Eq. 4.12:

$$QS_{pred} = QS_o \times \left(\frac{QD}{QD_o} \right) \qquad \textit{Eq. 4.12}$$

where:

QS_{pred} : predicted LFI at the subject site

QS_o : LFI at the subject site calculated from the overlap period

QD_o : LFI at the donor site calculated from the overlap period

QD : LFI at the donor site calculated from the entire observation period.

The second technique applies with the same principle, but a weighting coefficient $M(r)$ is included to account for the robustness of the correlation between subject and donor sites. The predicted low-flow indices at the subject site can be extrapolated using Eq. 4.13:

$$QS_{pred} = QS_o . \left(\frac{QD}{QD_o} \right)^{M(r)} \qquad \text{Eq. 4.13}$$

where the weighting coefficient $M(r)$ considers the length of the overlap period of the records in years (n_o) as well as the correlation coefficient (r) of annual low flows. $M(r)$ can be calculated using Eq. 4.14:

$$M(r) = \frac{(n_o - 3).r^3}{(n_o - 4).r^2 + 1} \qquad \textit{Eq. 4.14}$$

4.3 Evaluation of Methods Performance

To determine the most applicable method between the spatial regionalization and the temporal regionalization methods, the scatter plot between observed and predicted low-flow indices for each method will be constructed and the statistical indicators such as coefficient of determination (R^2), root-mean-square error (RMSE), and Nash-Sutcliffe efficiency (NSE) will be calculated to assess which method is the most applicable for this study.

4.3.1 Nash-Sutcliffe Efficiency (NSE)

The Nash-Sutcliffe efficiency is a normalized statistic that determines the relative magnitude of the residual variance compared to the measured data variance. NSE indicates how well the plot of observed versus predicted LFI fits the 1:1 line (Moriasi et al., 2007). NSE can be computed by using Eq. 4.15 below:

$$NSE = 1 - \left[\frac{\sum_{i=1}^{n} \left(O_i - P_i\right)^2}{\sum_{i=1}^{n} \left(O_i - \overline{O}\right)^2} \right] \qquad \textit{Eq. 4.15}$$

where:

O_i : i^{th} observed low-flow indices

P_i : i^{th} predicted low-flow indices

$\bar{O}$: mean of observed low-flow indices

n : total number of observations.

4.3.2 Root-Mean-Square Error (RMSE)

The root-mean-square error is the square root of the mean of the square of all errors. It is considered an excellent general-purpose error metric for numerical predictions (Neill and Hashemi, 2018). RMSE can be computed by Eq. 4.16.

$$RMSE = \sqrt{\frac{1}{n} \sum_{i=1}^{n} \left(O_i - P_i\right)^2} \qquad \textit{Eq. 4.16}$$

Neill and Hashemi (2018) confirm that the RMSE is a good measure of accuracy, but only to compare prediction errors of different models or model configurations for a particular variable and not between variables, as it is scale-dependent.

4.3.3 Coefficient of Determination (R^2)

The coefficient of determination is the criterion generally used in linear regression to test the adjustment of the model (Ait-Amir et al., 2020). The coefficient is defined as the squared value of the coefficient of correlation (Krause et al., 2005) and calculated by Eq. 4.17:

$$R^2 = \left(\frac{\sum_{i=1}^{n} \left(O_i - \overline{O}\right).\left(P_i - \overline{P}\right)}{\sqrt{\sum_{i=1}^{n} \left(O_i - \overline{O}\right)^2} \sqrt{\sum_{i=1}^{n} \left(P_i - \overline{P}\right)^2}} \right)^2 \qquad \textit{Eq. 4.17}$$

where:

$\overline{P}$: predicted low-flow indices

CHAPTER 5
RESULTS AND DISCUSSIONS

5.1 Low-flow Indices

The low-flow characteristics are defined based on three low-flow indices namely Q95, BFI, and 7Q10 where the computed values are presented and discussed in the section below.

5.1.1 Ninety-five-percentile Flow

Figure 5.1 illustrates the flow duration curves of the 25 selected flow stations. The flow duration curves developing from the three located mainstream stations namely P.73, P.1, and P.67 indicate the significantly higher overall compared to the others. The reason is probably that these three stations were located downstream of any stream junction which shares substantial inflow to the sub-basins or the side-flow effect to where they are located. The Q95 is then determined from the flow duration curve and can be summarized as shown in *Table 5.1*.

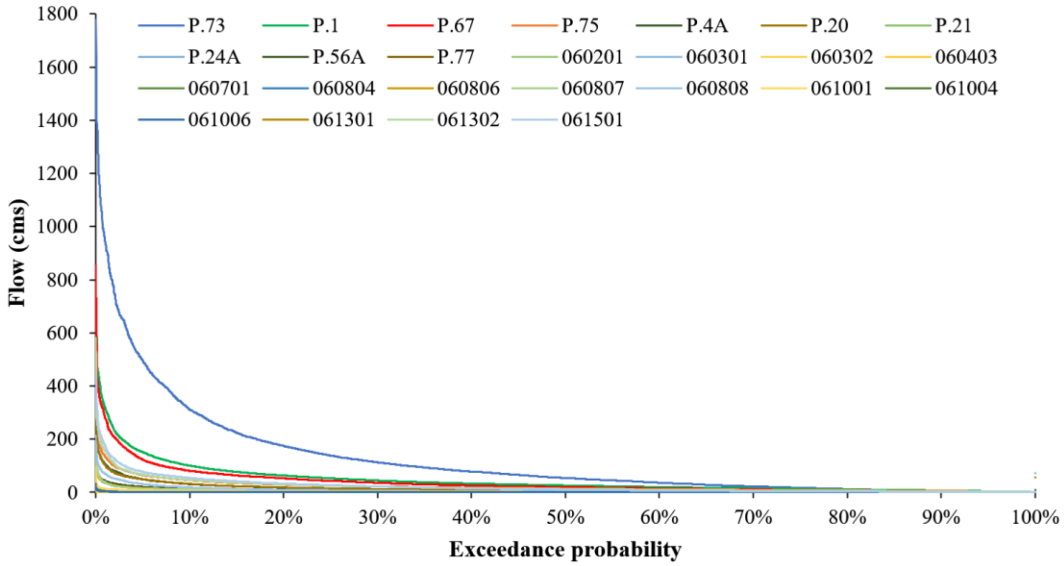

Figure 5.1 Flow duration curves for the 25 flow stations

5.1.2 Baseflow Index

Figure 5.2 demonstrates the baseflow hydrographs of the 25 flow stations. Similar to the flow duration curves, the baseflow hydrograph developing from the three located mainstream stations mentioned above indicates the significantly higher overall compared to the others. The reason may come from the presence of side flow as well. Because when the side flow is high, soil can retain water more than other areas that do not have much side flow. Therefore, most of the time, flow in the river could be maintained at any level. The plot also depicts that the daily baseflow in the 25 sub-basins has a similar pattern, but they are different in amount. The values of BFIs calculated based on the baseflow volume divided by the total streamflow volume are shown in *Table 5.1*.

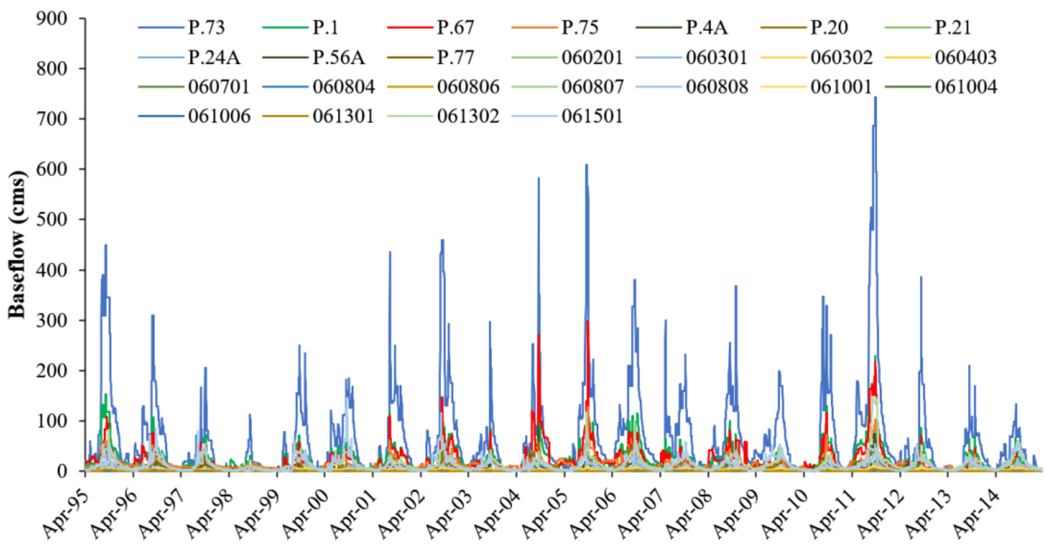

Figure 5.2 Baseflow time-series for the 25 flow stations

5.1.3 Annual Minimum 7-day Moving Average flow with a 10-year Recurrence Interval

Figure 5.3 shows the 7-day moving average flow of the 25 flow stations. The plot is much similar to that of the baseflow hydrograph due to the concept of developing both graphs being based on the moving window of flow time-series. However, they are different in terms of quantity. The result indicates that the three located mainstream stations (P.73, P.1, and P.67) mentioned above keep showing higher values. Moreover, station P.75 located upstream of the three stations is also found to present a significantly higher value of 7Q10 compared to the others.

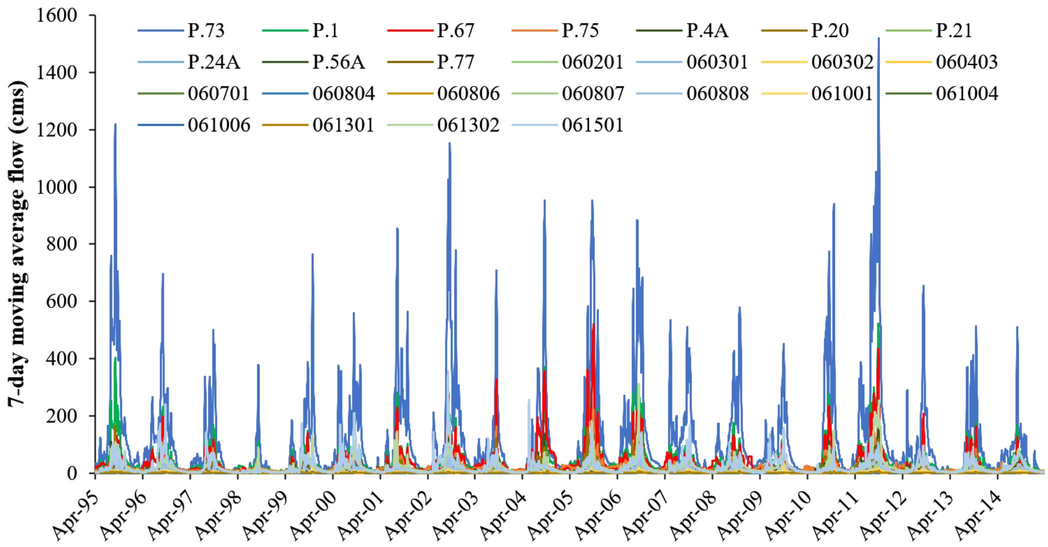

Figure 5.3 7-day moving average flow of the 25 flow stations

Figure 5.4 illustrates the goodness of fit test of the 25 flow stations with the commonly-used distributions for low-flow fitting including Log-Pearson type III, Normal, and Gumbel distributions by using the skewness and kurtosis L-moment ratio diagram (LMRD) as described in Wu et al. (2012). In order to read the information in the figure, it should be noticed that the continuous black line, red dot, and blue dot represent the perfect fit while the black, red, and blue dash lines represent the 95% confident interval of the Log-Pearson type III, Normal, and Gumbel distributions, respectively. Meaning that if any value of data falls in between or inside the dash lines, it can be informed that the value is fitted to the distribution with a 95% confident interval. In addition, there are two sets of data which are the black dot and orange dot. The black dot represents the data which are original value of each station fitting to the Normal and Gumbel distributions while the orange dot represents the logarithm of the data of each station fitting to the Pearson type III distribution or in other words it represents the data of each station fitting to the Log-Pearson type III distribution. The results indicate that the Log-Pearson type III distribution outperforms the Normal and Gumbel distributions since 22 out of the 25 flow stations are fitted with 95% confident interval while only 18 and 20 out of the 25 flow stations are fitted to the Normal and Gumbel distributions, respectively. Therefore, the 7Q10 in this study is determined by fitting the annual minimum 7 days average flow to the Log-Pearson type III distribution for further analysis. The L-moment ratio diagram for the goodness of fit tests of each station can be shown in *Appendix A*. The determined 7Q10 of all 25 gauged stations are summarized as shown in *Table 5.1*.

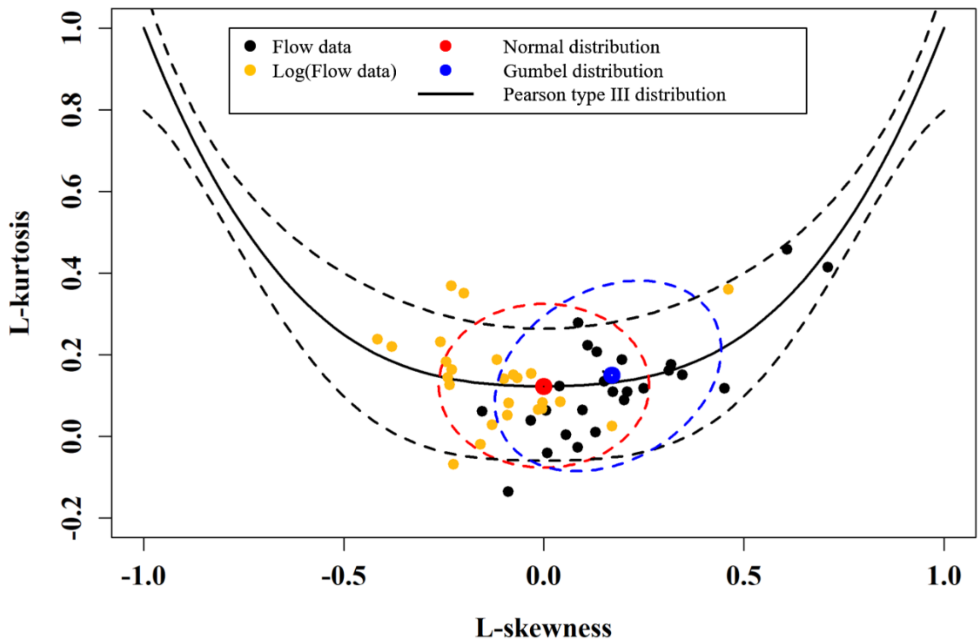

Figure 5.4 L-moment ratio diagram for the goodness of fit tests of all stations

Table 5.1 Summary of the computed LFI for the 25 flow stations

No.	Station	Q95 (cms)	BFI	7Q10 (cms)	No.	Station	Q95 (cms)	BFI	7Q10 (cms)
1	P.1	4.6	0.58	10.21	14	060403	0.11	0.81	0.19
2	P.4A	0.12	0.41	0.5	15	060701	0.12	0.60	0.18
3	P.20	0.96	0.57	2.49	16	060804	0.06	0.51	0.12
4	P.21	0.15	0.48	0.41	17	060806	0.21	0.45	0.43
5	P.24A	0.21	0.45	0.52	18	060807	0.88	0.59	1.39
6	P.56A	0.31	0.49	0.83	19	060808	0.22	0.42	0.42
7	P.67	3.44	0.56	7.53	20	061001	0.7	0.73	0.93
8	P.73	0.96	0.53	12.98	21	061004	0.11	0.66	0.18
9	P.75	4.23	0.63	8.58	22	061006	0.1	0.58	0.16
10	P.77	0.01	0.52	1.53	23	061301	0.11	0.73	0.27
11	060201	0.11	0.67	0.23	24	061302	3.48	0.67	4.51
12	060301	0.26	0.65	0.45	25	061501	1.2	0.54	1.82
13	060302	0.11	0.65	0.15					

5.2 Regionalization of Low-flow Indices Using Regression Method

In order to verify whether the regression method is applicable for the study or not, the calibration and validation process is investigated for two different periods where the land-use change has been recorded. The 15-yr calibration period is selected from 2000 to 2014 and the 5-yr validation period is from 1995 to 1999.

In the next section, the assessment for the low-flow characteristics using the regression method is firstly made for the whole observation period of 20-yr to identify the key basin characteristics which contribute to the low-flow characteristic and then investigate the change when turning to the calibration and validation process. As mentioned in Chapter 4, the pre-selection of independent basin characteristics is required to avoid the redundancy in the regression equation. As the result, only 15 independent basin characteristics are selected out of the total 51 basin characteristics. The abbreviated sub-basin properties with their statistical summary are described in *Table 5.2*. The correlation coefficient (r) and the scatter plots between the 15 independent basin characteristics are as shown in *Table 5.3*.

Table 5.2 The selected 15 basin characteristics with their statistical summary

N°	Acronym	Variable description	Unit	Min	Mean	Max
1	Ar	Basin area	km^2	23.43	1638.54	14536.02
2	El_{max}	Maximum elevation	m	1251.00	1968.12	2577.00
3	El_{min}	Minimum elevation	m	195.00	436.44	1024.00
4	Sl_{max}	Maximum slope	%	116.25	236.32	441.30
5	Sl_{mean}	Mean slope	%	24.93	31.30	41.82
6	AMR	Annual mean rainfall	mm	912.90	1117.43	1305.40
7	%A	Percentage of agriculture	%	0.01	14.43	31.17
8	%F	Percentage of forest	%	64.68	83.78	98.09
9	%M	Percentage of mixed-land use	%	0.00	0.42	3.37
10	%W	Percentage of open water	%	0.00	0.08	0.54
11	%G30	Percentage of soil type group 30	%	0.00	0.84	13.79
12	%G40	Percentage of soil type group 40	%	0.00	0.25	3.05
13	%G56	Percentage of soil type group 56	%	0.00	0.01	0.20
14	%G60	Percentage of soil type group 60	%	0.00	0.07	0.84
15	%G62	Percentage of soil type group 62	%	63.87	85.48	99.99

Table 5.3 Matrix of correlation coefficients (r) and scatter plots between the 15 independent sub-basin properties

Variables	Ar	El_{min}	El_{max}	Sl_{mean}	Sl_{max}	AMR	%G30	%G40	%G56	%G60	%G62	%A	%F	%W	%M
Ar	1														
El_{min}	-0.45	1													
El_{max}	0.39	-0.24	1												
Sl_{mean}	-0.35	0.20	-0.16	1											
Sl_{max}	0.69	-0.56	0.53	-0.26	1										
AMR	0.22	-0.45	-0.13	0.19	0.31	1									
%G30	-0.01	-0.09	-0.04	-0.16	-0.03	-0.19	1								
%G40	0.10	-0.11	0.48	-0.27	0.00	-0.11	-0.10	1							

Variables	Ar	El_{min}	El_{max}	Sl_{mean}	Sl_{max}	AMR	%G30	%G40	%G56	%G60	%G62	%A	%F	%W	%M
%G56	0.32	-0.26	-0.08	-0.43	0.03	0.25	0.07	0.01	1	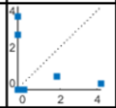	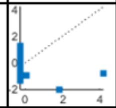	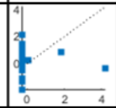	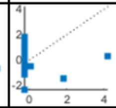	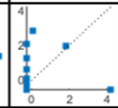	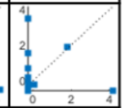
%G60	0.06	-0.17	-0.17	-0.11	0.00	0.11	0.05	-0.04	0.03	1	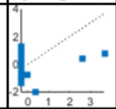	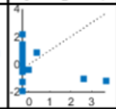	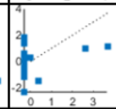	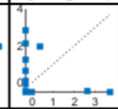	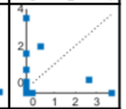
%G62	-0.54	0.36	-0.22	0.81	-0.54	0.03	-0.18	-0.08	-0.33	0.12	1	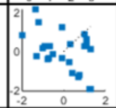	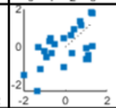	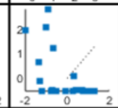	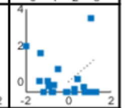
%A	0.17	0.28	-0.01	-0.34	0.10	-0.31	-0.25	-0.07	0.02	-0.31	-0.42	1	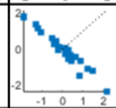	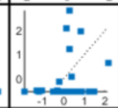	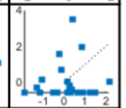
%F	-0.31	-0.15	0.00	0.40	-0.17	0.24	0.27	0.07	-0.09	0.27	0.51	-0.98	1	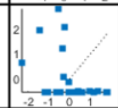	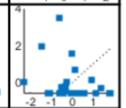
%W	0.77	-0.42	0.25	-0.32	0.73	0.33	-0.12	-0.01	0.12	-0.09	-0.57	0.30	-0.42	1	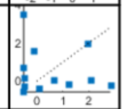
%M	0.33	-0.26	-0.04	-0.19	0.07	-0.14	-0.13	-0.05	0.08	-0.01	-0.20	0.17	-0.30	0.20	1

5.2.1 Ninety-five-percentile Flow

Based on the stepwise regression approach with the p-value of 0.05, only three standardized sub-basin descriptors namely proportions of agriculture (%A), forest (%F), and open water (%W) show a significant relationship to predict the Q95. The regression equation which relates the three descriptors to the predicted Q95 is as shown in Eq. 5.1. The presence of the three sub-basin descriptors tends to increase the value of Q95 in each sub-basin due to the positive sign of the regression coefficients. The obtained equation is considered to support what is described in the hydrologic cycle where land use plays an important role in determining infiltration and thus quick flow and slow flow. An increase in agriculture, forest, or water surface would contribute to the increase in Q95 because these types of land use can retain a relatively high amount of water and slowly flow to the river.

$$Q95_{pred} = 2.20 \times \%A + 2.63 \times \%F + 1.18 \times \%W \qquad \textit{Eq. 5.1}$$

Figure 5.5 shows the scatter plot between the Q95 predicted from the Eq. 5.1 and the observed Q95 determined from the flow duration curve developed from the 20-yr streamflow time series. The result shows that the regression equation could yield a relatively high NSE and R^2 of 0.78 with the RMSE of 0.65 cms which is good for the prediction.

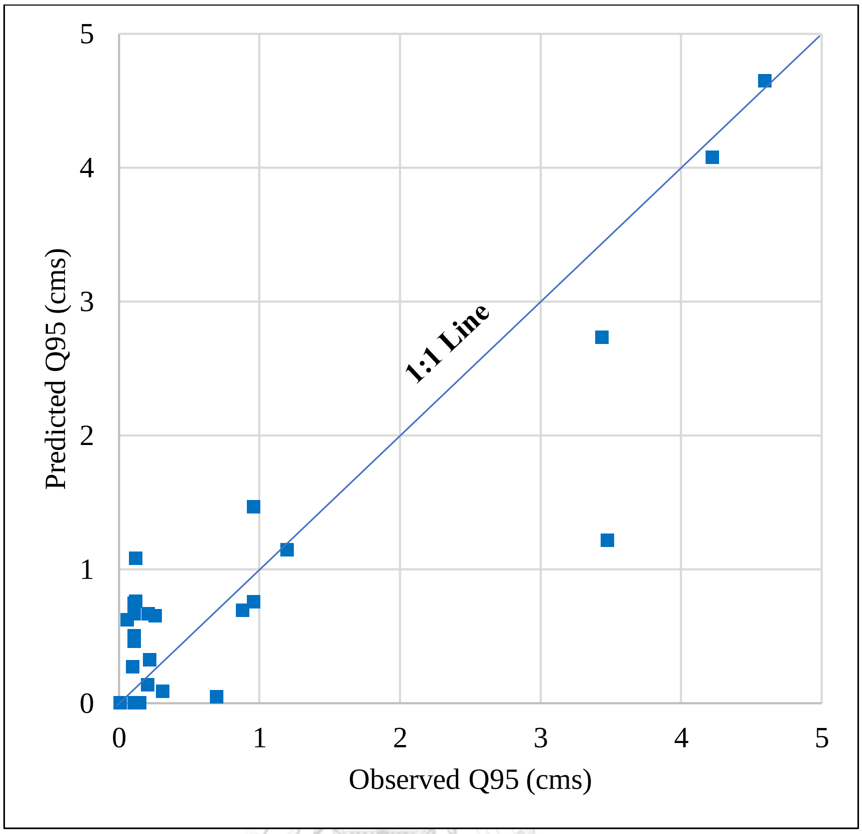

Figure 5.5 Predicted Q95 using regression method vs observed Q95

5.2.2 Baseflow Index

In the prediction of the baseflow index, there are three standardized sub-basin descriptors namely minimum elevation (El_{min}), mean slope (Sl_{mean}), and the proportion of soil type group 60 (%G60) which share substantial distribution to the prediction. The regression equation which relates the three descriptors to the predicted BFI is as shown in Eq. 5.2. The presence of El_{min}, and Sl_{mean} tends to increase the amount of BFI while the presence of %G60 tends to decrease the amount of BFI in each sub-basin.

$$BFI_{pred} = 0.43 \times El_{\min} + 0.37 \times Sl_{mean} - 0.34 \times \%G60 \qquad \textit{Eq. 5.2}$$

Figure 5.6 illustrates the scatter plot between the BFI predicted from the Eq. 5.2 and the observed BFI determined from the local minimum separation technique. The result shows that the regression equation could yield a relatively good NSE and R^2 of 0.58 with the RMSE of 0.07.

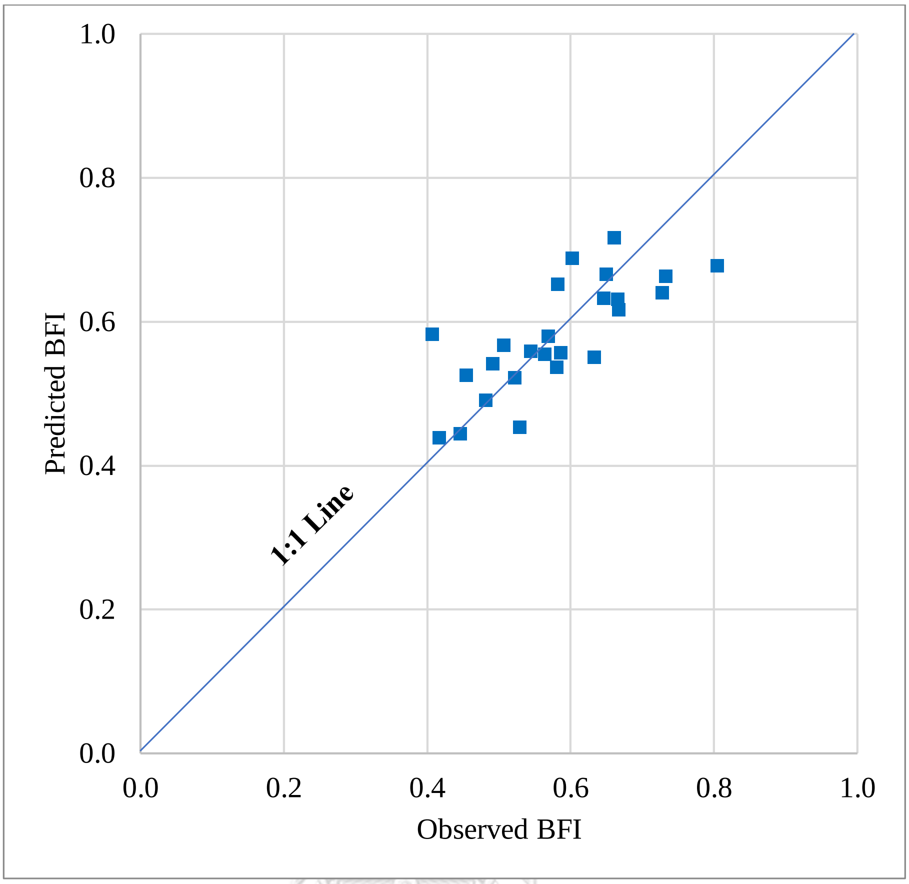

Figure 5.6 Predicted BFI using regression method vs observed BFI

5.2.3 Annual Minimum 7Q10

Unlike Q95 and BFI, the prediction of 7Q10 consists of five standardized sub-basin descriptors namely area (Ar), the proportions of agriculture (%A), forest (%F), and open water (%W) which share substantial distribution to the prediction. The regression equation which relates the four descriptors to the predicted 7Q10 is as shown in Eq. 5.3. The presence of them tends to increase the amount of 7Q10 in each sub-basin. Similar to what is described for the Q95, the obtained equation is considered to support what is described in the hydrologic cycle where land use plays an important role in determining infiltration and thus quick flow and slow flow. An increase in agriculture, forest, or water surface would contribute to the increase in 7Q10 because these types of land use can retain a relatively high amount of water and slowly flow to the river. Moreover, an increase in basin area would also increase in 7Q10 since bigger areas tend to have more flow to the stream.

$$7Q10_{pred} = 0.61 \times Ar + 0.74 \times \%A + 0.90 \times \%F + 0.58 \times \%W \qquad \textit{Eq. 5.3}$$

Figure 5.7 shows the scatter plot between the predicted 7Q10 determined from the Eq. 5.3 and the observed 7Q10. The result indicates that the regression equation could yield the best NSE and R^2 of 0.95 with the RMSE of 0.82 cms. The regression performs well in predicting high index values, but deteriorated performance is found for predicting low index values. The difficulty in predicting low index values is probably due to the inability to fit zero values to log-Pearson Type III.

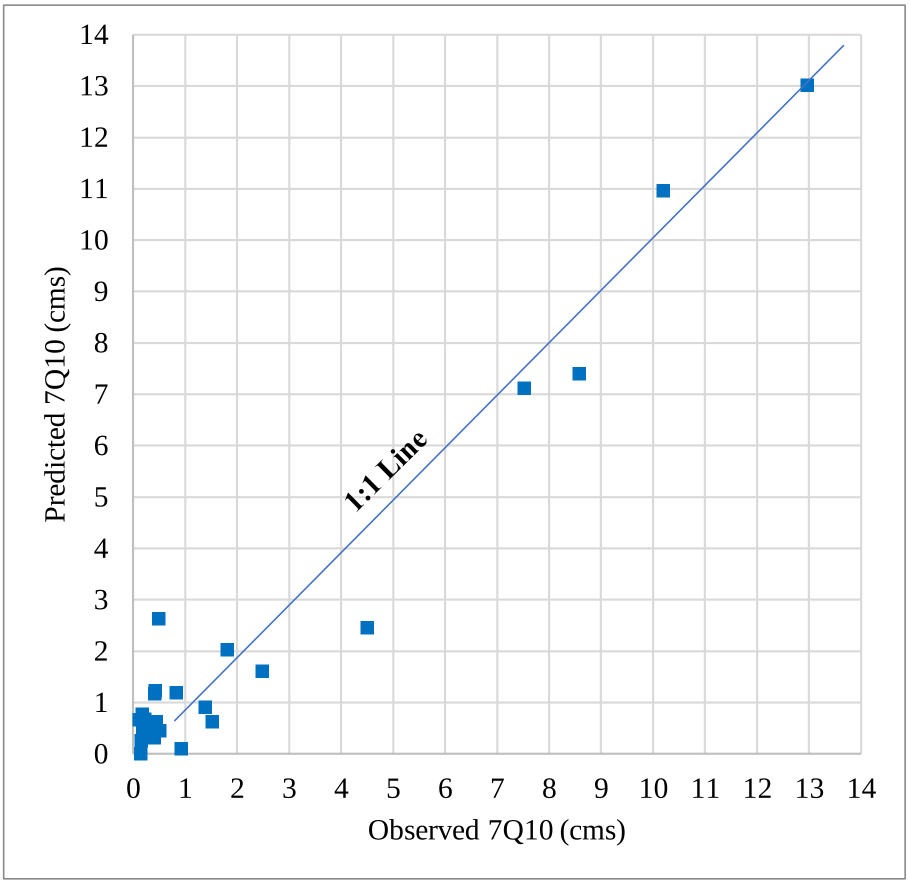

Figure 5.7 Predicted 7Q10 using regression method vs observed 7Q10

5.2.4 Calibration and Validation of the Regional regression Method

Figure 5.8 shows the performance of the regression method for the calibration and validation periods. It is found that the method performs more reliable for Q95 since it yields better statistical indicators for both calibration and validation while BFI performs the worst since it yields R^2 and NSE only 0.25 and 0.18, respectively for the validation. 7Q10, on the other hand, performs the best for the calibration period. However, one outlier causes the performance to drop significantly.

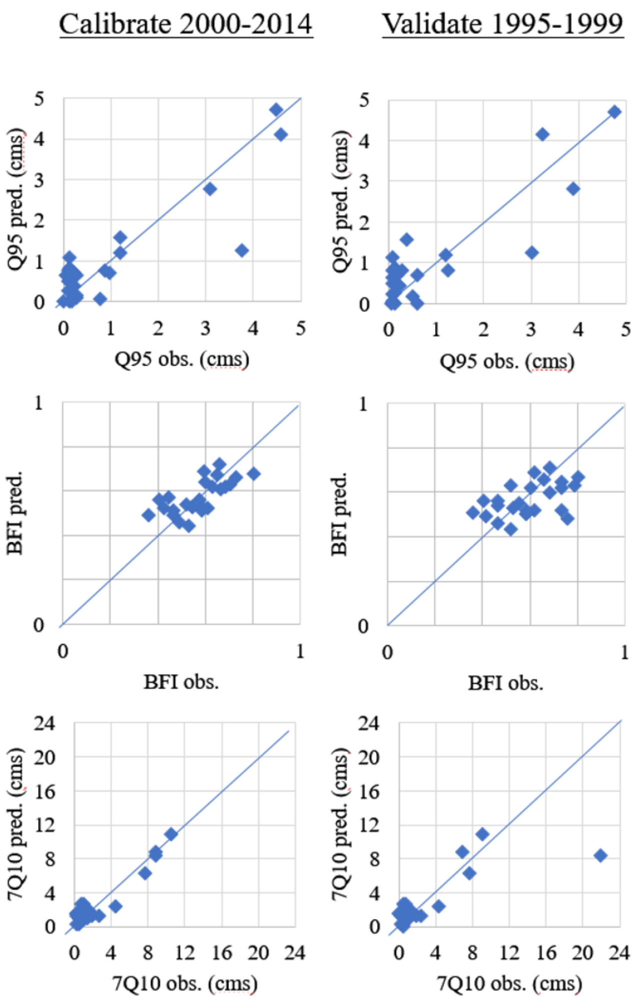

Equations & Summary results

$$Q95 = 2.10\%A + 2.53\%F + 1.17\%W$$

Q95	Calibrate	Validate
RMSE (cms)	0.65	0.66
R^2	0.78	0.76
NSE	0.78	0.75

$$BFI = 0.46El_{min} + 0.44Sl_{mean}$$

BFI	Calibrate	Validate
RMSE	0.08	0.11
R^2	0.49	0.25
NSE	0.49	0.18

$$7Q10 = 0.17El_{max} + 0.18\%F + 0.95\%W$$

7Q10	Calibrate	Validate
RMSE (cms)	0.95	2.96
R^2	0.92	0.68
NSE	0.92	0.65

Figure 5.8 Result of calibration and validation of the regression method

As the calibration and validation periods are considered for the period when there is a change in land use, it can therefore be expected from the equations with land-use variables to be able to represent the effect of land-use change from the calibration to validation periods. In this study, the land-use variables are significant for the prediction of Q95 and 7Q10 but not BFI. Based on the calibration and validation performance, the regression method with Q95 is most likely to be applicable for accounting for the effect of land-use change in the Upper Ping River basin with a reliable result. For 7Q10, the performance deteriorated when moving from calibration to validation period. BFI cannot reflect the effect of land-use change because no land-use variables were included in the regression equation. This is considered the weakness of the regression method. However, the land-use variable can be forced to appear in the regression equation if it is known to the modeler that it could play a significant role in the low-flow.

5.3 Regionalization of Low-flow Indices Using Sub-Basin Similarity Method

5.3.1 Number of Suitable Donor Sub-Basin Selection

In order to investigate the number of donor sub-basin which should be used in this method. The number of donor sub-basin from 1 to 5 are tested for Q95 and can be summarized as shown in *Figure 5.9*, BFI (*Figure 5.10*), and 7Q10 (*Figure 5.11*) while the plots in detail for each donor are as shown in *Appendix B*. The results clearly show that the number of donors does not show a clear difference to the prediction of Q95 using the sub-basin similarity method. For BFI, on the other hand, the method shows poor performance in terms of R^2 and NSE while they are not much different in terms of RMSE. However, the method indicates a clear deteriorated performance when applying a higher number of donor sub-basin for predicting 7Q10. Based on the result, it can be confirmed that the method performs the best when using only one donor sub-basin. Therefore, the application of the sub-basin similarity method using only one sub-basin as the donor is used for further analysis.

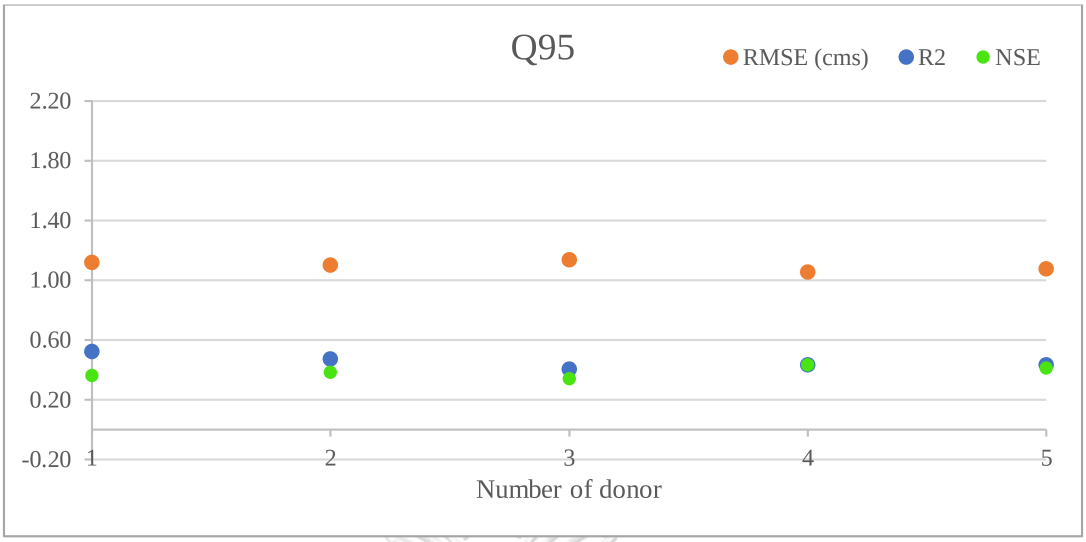

Figure 5.9 The method performance based on number of donor sub-basins for Q95

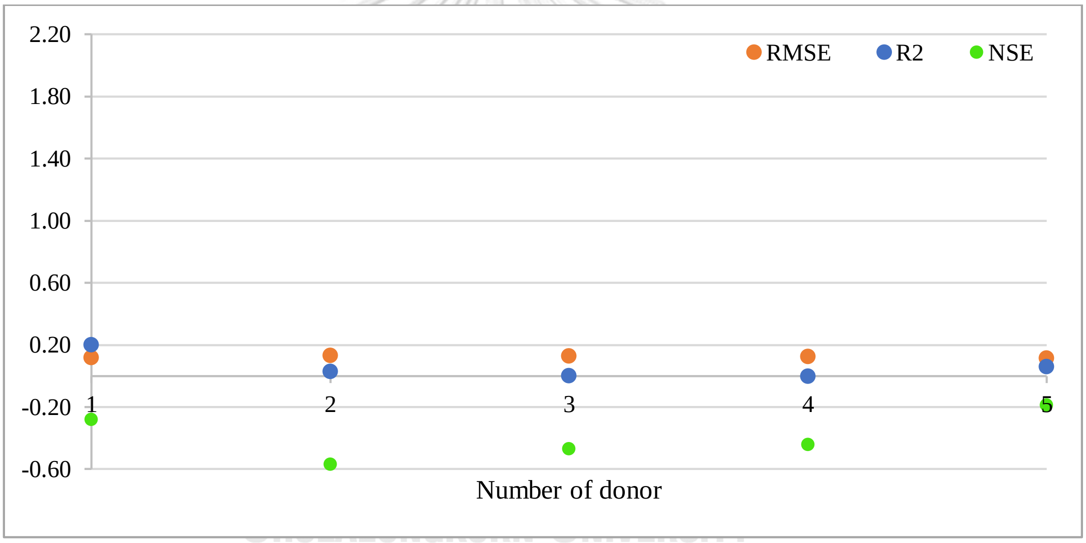

Figure 5.10 The method performance based on number of donor sub-basins for BFI

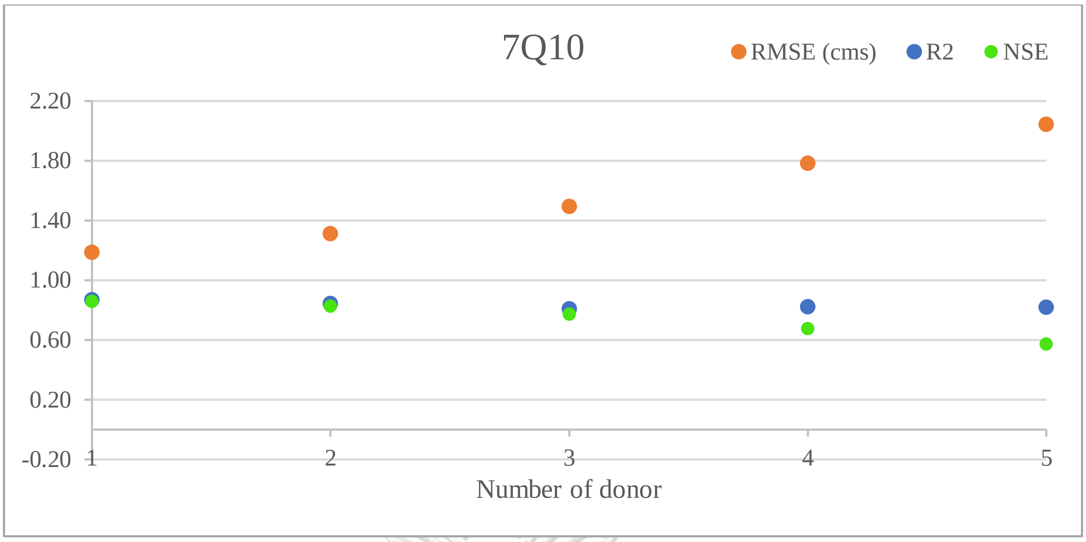

Figure 5.11 The method performance based on number of donor sub-basins for 7Q10

5.3.2 Regionalization Using Sub-Basin Similarity Method

Figure 5.12 demonstrates the scatter plot between the Q95 predicted using the sub-basin similarity method and the observed Q95 determined from the flow duration curve. The result shows that the method yields the R^2, NSE, and RMSE of 0.52, 0.36, and 1.12 cms, respectively. Apart from the statistical performance indices, it can be seen from *Figure 5.12* that the sub-basin similarity method cannot well predict Q95 because the deviations between the observed and predicted Q95 are generally large.

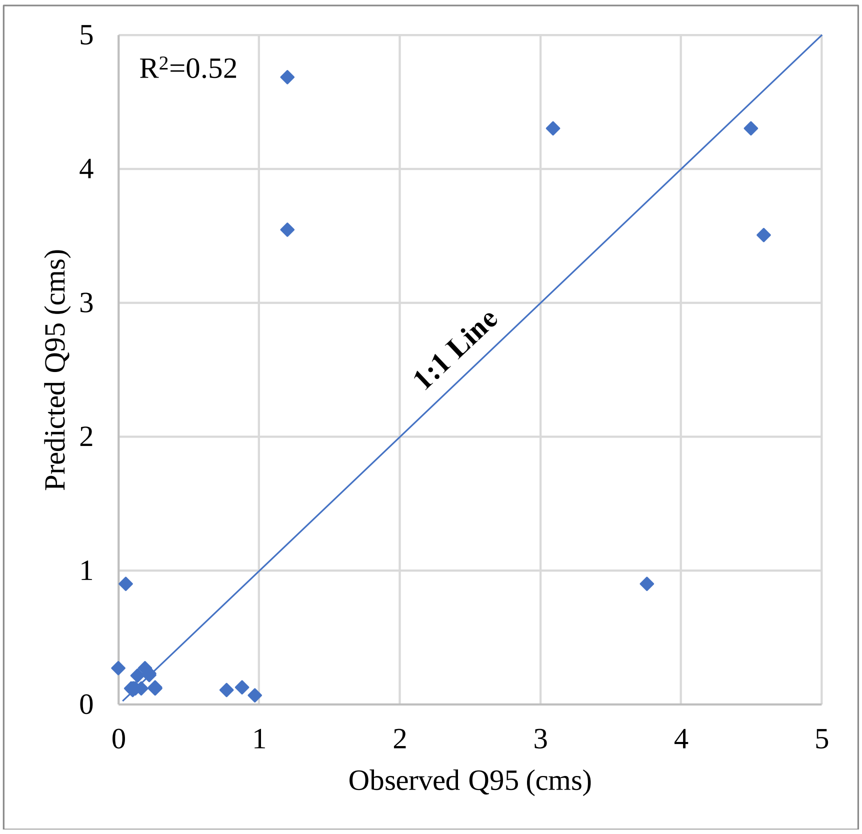

Figure 5.12 Predicted Q95 using sub-basin similarity method vs observed Q95

Figure 5.13 illustrates the scatter plot between the BFI predicted using the sub-basin similarity method and the observed BFI determined from the local minimum separation technique. The result shows that the method yields the low R^2 and NSE of 0.20, -0.28, respectively while it yields RMSE of 0.12 which is about 15% of the maximum observed BFI. Apart from the performance indices, it can be seen from *Figure 5.13* that the sub-basin similarity method also cannot well predict BFI because there are large deviations between the observed and predicted BFI for many stations.

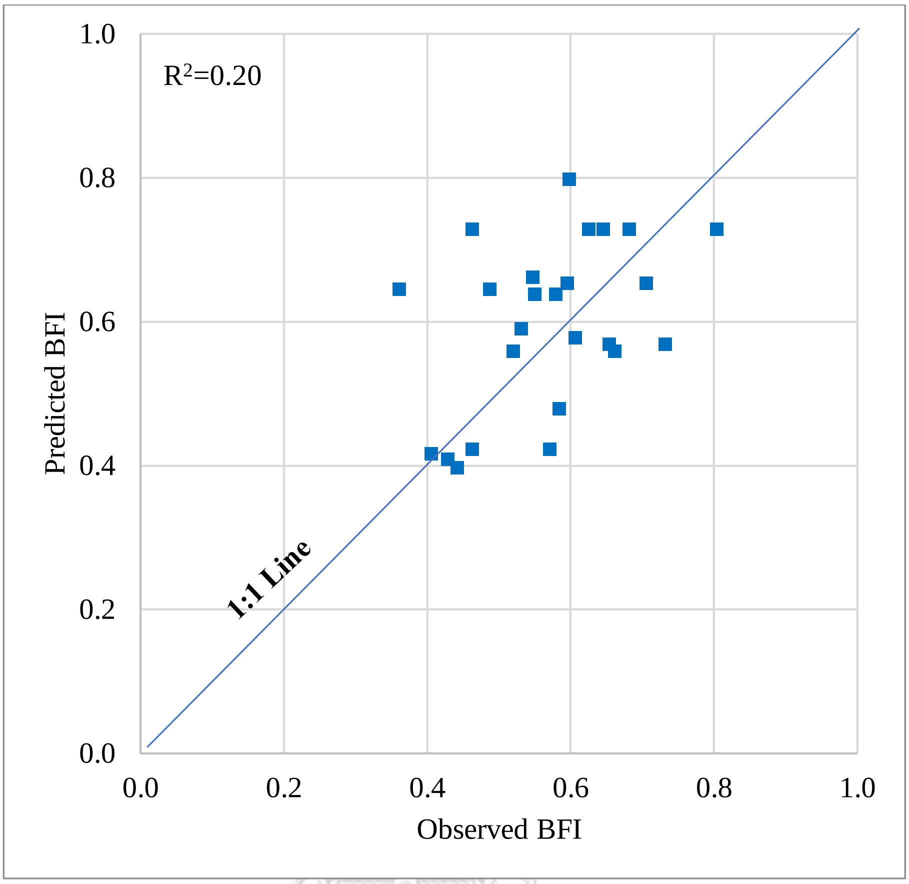

Figure 5.13 Predicted BFI using sub-basin similarity method vs observed BFI

Figure 5.14 shows the scatter plot between the 7Q10 predicted using the sub-basin similarity method and the observed 7Q10 calculated by fitting the annual minimum 7-day average flow to the Log-Pearson type III. The result shows that the method yields a high R^2, and NSE of 0.87, 0.85, respectively while it yields RMSE of 1.19 cms. However, it can be noticed that it is most likely that the prediction generally underestimates the observed 7Q10.

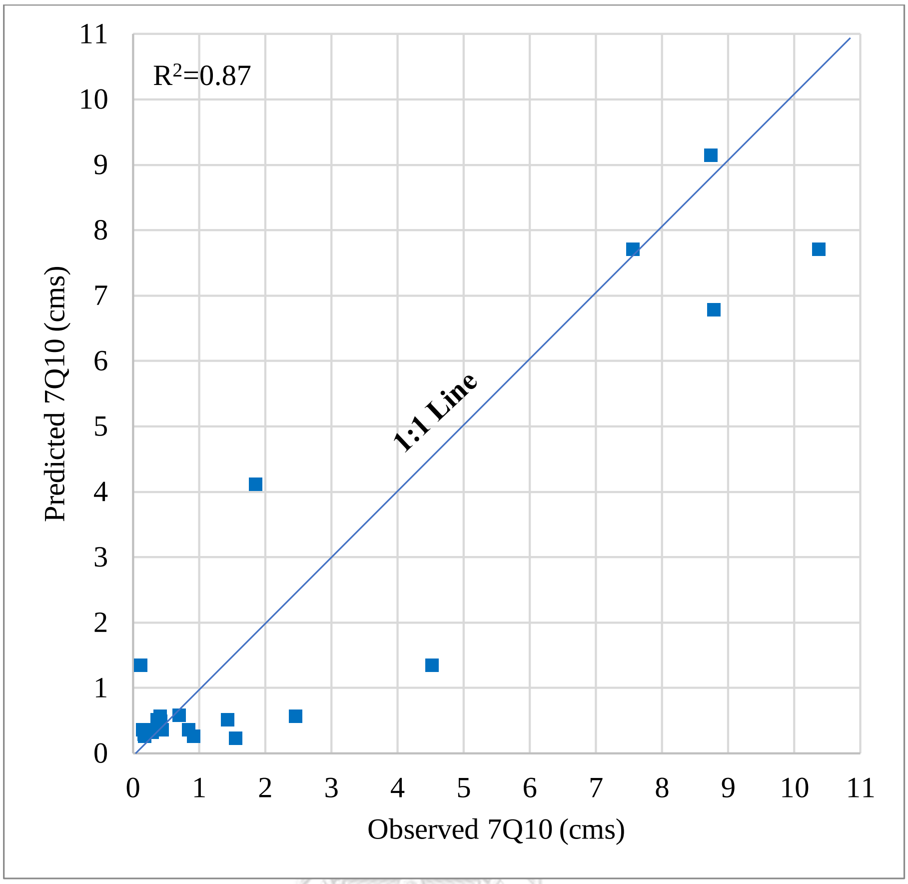

Figure 5.14 Predicted 7Q10 using sub-basin similarity method vs observed 7Q10

5.4 Regionalization of Low-flow Indices Using Climate Adjustment Method

5.4.1 Effect of the Overlap Period on the Prediction

The climate adjustment method can be applied using different overlap periods. The effects of different overlap periods with different base years are investigated in the prediction. A sample of the Q95 which is predicted from various overlap periods of 1-yr, 5-yr, 10-yr, and 15-yr with the base year of 1995 is assessed using both augmentation techniques. The predicted Q95 values obtained from using different overlap periods are plotted versus the observed Q95 estimated from the overall 20-yr period using the 1st and 2nd techniques as shown in *Figure 5.15* and *Figure 5.16*, respectively. The results indicate that the appropriate length of overlap period is necessary for the prediction to obtain a reliable result. The figure clearly shows that for the overlap period of 1-yr, the prediction using the 1st technique performs better than the 2nd technique. However, for the overlap period of 5-yr or more, the 2nd technique shows better performance overall.

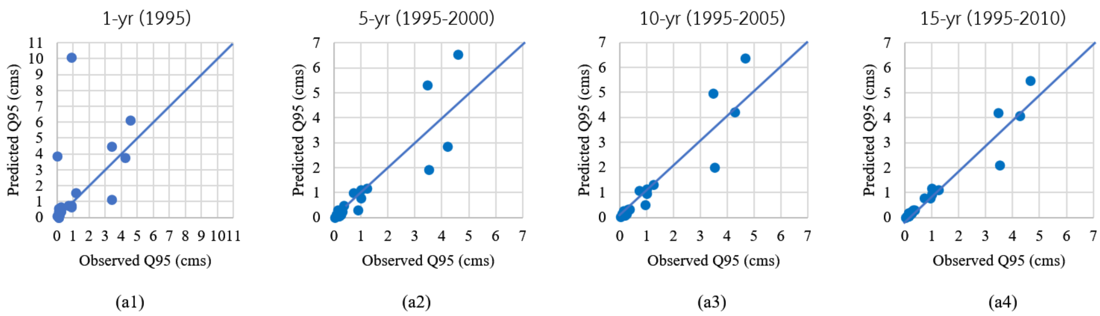

Figure 5.15 Q95 estimated from various overlap periods using 1st technique plotted versus observed Q95

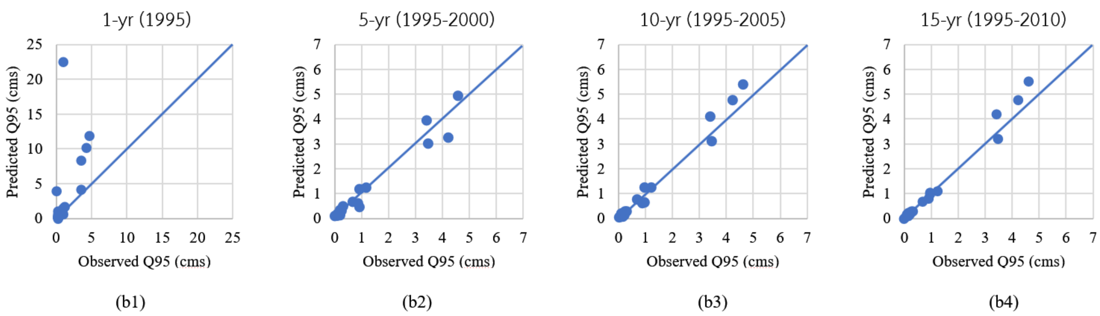

Figure 5.16 Q95 estimated from various overlap periods using 2nd technique plotted versus observed Q95

5.4.2 Calibration and Validation of Climate Adjustment Method

The calibration and validation process of the climate adjustment method is tested if the method is applicable for the study or not. The processes are investigated with three conditions which are 1) 1-yr overlap period with 1st technique; 2) 5-yr overlap period with 1st technique, and 3) 5-yr overlap period with 2nd technique.

Figure 5.17 shows the results of the calibration and validation of the climate adjustment method for Q95. It is found that the method seems to perform less reliable for the first conditions since the plot shows a noticeable deviation for validation compared to those of the calibration periods. For the second condition, the method can yield a reliable performance since there is a noticeable improvement for the validation compared to the first condition while another improvement is found when applying the third condition which the 2nd augmentation technique is used.

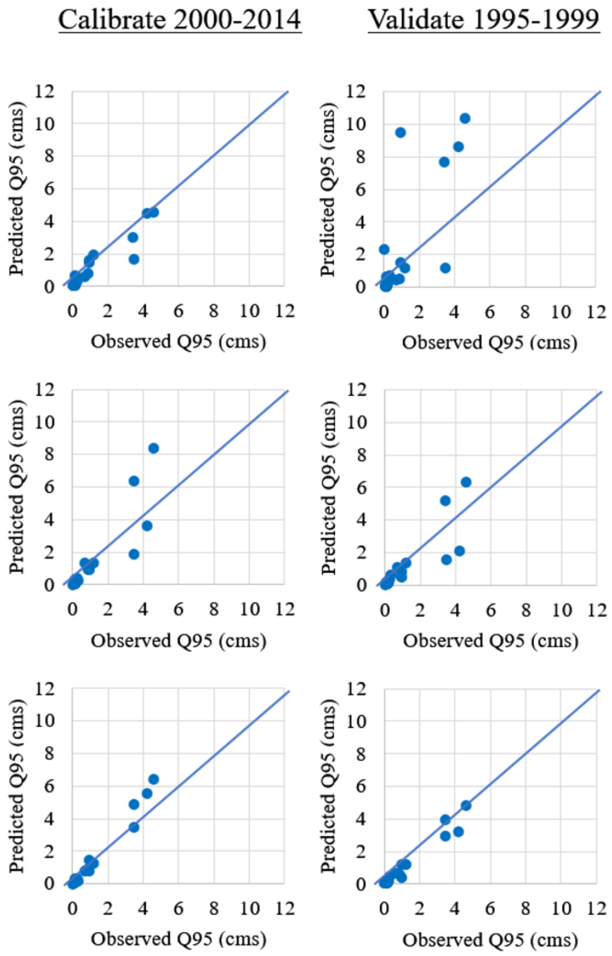

Conditions & Summary results

Overlap 1-yr + 1st Technique

Q95	Calibrate	Validate
RMSE (cms)	0.46	2.50
R^2	0.89	0.56
NSE	0.89	-2.30

Overlap 5-yr + 1st Technique

Q95	Calibrate	Validate
RMSE (cms)	1.03	0.77
R^2	0.80	0.73
NSE	0.44	0.69

Overlap 5-yr + 2nd Technique

Q95	Calibrate	Validate
RMSE (cms)	0.55	0.30
R^2	0.98	0.92
NSE	0.84	0.95

Figure 5.17 Results of calibration and validation of the CAM for Q95

Figure 5.18 demonstrates the performance of the climate adjustment method for BFI. It can be noticed that the performance for BFI is much similar to that of Q95. However, the performance for Q95 is better overall.

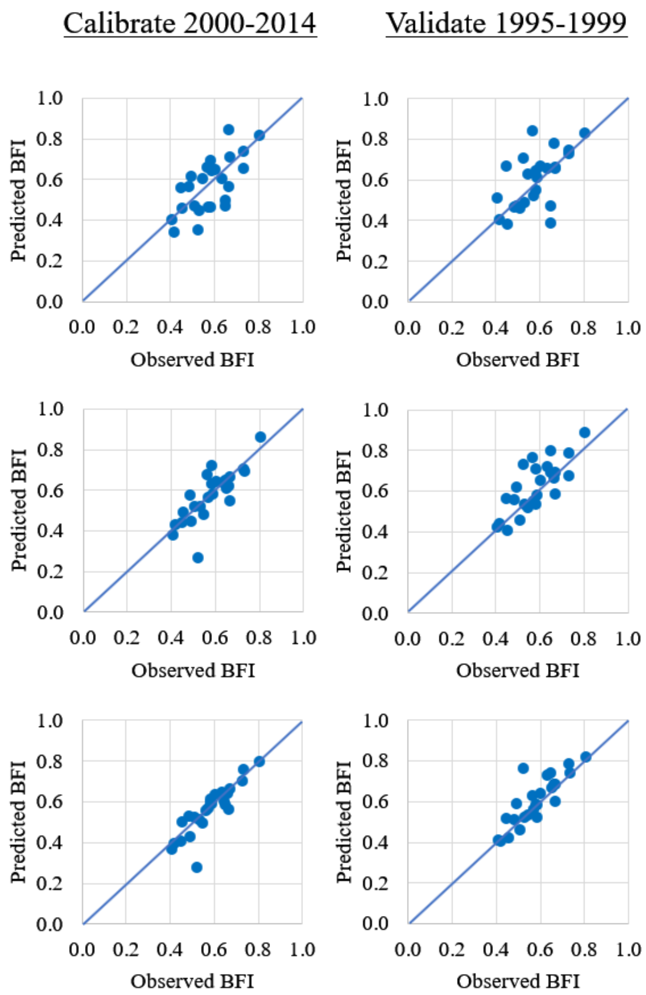

Conditions & Summary results

Overlap 1-yr + 1st Technique

BFI	Calibrate	Validate
RMSE	0.10	0.11
R^2	0.46	0.33
NSE	0.05	-0.25

Overlap 5-yr + 1st Technique

BFI	Calibrate	Validate
RMSE	0.08	0.09
R^2	0.63	0.52
NSE	0.43	0.20

Overlap 5-yr + 2nd Technique

BFI	Calibrate	Validate
RMSE	0.06	0.07
R^2	0.76	0.62
NSE	0.62	0.54

Figure 5.18 Results of calibration and validation of the CAM for BFI

Figure 5.19 shows the performance of the climate adjustment method for 7Q10. For the 7Q10, the method can only be performed for the second condition where a 5-yr overlap period with the first technique is applied since the first and the conditions required the annual 7Q10 which cannot be determined. The result indicates that the overall performance is much better compared to BFI and Q95 when applying the same condition.

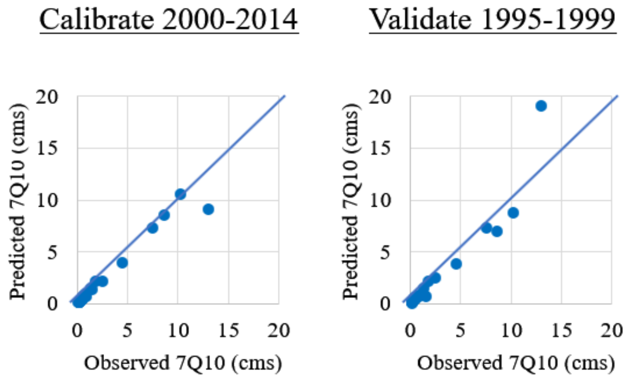

Conditions & Summary results

Overlap 5-yr + 1st Technique

7Q10	Calibrate	Validate
RMSE	0.78	1.31
R^2	0.96	0.91
NSE	0.95	0.86

Figure 5.19 Results of calibration and validation of the CAM for 7Q10

5.5 Performance Measurement

This section aims to suggest the most applicable method among the selected methods. the three statistical indicators including Nash-Sutcliffe efficiency (NSE), coefficient of determination (R^2), and root-mean-square-error (RMSE) are chosen to represent the performance of the regionalization methods.

The tables which show the observed low-flow indices value and the predicted values by all methods can be presented in *Appendix C* while the maps showing the low-flow value for the main stations along the Ping River are presented in *Appendix D*. *Figure 5.20* summarizes the performance of all methods used in this study in terms of R^2. The plot illustrates that the climate adjustment method with the third condition performs the best overall followed by the climate adjustment method with the second condition and the regression method. The climate adjustment method with the first condition is found to perform the poorest performance while the sub-basin similarity method indicates a moderate performance. As mentioned earlier, the climate adjustment method with the first and the third conditions which required the value of annual 7Q10 cannot be defined and shown in the plot.

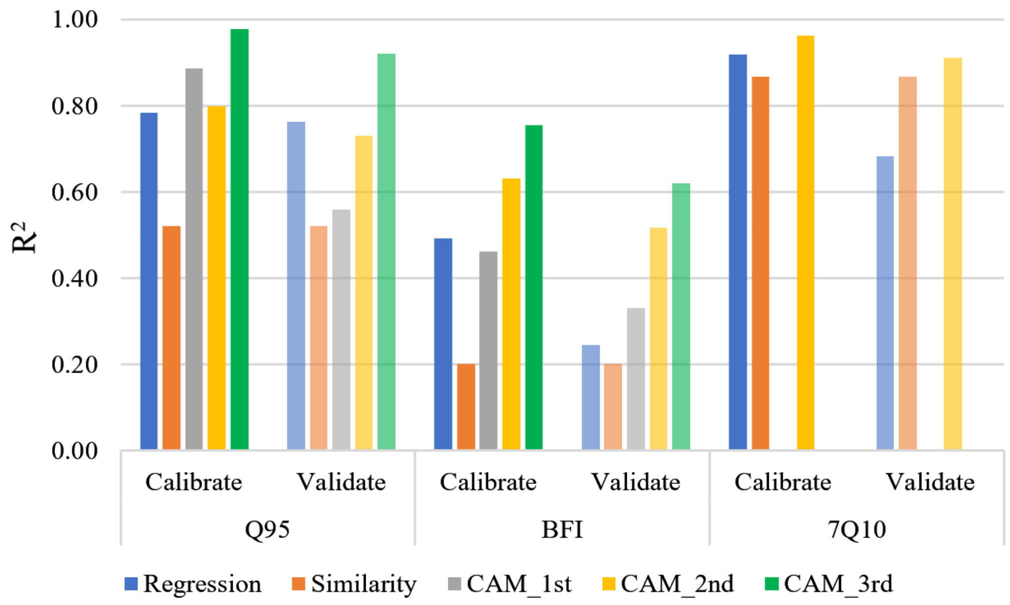

Figure 5.20 Summary of all methods' performance in terms of R^2

Figure 5.21 summarizes the performance of all methods used in terms of the normalized RMSE. The plot shows that the climate adjustment method with the third condition yields the lowest RMSE overall. The regression method seems to be the second-best method for the regionalization except for 7Q10 which method yields a high RMSE in the validation process. The climate adjustment method with the second condition and the sub-basin similarity method is found to perform a comparably moderate performance except for BFI for the sub-basin similarity method. Again, the climate adjustment method with the first condition is found to perform the poorest performance.

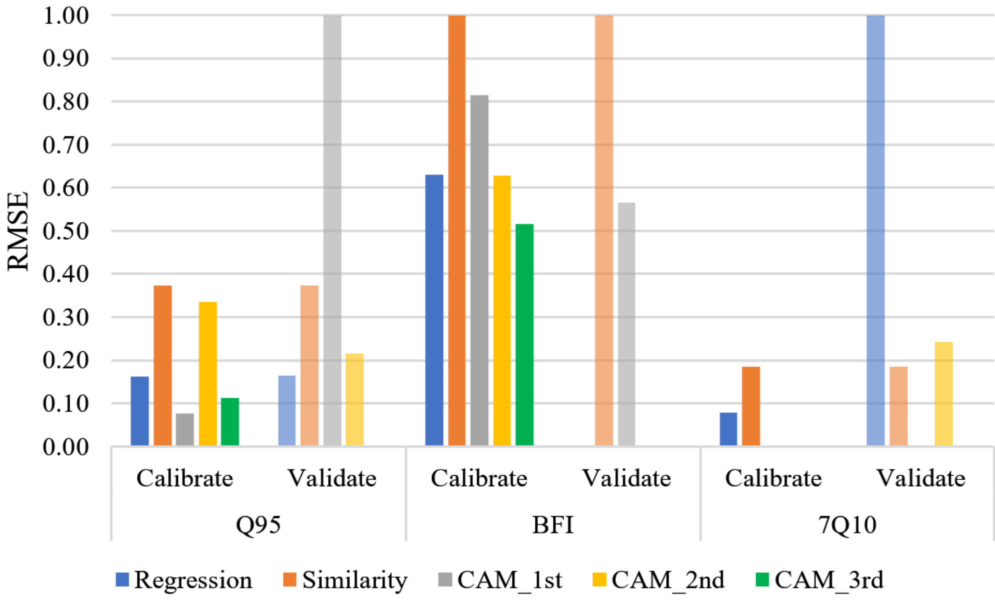

Figure 5.21 Summary of all methods' performance in terms of RMSE

Figure 5.22 summarizes the performance of all methods used in this study in terms of NSE. The plot demonstrates that the climate adjustment method with the third condition performs the best overall followed by the climate adjustment method with the second condition and the regression method. The climate adjustment method with the first condition is found to perform the poorest performance while the sub-basin similarity method indicates a moderate performance, but it seems to be failed in predicting BFI.

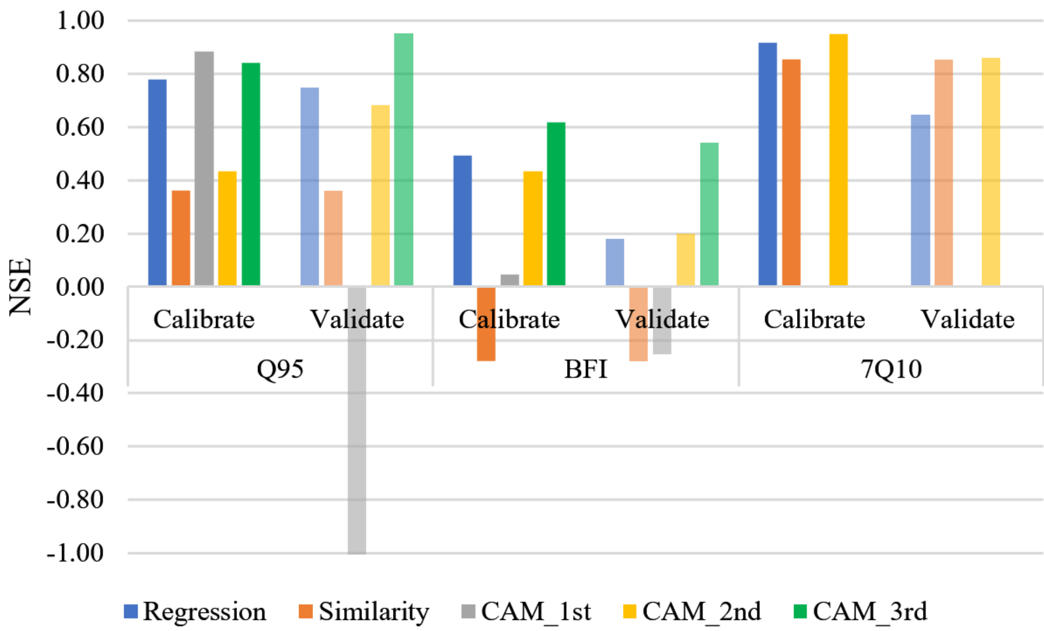

Figure 5.22 Summary of all methods' performance in terms of NSE

5.6 Proposed Procedure for Low-flow assessment in Ungauged Basin

Figure 5.23 demonstrates a proposed procedure for assessing low-flow characteristics in the ungauged basin which is applied in this study. The procedure consists of 3 steps and can be described as below:

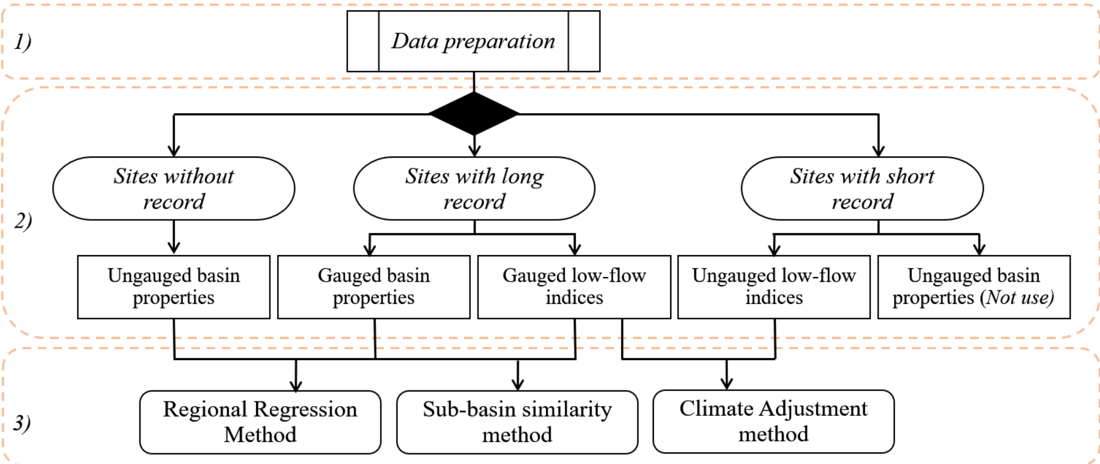

Figure 5.23 Proposed procedure for low-flow assessment in the ungauged sub-basin

1. *Data preparation*:
    a. Data collection: Collect all available and required data such as flow time series, rainfall time series, and other basin properties.
    b. Data cleaning: All data must be checked; for instance, the consistency test of rainfall, and convert to be computable data
2. *Site classification*:
    a. Gauged site (possible donor): site with longer flow record
    b. Ungauged site (subject site):
        i. site with a shorter flow record
        ii. site without flow record
3. *Regionalization*:
    a. Regional regression method:
        i. Develop regression equation for the donor site
        ii. Calculate predicted LFI by substituting the ungauged basin properties into the equation
    b. Sub-basin similarity method:
        i. Calculate the weight of each basin descriptor
        ii. Calculate inverse physical distance
        iii. Calculate physical weight
        iv. Select donor site
        v. Calculate inverse spatial distance
        vi. Calculate spatial weight
        vii. Calculate integrated weight
        viii. Calculate predicted LFI by scaling the LFI at the donor site with the integrated weight
    c. Climate adjustment method:
        i. Select donor
        ii. Calculate predicted LFI by applying record augmentation techniques. It is noted that thought the ungauged basin properties are obtainable but are not required for LFI estimation based on this method.

5.7 Conclusion

The results of the regional regression method using stepwise linear regression analysis on 25 gauged basins indicated that the Q95 and 7Q10 except BFI could be explained by the basin properties with reliable precision and they are most likely to be applicable for accounting the effect of land-use change in the Upper Ping River basin. Regarding the sub-basin similarity method, it is shown that the 7Q10 can be explained by the physical similarity and spatial proximity between a donor and a subject site with a reliable precision while the precision for Q95 and BFI are not reliable. For the climate adjustment method, it is noticed that the appropriate length of overlap period and augmentation technique with the proper donor selection technique can crucially explain the three low-flow indices (Q95, BFI, and 7Q10) with reliable precision.

CHAPTER 6
CONCLUSIONS AND RECOMMENDATIONS

6.1 Conclusions

The assessment of low-flow in ungauged basins remains a challenging issue especially for developing countries where the flow gauging network is limited. Regionalization using the regression method, similarity method, and climate adjustment methods was found to be applicable for the prediction of low-flow in the Upper Ping River basin which is the study area but with a different predictive degree. The difference is due to the methods themself and the selection of the low-flow indices. In terms of Q95, the climate adjustment method with the third condition was found to perform the best, followed by the regional regression method and the climate adjustment method with the second condition while the sub-basin similarity method shows a moderate performance. Similar to the Q95, the climate adjustment method with the third condition and the second condition still performs better than the others in predicting BFI. In terms of 7Q10, the three available methods are found to be applicable for the prediction. However, the climate adjustment method with the second condition shows the best performance compared to the sub-basin similarity and the regional regression methods. The climate adjustment method with the first condition performs the worst overall in predicting all low-flow indices. All in all, the climate adjustment method with the third condition generally outperforms the regression and sub-basin similarity methods as it yields better performance indices. The longer the overlap period used for the climate adjustment method, the better the performance. The 2nd augmentation technique of the climate adjustment method where the weighting coefficient was applied further improves the performance over its 1st technique.

6.2 Recommendations

According to what the study found for the study area of the Upper Ping River basin; it is recommended to apply the climate adjustment method with 7Q10 for assessing the low-flow characteristics when there are available flow records at least 5 years. On the other hand, applying the regional regression method with Q95 is more recommended than the sub-basin similarity method or with 7Q10 and BFI when there is no flow record available or available with a period of fewer than 5 years. Moreover, it is recommended to try other regionalization methods, especially the methods that can represent uncertainty with the hope of improving the method performance. On the other hand, more low-flow indices should be considered when applying to other study area or any specific purpose since various region or purpose seems to have various flow characteristics and requires different informative low-flow characteristic. Furthermore, applying more stations with longer records and up to date when they are available would be more beneficial to the research and the water resources management and planning.

REFERENCES

AIT-AMIR, B., POUGNET, P. & EL HAMI, A. 2020. Meta-Model Development. *Embedded Mechatronic Systems 2.* Elsevier.

ARIHOOD, L. D. & GLATFELTER, D. R. 1991. Method for estimating low-flow characteristics of ungauged streams in Indiana. United States Government Printing Office.

BAO, Z., ZHANG, J., LIU, J., FU, G., WANG, G., HE, R., YAN, X., JIN, J. & LIU, H. 2012. Comparison of regionalization approaches based on regression and similarity for predictions in ungauged catchments under multiple hydro-climatic conditions. *Journal of Hydrology,* 466, 37-46.

BENDEL, R. B. & AFIFI, A. A. 1977. Comparison of Stopping Rules in Forward "Stepwise" Regression. *Journal of the American Statistical Association,* 72, 46-53.

BERAN, M. & RODIER, J. 1985. Hydrological aspects of drought. Studies and reports in hydrology 39. *UNESCOWMO, Paris, France*.

BLÖSCHL, G. 2006. Rainfall-runoff modeling of ungauged catchments. *Encyclopedia of hydrological sciences*.

CARTHAIGH, M. 1987. *A Statistical Analysis Of River Flows - The South Western Region.pdf*.

ENGELAND, K. & HISDAL, H. 2009. A comparison of low flow estimates in ungauged catchments using regional regression and the HBV-model. *Water Resources Management,* 23, 2567-2586.

ESLAMIAN, S. 2018. *Handbook of Engineering Hydrology (Three-Volume Set),* CRC Press.

GUPTA, A. D. 2001. Challenges and opportunities for water resources management in Southeast Asia. *Hydrological sciences journal,* 46, 923-935.

GUSTARD, A., BULLOCK, A. & DIXON, J. 1992. *Low flow estimation in the United Kingdom,* Institute of Hydrology.

HAVENS, A. V. 1954. Drought and Agriculture. *Weatherwise,* 7, 51-68.

HELSEL, D. R. & HIRSCH, R. M. 1992. *Statistical methods in water resources*, Elsevier.

HYDROLOGY, I. O. 1980. *Low Flow Studies Reports,* Institute of Hydrology.

KARAMOUZ, M., SZIDAROVSZKY, F. & ZAHRAIE, B. 2003. *Water resources systems analysis,* CRC Press.

KIMHUY, S. 2018. *DROUGHT ASSESSMENT FOR THE GREATER BARIBO BASIN IN CAMBODIA.* Master, Chulalongkorn University.

KRAUSE, P., BOYLE, D. & BÄSE, F. 2005. Comparison of different efficiency criteria for hydrological model assessment.

KUNDZEWICZ, Z. W. 1997. Water resources for sustainable development. *Hydrological Sciences Journal,* 42, 467-480.

LAAHA, G. & BLÖSCHL, G. 2005. Low flow estimates from short stream flow records—a comparison of methods. *Journal of Hydrology,* 306, 264-286.

LAAHA, G. & BLÖSCHL, G. 2007. A national low flow estimation procedure for Austria. *Hydrological Sciences Journal,* 52, 625-644.

LAAHA, G., HISDAL, H., KROLL, C., VAN LANEN, H., NESTER, T., ROGGER, M., SAUQUET, E., TALLAKSEN, L., WOODS, R. & YOUNG, A. 2013.

Prediction of low flows in ungauged basins. *Run-off Prediction in Ungauged Basins, Synthesis across Processes, Places and Scales.* Cambridge University Press.

LAN, Y. & GUO, S. Multiple stepwise regression analysis on knowledge evaluation. 2008 International Conference on Management of e-Commerce and e-Government, 2008. IEEE, 297-302.

LDD. 2014. *Classification and kind of soil in Thailand* [Online]. Land Development Department. Available: http://www.ldd.go.th/ldd_en/en-US/classification-and-kinds-of-soil/ [Accessed].

LI, M., SHAO, Q., ZHANG, L. & CHIEW, F. H. 2010. A new regionalization approach and its application to predict flow duration curve in ungauged basins. *Journal of Hydrology,* 389**,** 137-145.

MORIASI, D. N., ARNOLD, J. G., VAN LIEW, M. W., BINGNER, R. L., HARMEL, R. D. & VEITH, T. L. 2007. Model evaluation guidelines for systematic quantification of accuracy in watershed simulations. *Transactions of the ASABE,* 50**,** 885-900.

NATHAN, R. J. & MCMAHON, T. A. 1992. Estimating low flow characteristics in ungauged catchments. *Water Resources Management,* 6**,** 85-100.

NEILL, S. P. & HASHEMI, M. R. 2018. *Fundamentals of ocean renewable energy: generating electricity from the sea*, Academic Press.

OUARDA, T. B., CHARRON, C. & ST-HILAIRE, A. 2008. Statistical models and the estimation of low flows. *Canadian Water Resources Journal,* 33**,** 195-206.

OUDIN, L., ANDRÉASSIAN, V., PERRIN, C., MICHEL, C. & LE MOINE, N. 2008. Spatial proximity, physical similarity, regression and ungaged catchments: A comparison of regionalization approaches based on 913 French catchments. *Water Resources Research,* 44.

PEREIRA, L. S., CORDERY, I. & IACOVIDES, I. 2009. *Coping with water scarcity: Addressing the challenges*, Springer Science & Business Media.

POST, D., JONES, J. & GRANT, G. 1998. An improved methodology for predicting the daily hydrologic response of ungauged catchments. *Environmental modelling & software,* 13**,** 395-403.

PRATOOMCHAI, W., KAZAMA, S., EKKAWATPANIT, C. & KOMORI, D. 2015. Opportunities and constraints in adapting to flood and drought conditions in the Upper Chao Phraya River basin in Thailand. *International Journal of River Basin Management,* 13**,** 413-427.

PYRCE, R. 2004. Hydrological low flow indices and their uses. *Watershed Science Centre,(WSC) Report*.

RAZAVI, T. & COULIBALY, P. 2013. Streamflow prediction in ungauged basins: review of regionalization methods. *Journal of hydrologic engineering,* 18**,** 958-975.

REDA, A. G., TRIPATHI, N. K., SONI, P. & TIPDECHO, T. 2015. Rain fed rice agriculture under climate variability in Southeast Asia: The case of Thailand. *Journal of Earth Science & Climatic Change,* 6**,** 1.

RIGGS, H. C. 1985. *Streamflow characteristics*, Elsevier.

ROBSON, A. & REED, D. 1999. *Flood estimation handbook: Statistical procedures for flood frequency estimation*, Institute of Hydrology Wallingford, UK.

SAMUEL, J., COULIBALY, P. & METCALFE, R. A. 2011. Estimation of continuous

streamflow in Ontario ungauged basins: comparison of regionalization methods. *Journal of Hydrologic Engineering,* 16**,** 447-459.
SEARCY, J. K. 1959. Manual of hydrology; part 2, Low-flow techniques. *US Geological Survey Water-Supply Paper*.
SHARMA, D. & BABEL, M. S. 2014. Trends in extreme rainfall and temperature indices in the western Thailand. *International Journal of Climatology,* 34**,** 2393-2407.
SHARMA, D., GUPTA, A. D. & BABEL, M. 2007. Spatial disaggregation of bias-corrected GCM precipitation for improved hydrologic simulation: Ping River Basin, Thailand. *Hydrology and Earth System Sciences Discussions,* 11**,** 1373-1390.
SIVAPALAN, M., TAKEUCHI, K., FRANKS, S., GUPTA, V., KARAMBIRI, H., LAKSHMI, V., LIANG, X., MCDONNELL, J., MENDIONDO, E. & O'CONNELL, P. 2003. IAHS Decade on Predictions in Ungauged Basins (PUB), 2003–2012: Shaping an exciting future for the hydrological sciences. *Hydrological sciences journal,* 48**,** 857-880.
SLOTO, R. A. & CROUSE, M. Y. 1996. HYSEP: A computer program for streamflow hydrograph separation and analysis. *Water-resources investigations report,* 96**,** 4040.
SMAKHTIN, V. U. 2001. Low flow hydrology: a review. *Journal of hydrology,* 240**,** 147-186.
TALLAKSEN, L. M. & VAN LANEN, H. A. 2004. *Hydrological drought: processes and estimation methods for streamflow and groundwater*, Elsevier.
TASKER, G. D. 1987. A COMPARISON OF METHODS FOR ESTIMATING LOW FLOW CHARACTERISTICS OF STREAMS 1. *JAWRA Journal of the American Water Resources Association,* 23**,** 1077-1083.
VATCHARASINTHU, C. & BABEL, M. Hydropower potential and water diversion from the Salween Basin. Workshop on Transboundary Waters: The Salween Basin. Organised by AIT Regional Environmental Management Centre, Oregon State University, University of Victoria, Chiang Mai, 1999. 13-16.
VOGEL, R. M. & KROLL, C. N. 1991. The value of streamflow record augmentation procedures in low-flow and flood-flow frequency analysis. *Journal of hydrology,* 125**,** 259-276.
WHITE, K. E. & SLOTO, R. A. 1990. *Base-flow frequency characteristics of selected Pennsylvania Streams*, US Department of the Interior, US Geological Survey.
WMO 1974. International glossary of hydrology. Geneva: WMO.
WMO 2008. *Manual on Low-flow Estimation and Prediction*, World Meteorological Organization.
WU, Y.-C., LIOU, J.-J., SU, Y.-F. & CHENG, K.-S. 2012. Establishing acceptance regions for L-moments based goodness-of-fit tests for the Pearson type III distribution. *Stochastic Environmental Research and Risk Assessment,* 26**,** 873-885.
YEVJEVICH, V. M. 1967. Objective approach to definitions and investigations of continental hydrologic droughts, An. *Hydrology papers (Colorado State University); no. 23*.
ZALANTS, M. G. 1991. *Low-flow frequency and flow duration of selected south Carolina streams through 1987*, US Department of the Interior, US Geological

Survey.
ZELENHASIĆ, E. & SALVAI, A. 1987. A method of streamflow drought analysis. *Water resources research*, 23**,** 156-168.
ZHANG, Y., AHIABLAME, L., ENGEL, B. & LIU, J. 2013. Regression modeling of baseflow and baseflow index for Michigan USA. *Water,* 5**,** 1797-1815.
ZHANG, Y. & CHIEW, F. H. 2009. Relative merits of different methods for runoff predictions in ungauged catchments. *Water Resources Research,* 45.

APPENDICES

Appendix A L-moment ratio diagram for the goodness of fit tests of each station

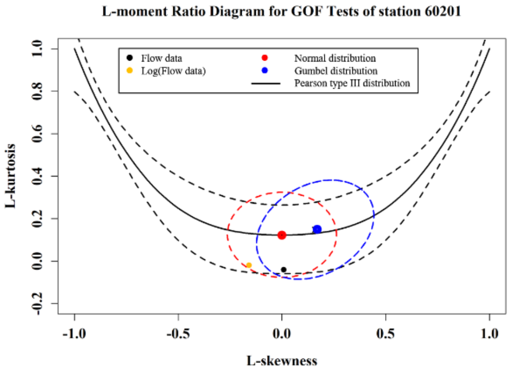

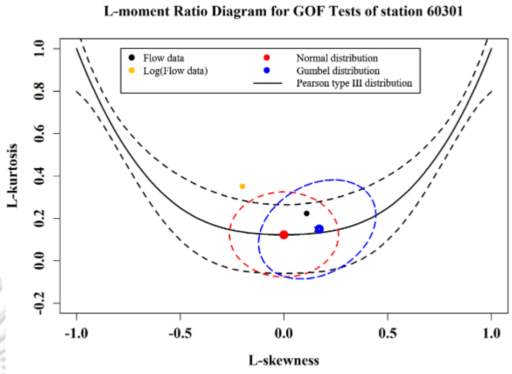

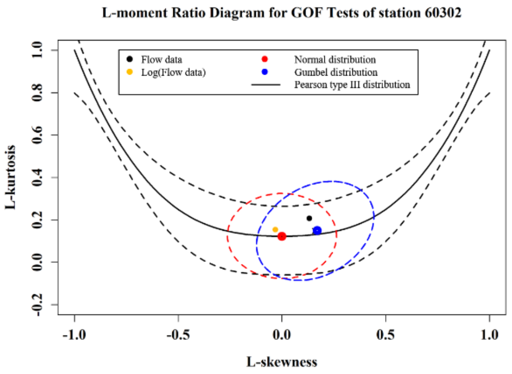

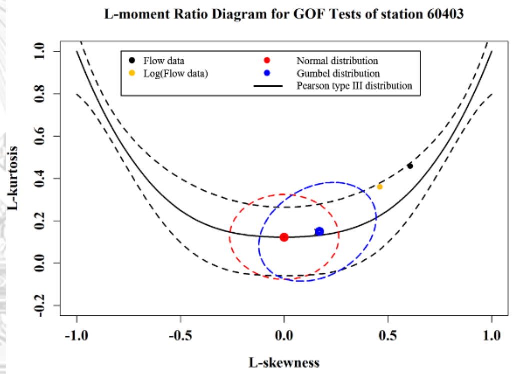

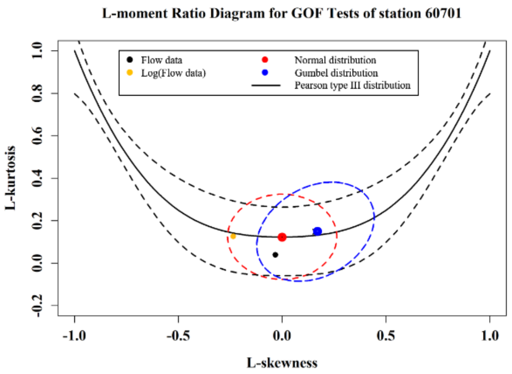

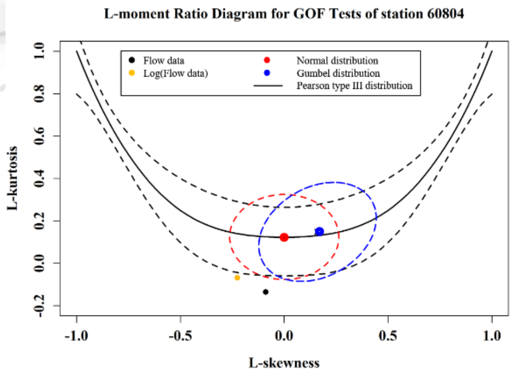

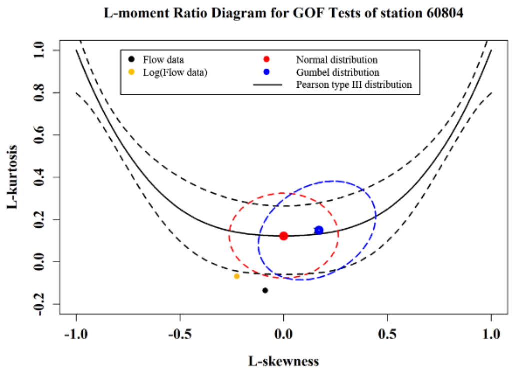
L-moment Ratio Diagram for GOF Tests of station 60804
Flow data
Log(Flow data)
Normal distribution
Gumbel distribution
Pearson type III distribution
L-kurtosis
L-skewness

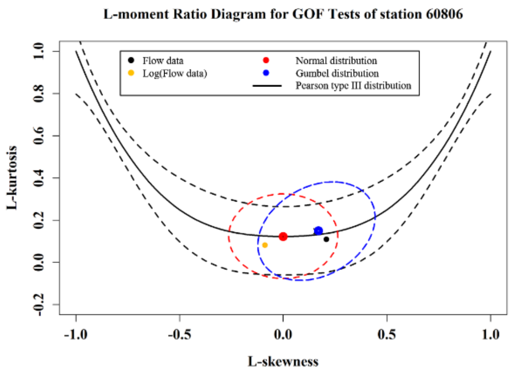
L-moment Ratio Diagram for GOF Tests of station 60806
Flow data
Log(Flow data)
Normal distribution
Gumbel distribution
Pearson type III distribution
L-kurtosis
L-skewness

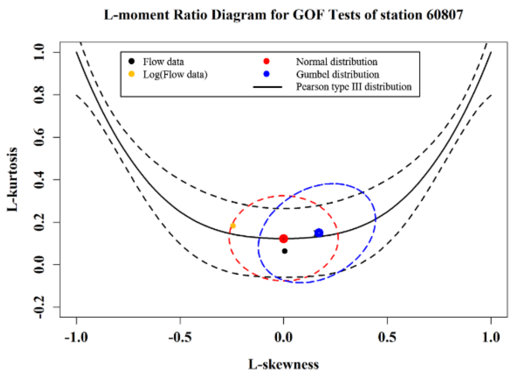
L-moment Ratio Diagram for GOF Tests of station 60807
Flow data
Log(Flow data)
Normal distribution
Gumbel distribution
Pearson type III distribution
L-kurtosis
L-skewness

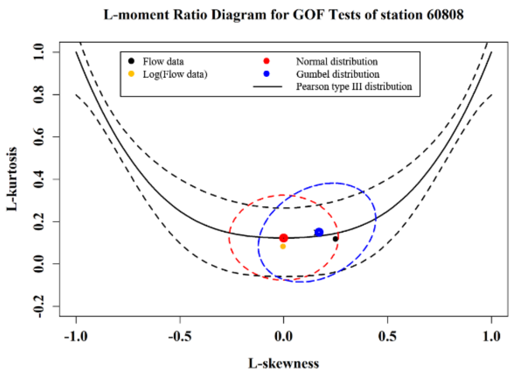
L-moment Ratio Diagram for GOF Tests of station 60808
Flow data
Log(Flow data)
Normal distribution
Gumbel distribution
Pearson type III distribution
L-kurtosis
L-skewness

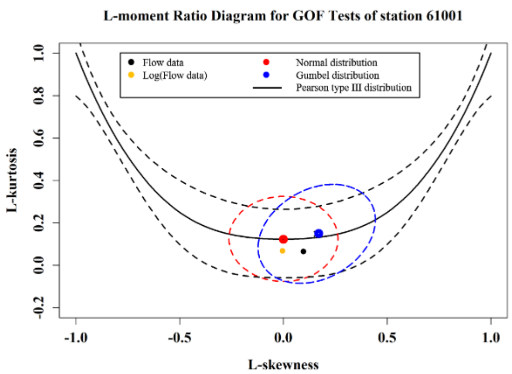
L-moment Ratio Diagram for GOF Tests of station 61001
Flow data
Log(Flow data)
Normal distribution
Gumbel distribution
Pearson type III distribution
L-kurtosis
L-skewness

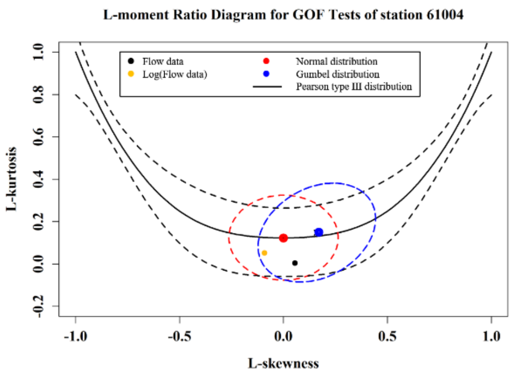
L-moment Ratio Diagram for GOF Tests of station 61004
Flow data
Log(Flow data)
Normal distribution
Gumbel distribution
Pearson type III distribution
L-kurtosis
L-skewness

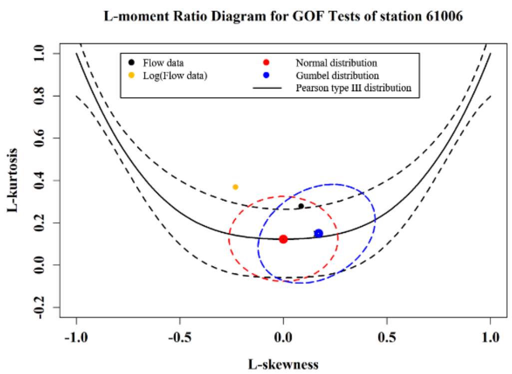
L-moment Ratio Diagram for GOF Tests of station 61006
Flow data
Log(Flow data)
Normal distribution
Gumbel distribution
Pearson type III distribution
L-kurtosis
L-skewness

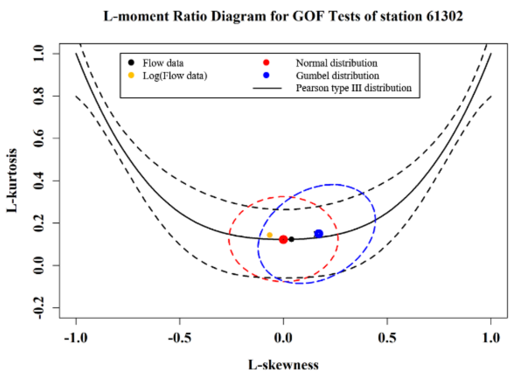
L-moment Ratio Diagram for GOF Tests of station 61302
Flow data
Log(Flow data)
Normal distribution
Gumbel distribution
Pearson type III distribution
L-kurtosis
L-skewness

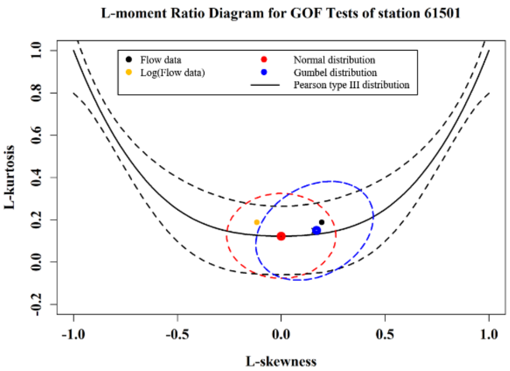
L-moment Ratio Diagram for GOF Tests of station 61501
Flow data
Log(Flow data)
Normal distribution
Gumbel distribution
Pearson type III distribution
L-kurtosis
L-skewness

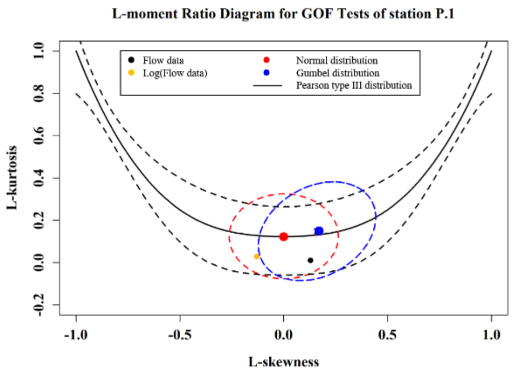
L-moment Ratio Diagram for GOF Tests of station P.1
Flow data
Log(Flow data)
Normal distribution
Gumbel distribution
Pearson type III distribution
L-kurtosis
L-skewness

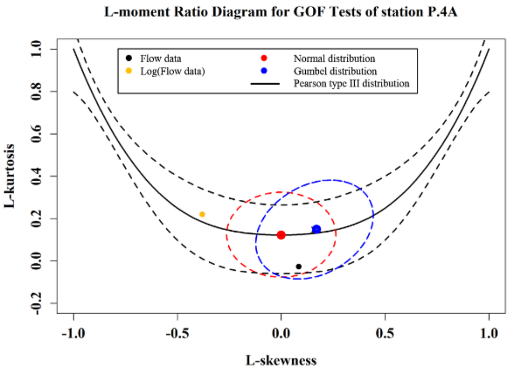
L-moment Ratio Diagram for GOF Tests of station P.4A
Flow data
Log(Flow data)
Normal distribution
Gumbel distribution
Pearson type III distribution
L-kurtosis
L-skewness

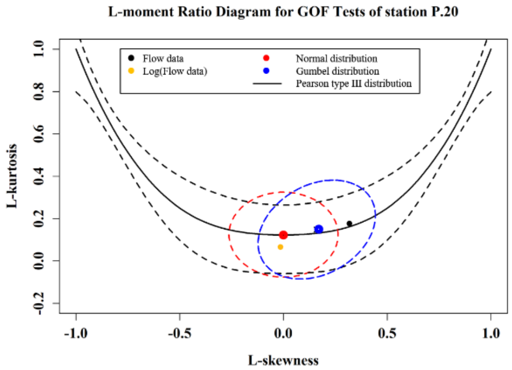
L-moment Ratio Diagram for GOF Tests of station P.20
Flow data
Log(Flow data)
Normal distribution
Gumbel distribution
Pearson type III distribution
L-kurtosis
L-skewness

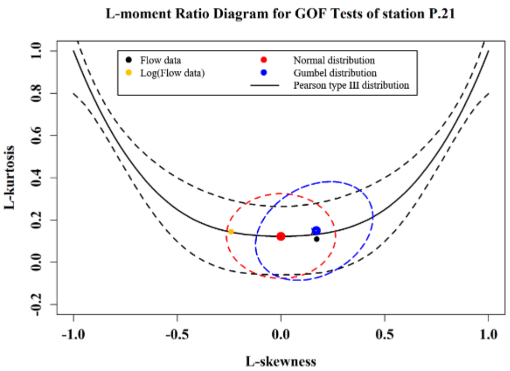
L-moment Ratio Diagram for GOF Tests of station P.21
Flow data
Log(Flow data)
Normal distribution
Gumbel distribution
Pearson type III distribution
L-kurtosis
L-skewness

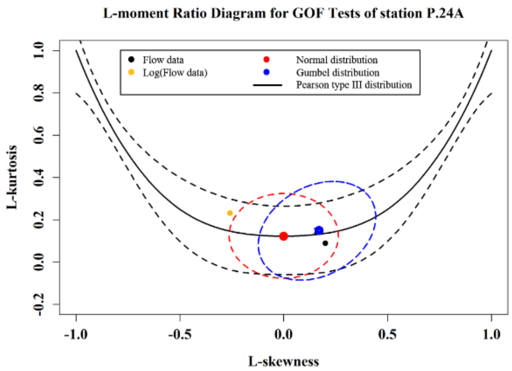
L-moment Ratio Diagram for GOF Tests of station P.24A
Flow data
Log(Flow data)
Normal distribution
Gumbel distribution
Pearson type III distribution
L-kurtosis
L-skewness

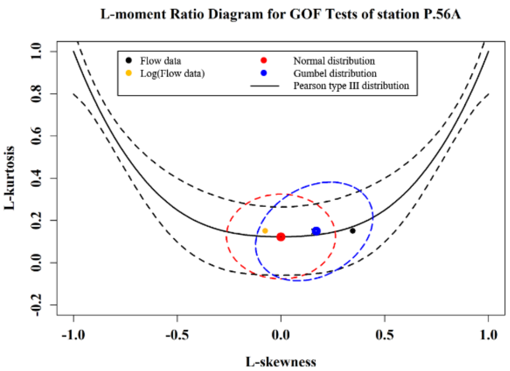
L-moment Ratio Diagram for GOF Tests of station P.56A
Flow data
Log(Flow data)
Normal distribution
Gumbel distribution
Pearson type III distribution
L-kurtosis
L-skewness

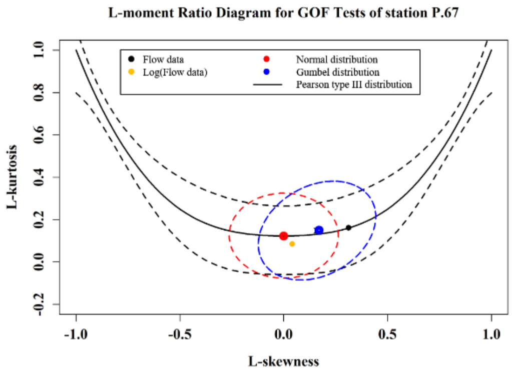
L-moment Ratio Diagram for GOF Tests of station P.67
Flow data
Log(Flow data)
Normal distribution
Gumbel distribution
Pearson type III distribution
L-kurtosis
L-skewness

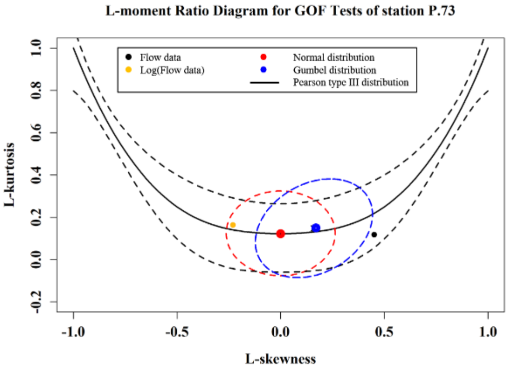
L-moment Ratio Diagram for GOF Tests of station P.73
Flow data
Log(Flow data)
Normal distribution
Gumbel distribution
Pearson type III distribution
L-kurtosis
L-skewness
-1.0
-0.5
0.0
0.5
1.0
-0.2
0.0
0.2
0.4
0.6
0.8
1.0

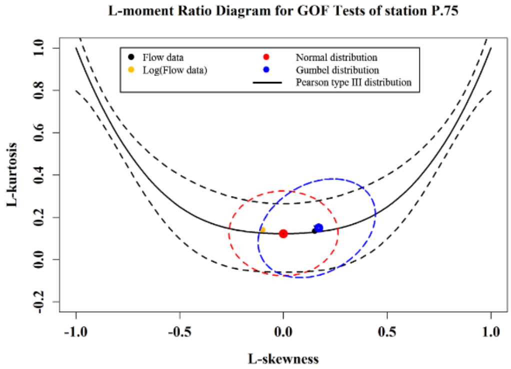
L-moment Ratio Diagram for GOF Tests of station P.75
Flow data
Log(Flow data)
Normal distribution
Gumbel distribution
Pearson type III distribution
L-kurtosis
L-skewness
-1.0
-0.5
0.0
0.5
1.0
-0.2
0.0
0.2
0.4
0.6
0.8
1.0

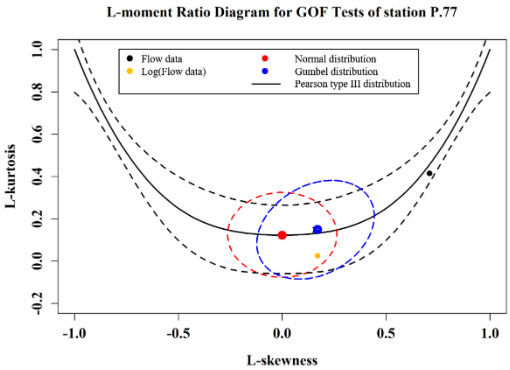
L-moment Ratio Diagram for GOF Tests of station P.77
Flow data
Log(Flow data)
Normal distribution
Gumbel distribution
Pearson type III distribution
L-kurtosis
L-skewness
-1.0
-0.5
0.0
0.5
1.0
-0.2
0.0
0.2
0.4
0.6
0.8
1.0

Appendix B Results of identifying the suitable number of the donor (from 1 to 5 donors)

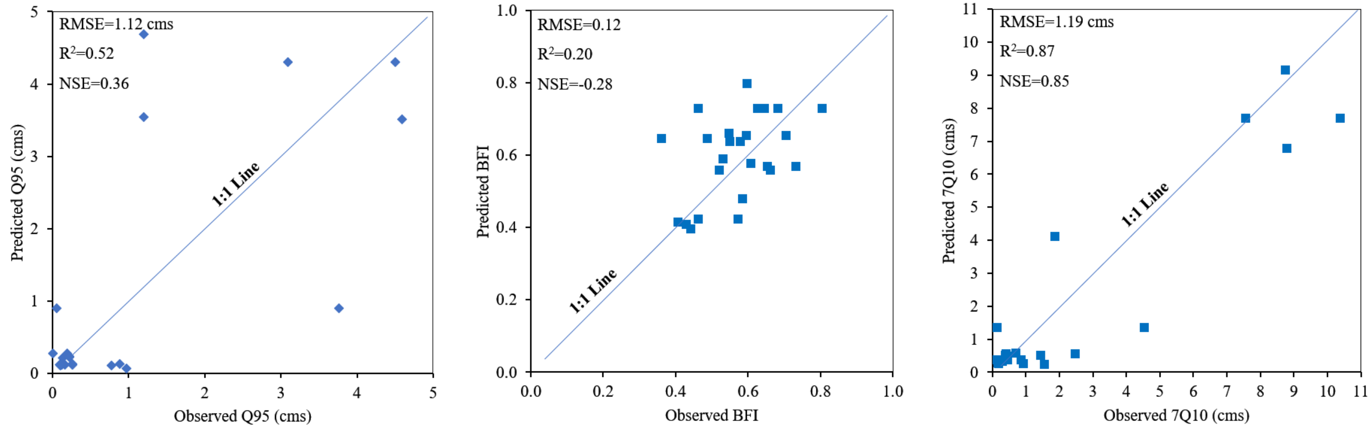

(a)

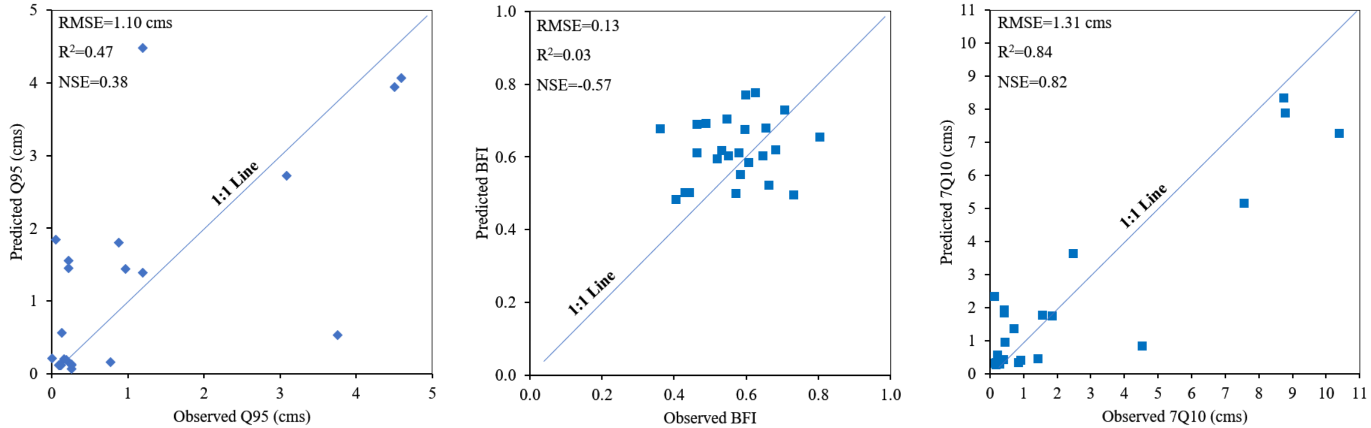

(b)

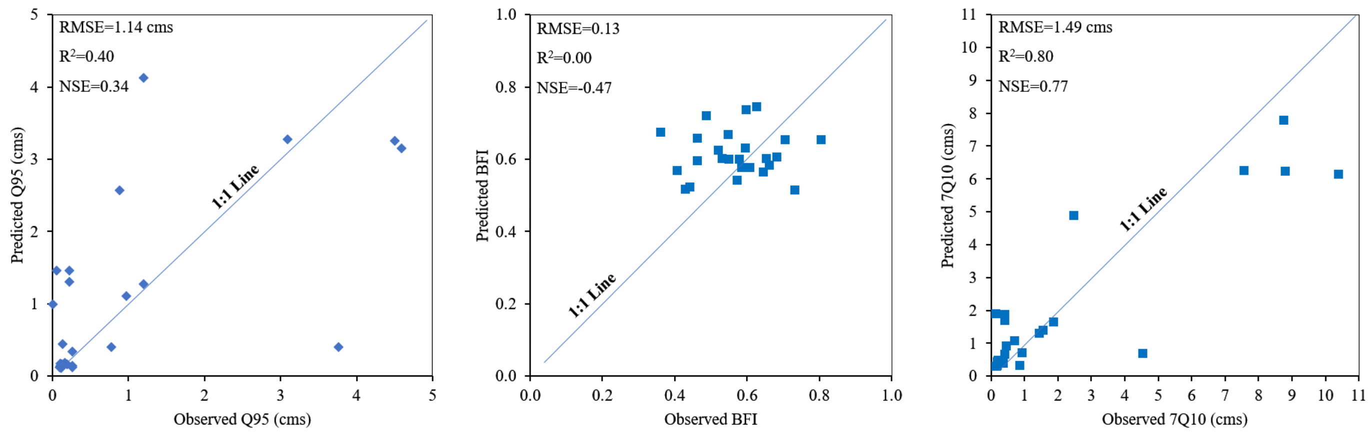

RMSE=1.14 cms
R²=0.40
NSE=0.34
1:1 Line
Predicted Q95 (cms)
Observed Q95 (cms)
RMSE=0.13
R²=0.00
NSE=-0.47
1:1 Line
Predicted BFI
Observed BFI
RMSE=1.49 cms
R²=0.80
NSE=0.77
1:1 Line
Predicted 7Q10 (cms)
Observed 7Q10 (cms)

(c)

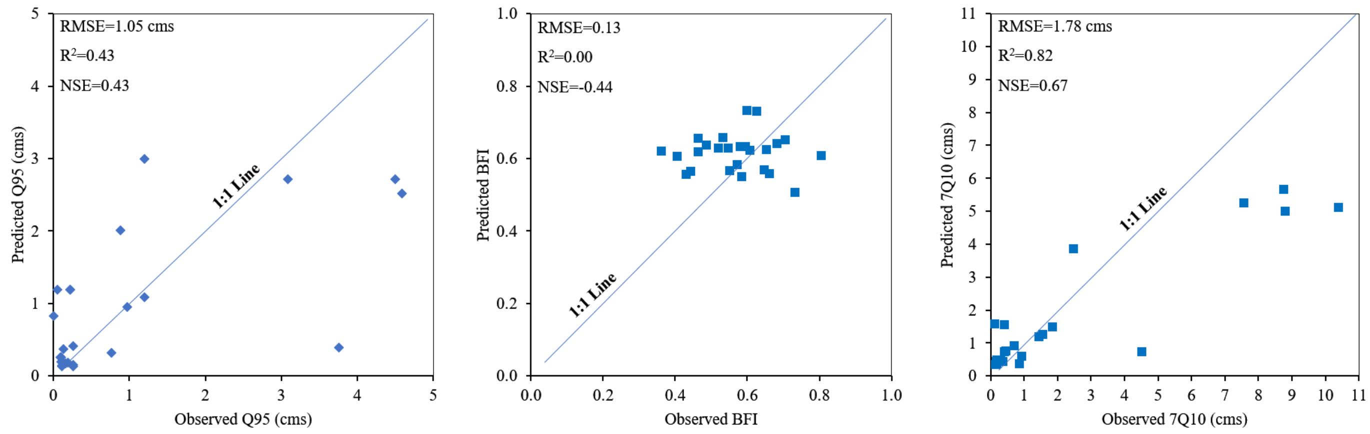

RMSE=1.05 cms
R²=0.43
NSE=0.43
1:1 Line
Predicted Q95 (cms)
Observed Q95 (cms)
RMSE=0.13
R²=0.00
NSE=-0.44
1:1 Line
Predicted BFI
Observed BFI
RMSE=1.78 cms
R²=0.82
NSE=0.67
1:1 Line
Predicted 7Q10 (cms)
Observed 7Q10 (cms)

(d)

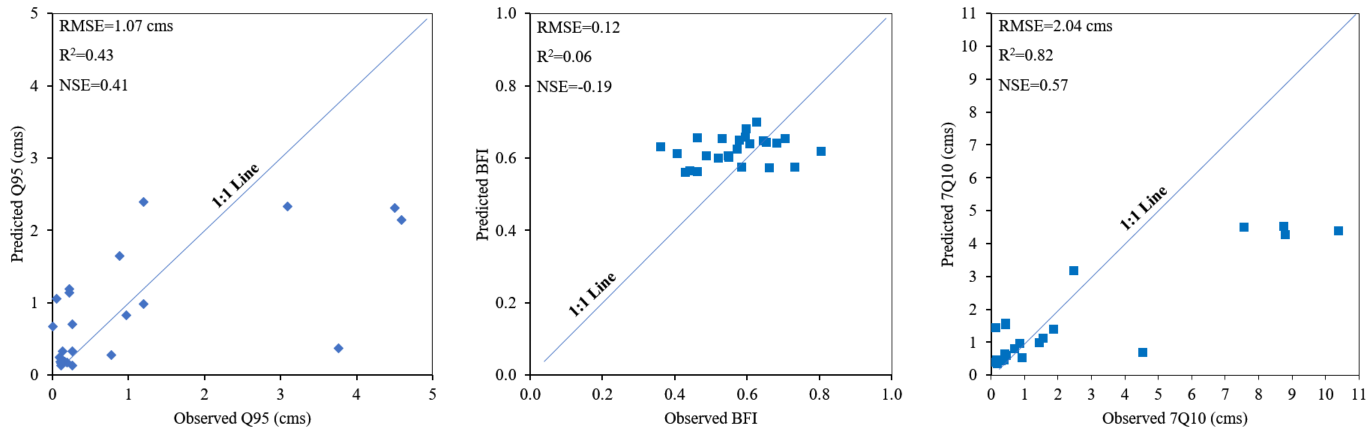
RMSE=1.07 cms
R²=0.43
NSE=0.41
1:1 Line
Predicted Q95 (cms)
Observed Q95 (cms)
RMSE=0.12
R²=0.06
NSE=-0.19
1:1 Line
Predicted BFI
Observed BFI
RMSE=2.04 cms
R²=0.82
NSE=0.57
1:1 Line
Predicted 7Q10 (cms)
Observed 7Q10 (cms)

(E)

Appendix C Results of observed and predicted low-flow indices by all methods

No.	Station	Q95 (cms)					
		Observed	Regression	Similarity	CAM_1st	CAM_2nd	CAM_3rd
1	P.1	4.60	0.00	0.12	10.40	6.33	4.84
2	P.4A	0.12	0.82	0.12	0.66	0.11	0.10
3	P.20	0.96	0.15	0.12	1.53	0.80	1.23
4	P.21	0.15	0.77	0.13	0.15	0.09	0.08
5	P.24A	0.21	0.80	0.12	0.14	0.13	0.12
6	P.56A	0.31	4.14	3.51	0.72	0.59	0.49
7	P.67	3.44	0.49	0.12	7.70	5.17	3.95
8	P.73	0.96	1.12	0.22	9.51	0.48	0.40
9	P.75	4.23	2.79	4.31	8.60	2.09	3.21
10	P.77	0.01	0.04	0.27	2.31	0.04	0.04
11	60201	0.11	0.82	0.12	0.19	0.06	0.08
12	60301	0.26	4.69	4.31	0.37	0.32	0.26
13	60302	0.11	0.62	0.90	0.06	0.15	0.11
14	60403	0.11	0.71	0.07	0.03	0.05	0.10
15	60701	0.12	0.70	0.23	0.06	0.21	0.14
16	60804	0.06	0.40	0.22	0.06	0.11	0.11
17	60806	0.21	0.00	0.11	0.16	0.23	0.21
18	60807	0.88	0.25	0.13	0.53	0.58	0.58
19	60808	0.22	0.82	0.11	0.21	0.31	0.28
20	61001	0.70	0.00	0.27	0.40	1.11	0.63
21	61004	0.11	1.54	4.69	0.10	0.14	0.12
22	61006	0.10	0.22	0.12	0.07	0.10	0.10
23	61301	0.11	1.25	0.90	0.29	0.18	0.17
24	61302	3.48	0.39	0.12	1.19	1.58	2.91
25	61501	1.20	1.17	3.55	1.19	1.33	1.22

No.	Station	BFI					
		Observed	Regression	Similarity	CAM_1st	CAM_2nd	CAM_3rd
1	P.1	0.58	0.62	0.73	0.64	0.71	0.59
2	P.4A	0.41	0.66	0.73	0.51	0.42	0.41
3	P.20	0.57	0.51	0.73	0.52	0.55	0.56
4	P.21	0.48	0.56	0.42	0.47	0.56	0.51
5	P.24A	0.45	0.62	0.73	0.38	0.41	0.42
6	P.56A	0.49	0.52	0.58	0.47	0.62	0.59
7	P.67	0.56	0.67	0.73	0.84	0.76	0.63
8	P.73	0.53	0.56	0.42	0.49	0.54	0.52
9	P.75	0.63	0.53	0.64	0.66	0.72	0.73
10	P.77	0.52	0.46	0.65	0.71	0.73	0.76
11	60201	0.67	0.69	0.65	0.66	0.59	0.60
12	60301	0.65	0.51	0.64	0.48	0.69	0.67
13	60302	0.65	0.54	0.56	0.39	0.80	0.74
14	60403	0.81	0.53	0.48	0.83	0.89	0.82
15	60701	0.60	0.56	0.40	0.67	0.65	0.64
16	60804	0.51	0.51	0.41	0.46	0.46	0.46
17	60806	0.45	0.65	0.57	0.67	0.56	0.52
18	60807	0.59	0.49	0.42	0.61	0.58	0.59
19	60808	0.42	0.71	0.57	0.40	0.44	0.40
20	61001	0.73	0.49	0.65	0.75	0.67	0.74
21	61004	0.66	0.44	0.59	0.78	0.67	0.69
22	61006	0.58	0.64	0.80	0.55	0.54	0.52
23	61301	0.73	0.60	0.56	0.73	0.79	0.79
24	61302	0.67	0.63	0.65	0.66	0.69	0.69
25	61501	0.54	0.53	0.66	0.63	0.52	0.53

No.	Station	7Q10 (cms)					
		Observed	Regression	Similarity	CAM_1st	CAM_2nd	CAM_3rd
1	P.1	10.21	0.00	0.36	-	8.81	-
2	P.4A	0.50	0.03	0.36	-	0.52	-
3	P.20	2.49	2.44	0.36	-	2.52	-
4	P.21	0.41	1.15	0.56	-	0.44	-
5	P.24A	0.52	1.29	0.36	-	0.66	-
6	P.56A	0.83	8.72	6.78	-	0.89	-
7	P.67	7.53	0.00	0.36	-	7.36	-
8	P.73	12.98	2.54	0.58	-	19.05	-
9	P.75	8.58	6.10	7.71	-	6.98	-
10	P.77	1.53	0.14	0.51	-	0.74	-
11	60201	0.23	1.43	0.32	-	0.23	-
12	60301	0.45	10.74	7.71	-	0.57	-
13	60302	0.15	1.57	1.35	-	0.13	-
14	60403	0.19	1.69	0.23	-	0.21	-
15	60701	0.18	0.86	0.49	-	0.16	-
16	60804	0.12	0.90	0.50	-	0.11	-
17	60806	0.43	0.74	0.26	-	0.45	-
18	60807	1.39	1.46	0.56	-	1.53	-
19	60808	0.42	0.23	0.26	-	0.41	-
20	61001	0.93	0.87	0.51	-	0.71	-
21	61004	0.18	8.18	9.15	-	0.21	-
22	61006	0.16	0.00	0.29	-	0.19	-
23	61301	0.27	2.31	1.35	-	0.37	-
24	61302	4.51	0.00	0.32	-	3.81	-
25	61501	1.82	1.18	4.11	-	2.14	-

Appendix D Low-flow values along the Ping River

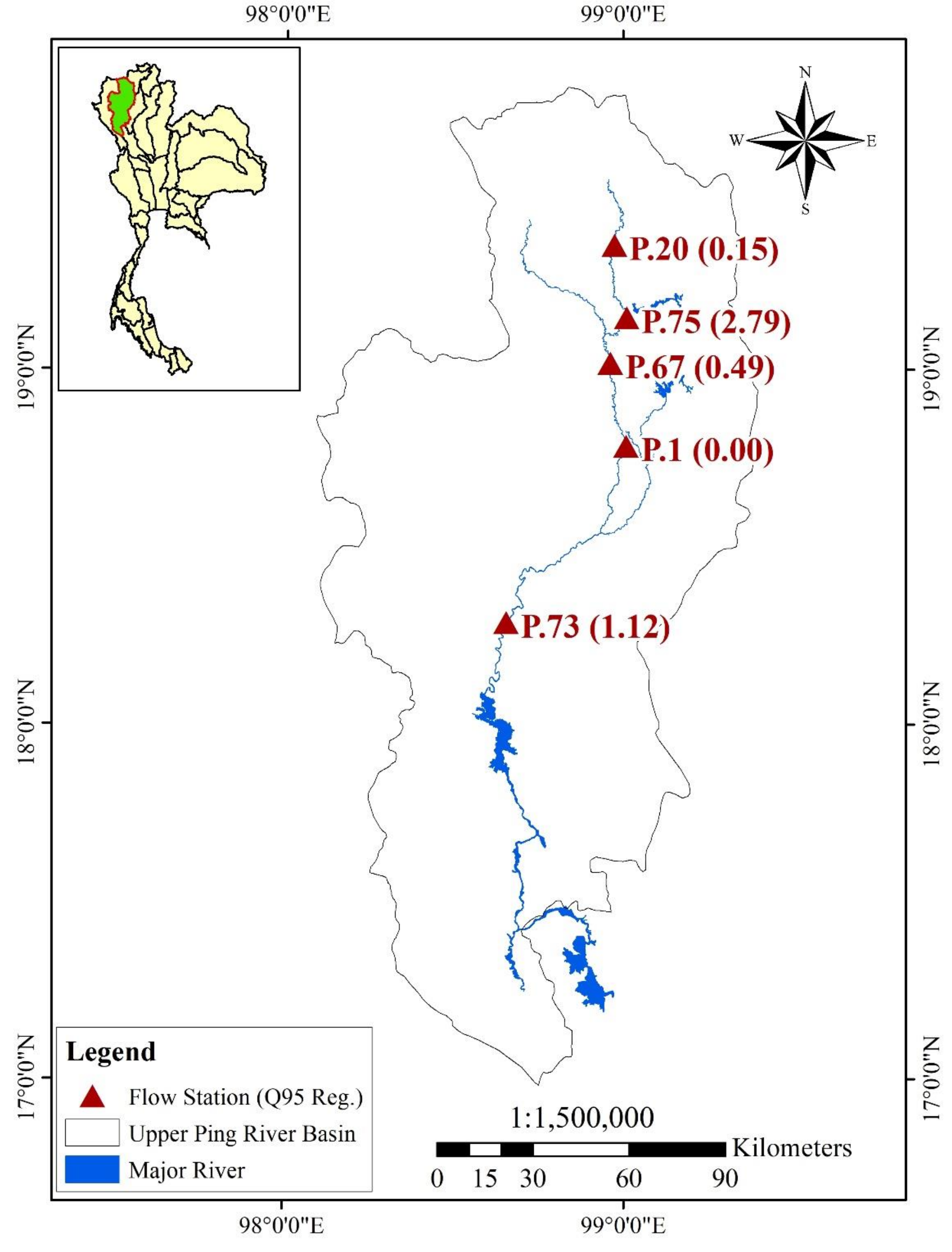

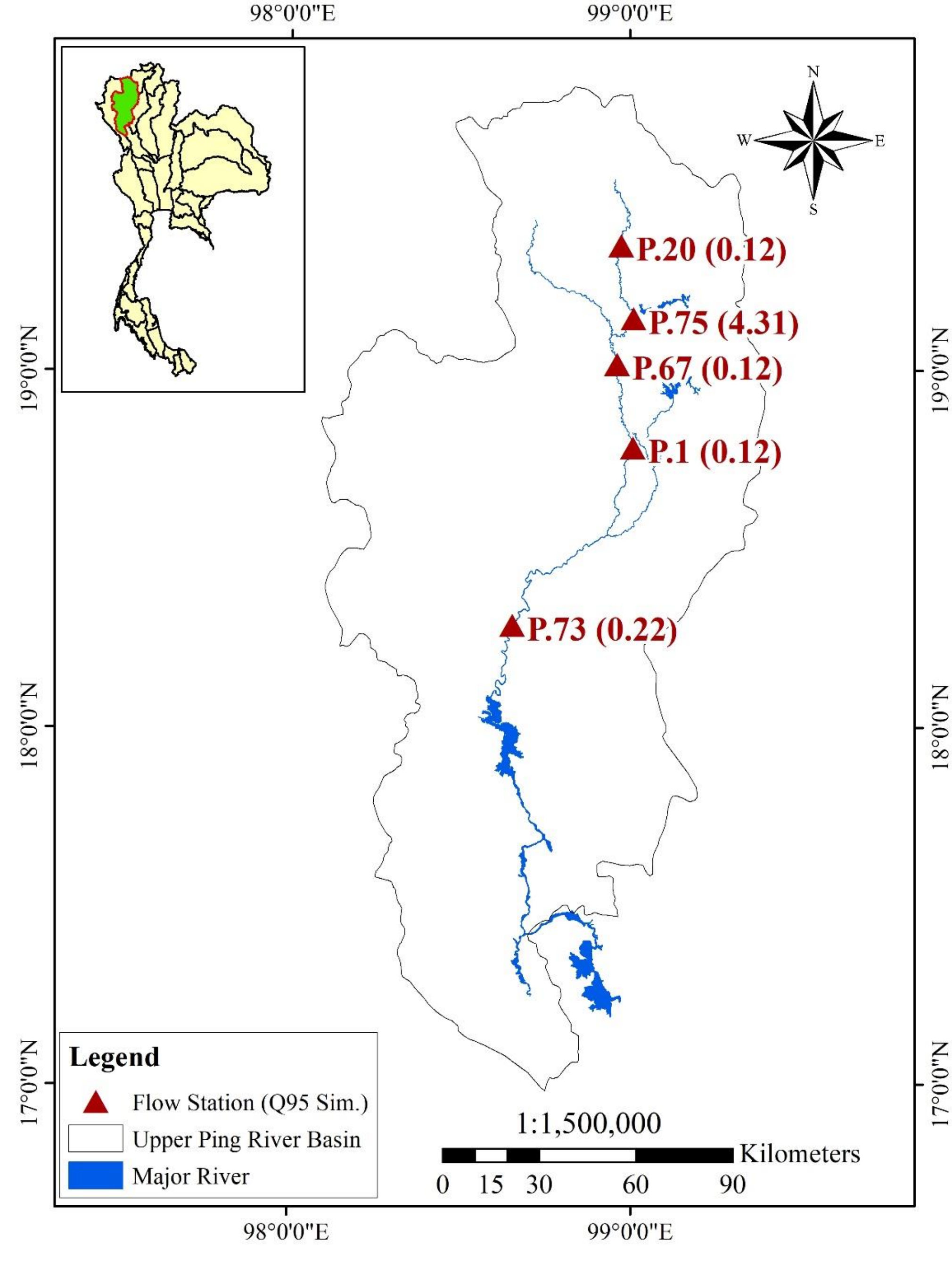
98°0'0"E
99°0'0"E
N
W
E
S
P.20 (0.12)
P.75 (4.31)
P.67 (0.12)
P.1 (0.12)
P.73 (0.22)
19°0'0"N
18°0'0"N
17°0'0"N
Legend
Flow Station (Q95 Sim.)
Upper Ping River Basin
Major River
1:1,500,000
0 15 30 60 90
Kilometers

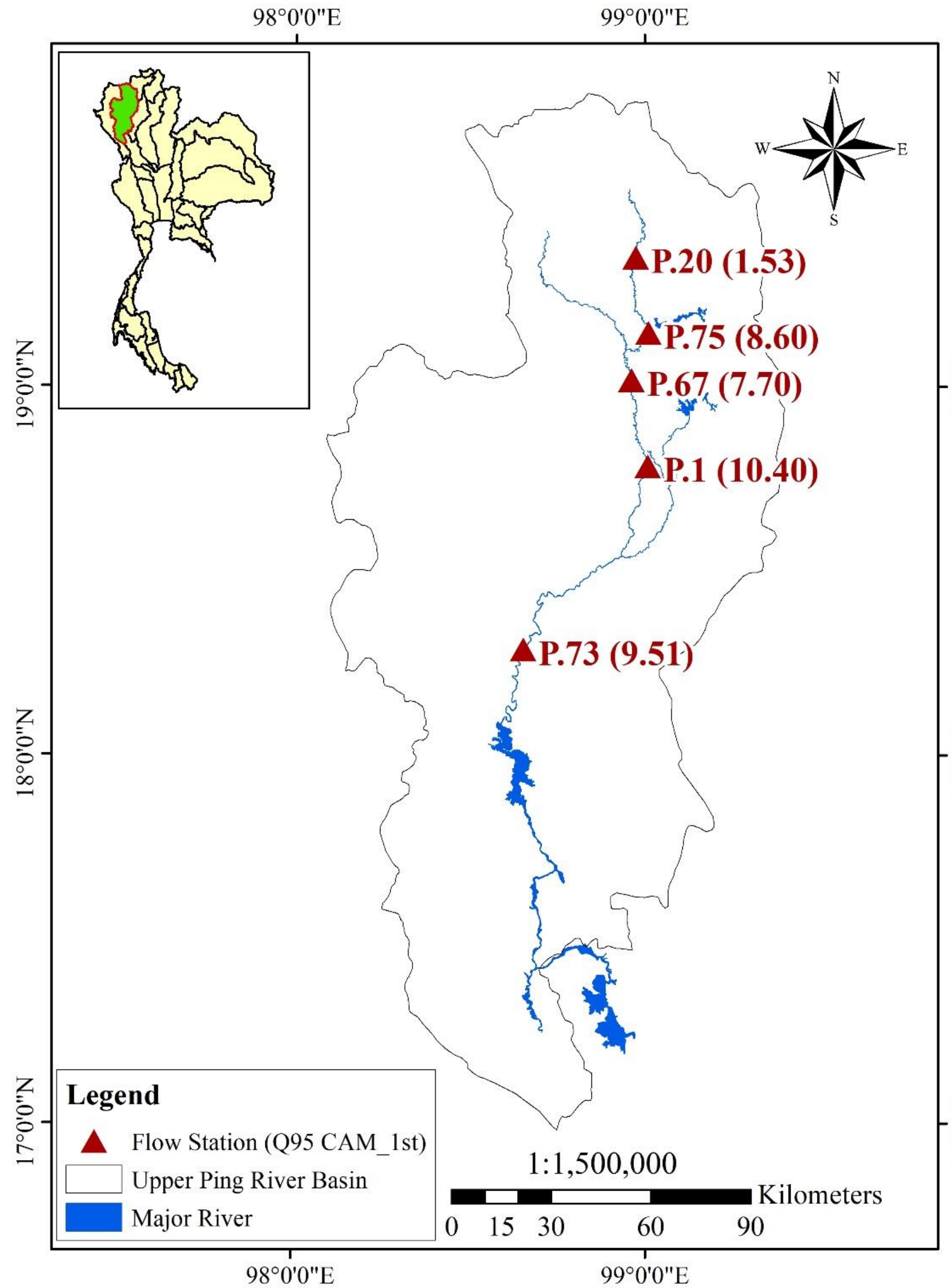
98°0'0"E
99°0'0"E
N
W
E
S
P.20 (1.53)
P.75 (8.60)
P.67 (7.70)
P.1 (10.40)
P.73 (9.51)
19°0'0"N
18°0'0"N
17°0'0"N
Legend
Flow Station (Q95 CAM_1st)
Upper Ping River Basin
Major River
1:1,500,000
0 15 30 60 90
Kilometers

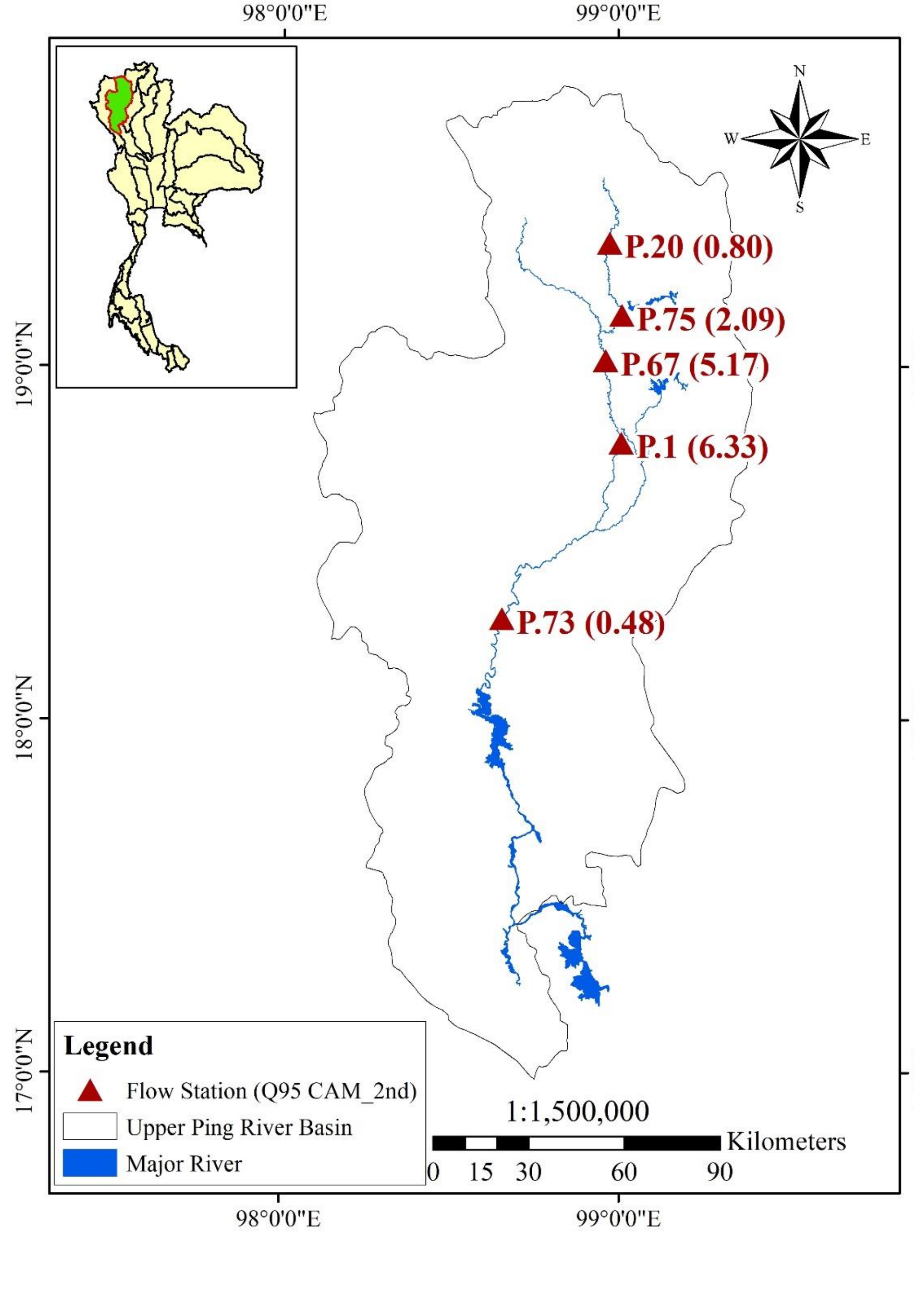
98°0'0"E
99°0'0"E
19°0'0"N
18°0'0"N
17°0'0"N
N
W
E
S
P.20 (0.80)
P.75 (2.09)
P.67 (5.17)
P.1 (6.33)
P.73 (0.48)
Legend
Flow Station (Q95 CAM_2nd)
Upper Ping River Basin
Major River
1:1,500,000
Kilometers
0 15 30 60 90

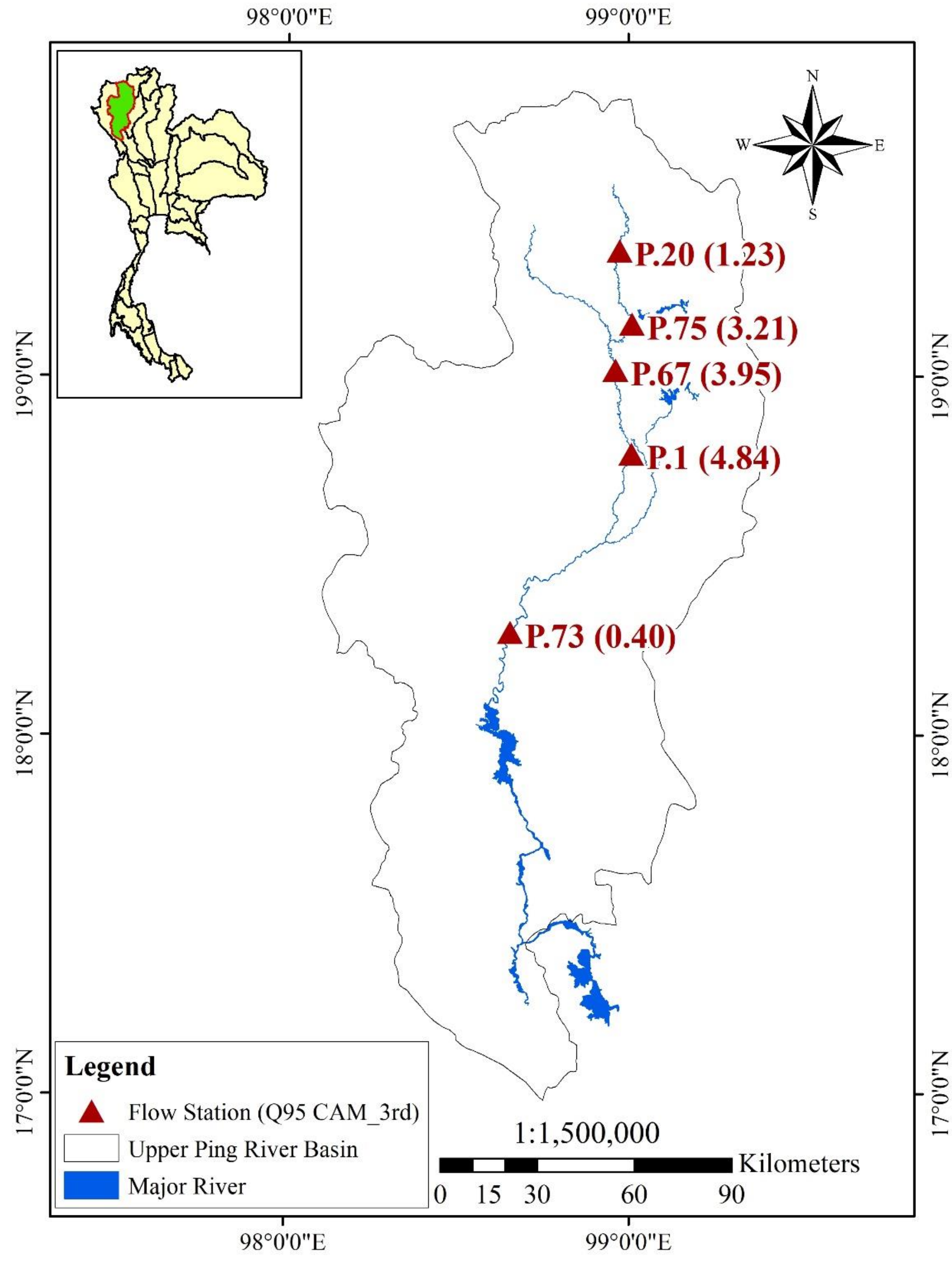

98°0'0"E
99°0'0"E
19°0'0"N
18°0'0"N
17°0'0"N
N
W
E
S
P.20 (1.23)
P.75 (3.21)
P.67 (3.95)
P.1 (4.84)
P.73 (0.40)
Legend
Flow Station (Q95 CAM_3rd)
Upper Ping River Basin
Major River
1:1,500,000
Kilometers
0 15 30 60 90

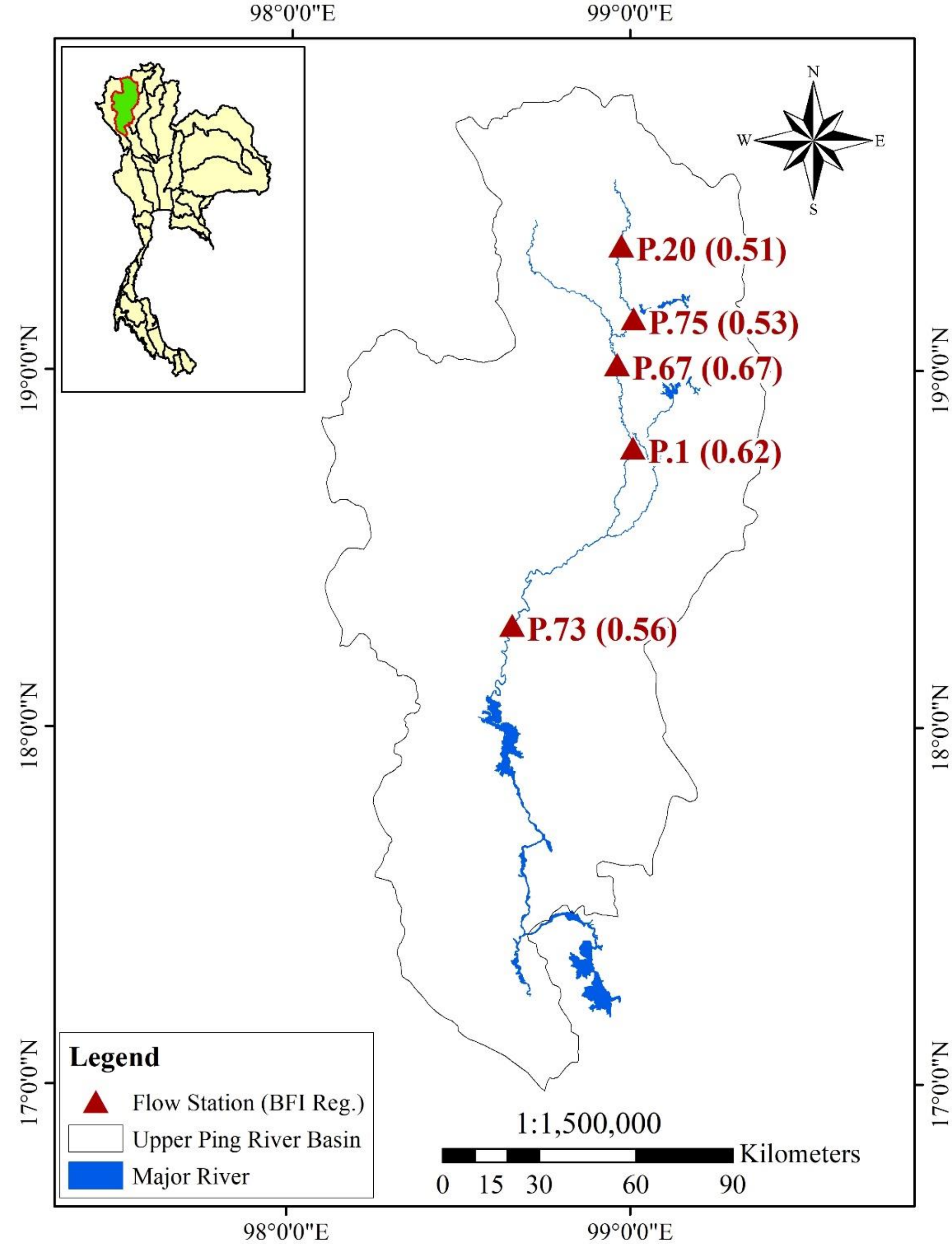
98°0'0"E
99°0'0"E
19°0'0"N
18°0'0"N
17°0'0"N
N
S
W
E
P.20 (0.51)
P.75 (0.53)
P.67 (0.67)
P.1 (0.62)
P.73 (0.56)
Legend
Flow Station (BFI Reg.)
Upper Ping River Basin
Major River
1:1,500,000
Kilometers
0 15 30 60 90

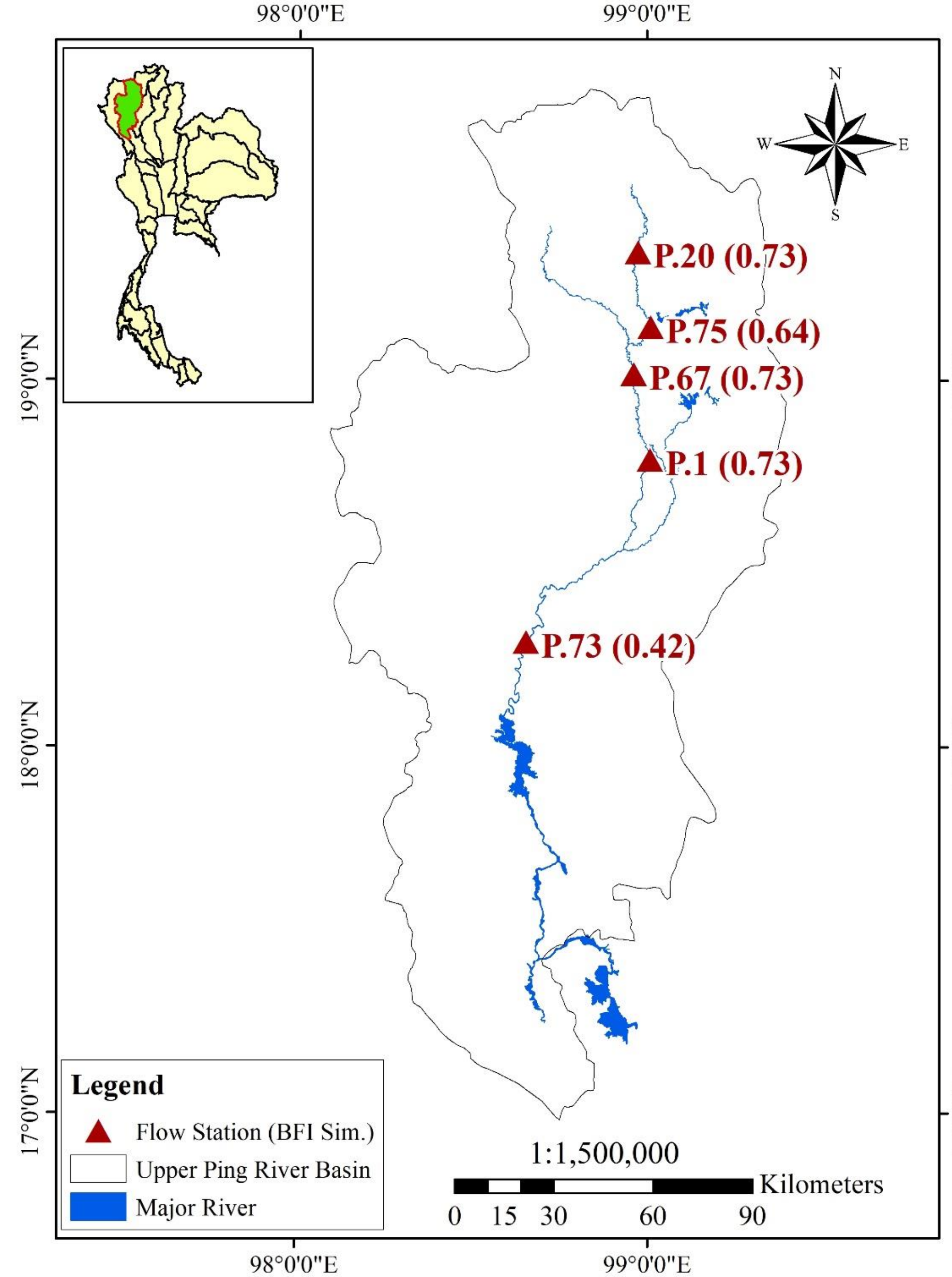
98°0'0"E
99°0'0"E
19°0'0"N
18°0'0"N
17°0'0"N
N
W
E
S
P.20 (0.73)
P.75 (0.64)
P.67 (0.73)
P.1 (0.73)
P.73 (0.42)
Legend
Flow Station (BFI Sim.)
Upper Ping River Basin
Major River
1:1,500,000
0 15 30 60 90
Kilometers

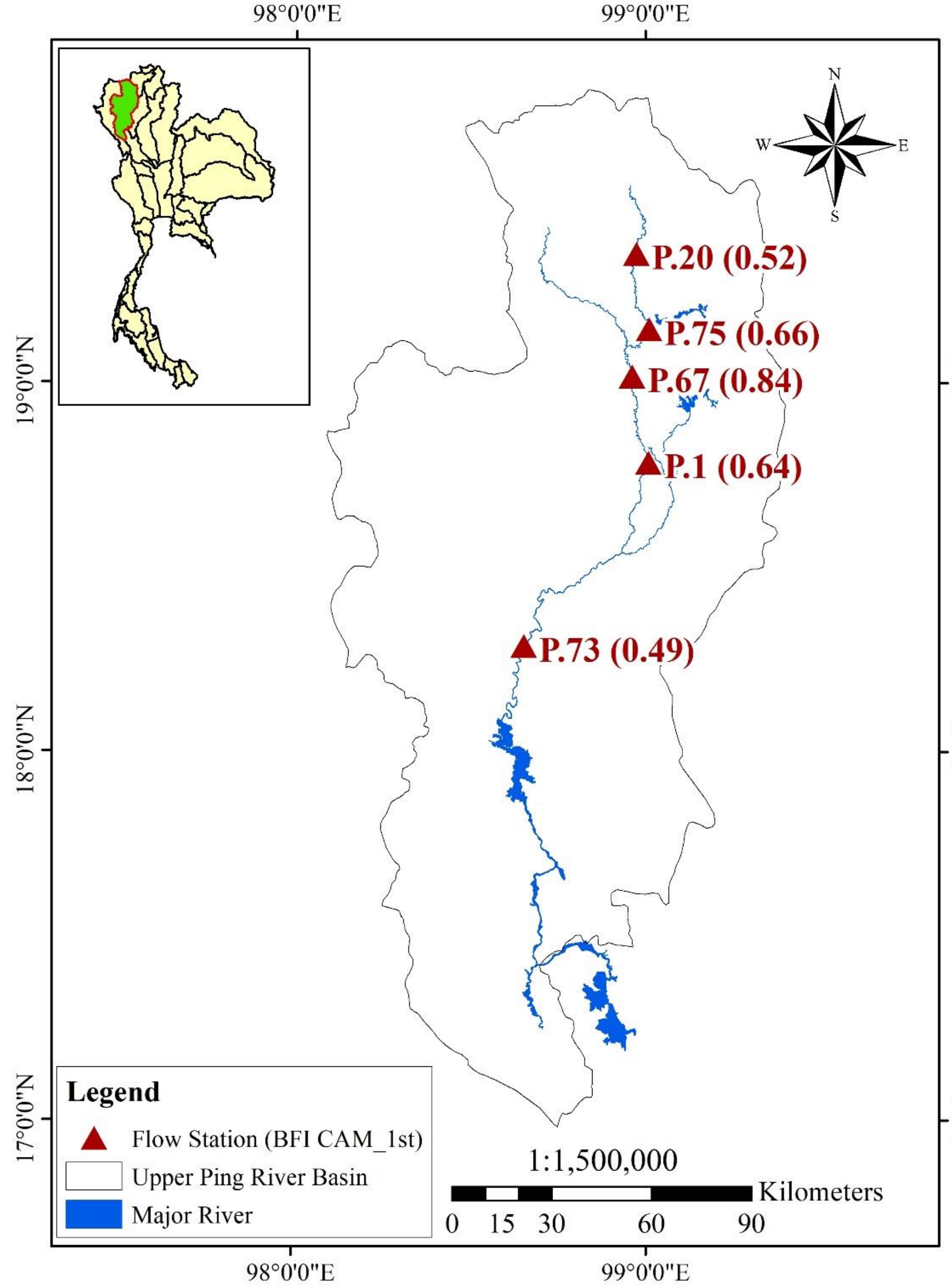
98°0'0"E
99°0'0"E
19°0'0"N
18°0'0"N
17°0'0"N
N
W
E
S
P.20 (0.52)
P.75 (0.66)
P.67 (0.84)
P.1 (0.64)
P.73 (0.49)
Legend
Flow Station (BFI CAM_1st)
Upper Ping River Basin
Major River
1:1,500,000
0 15 30 60 90
Kilometers

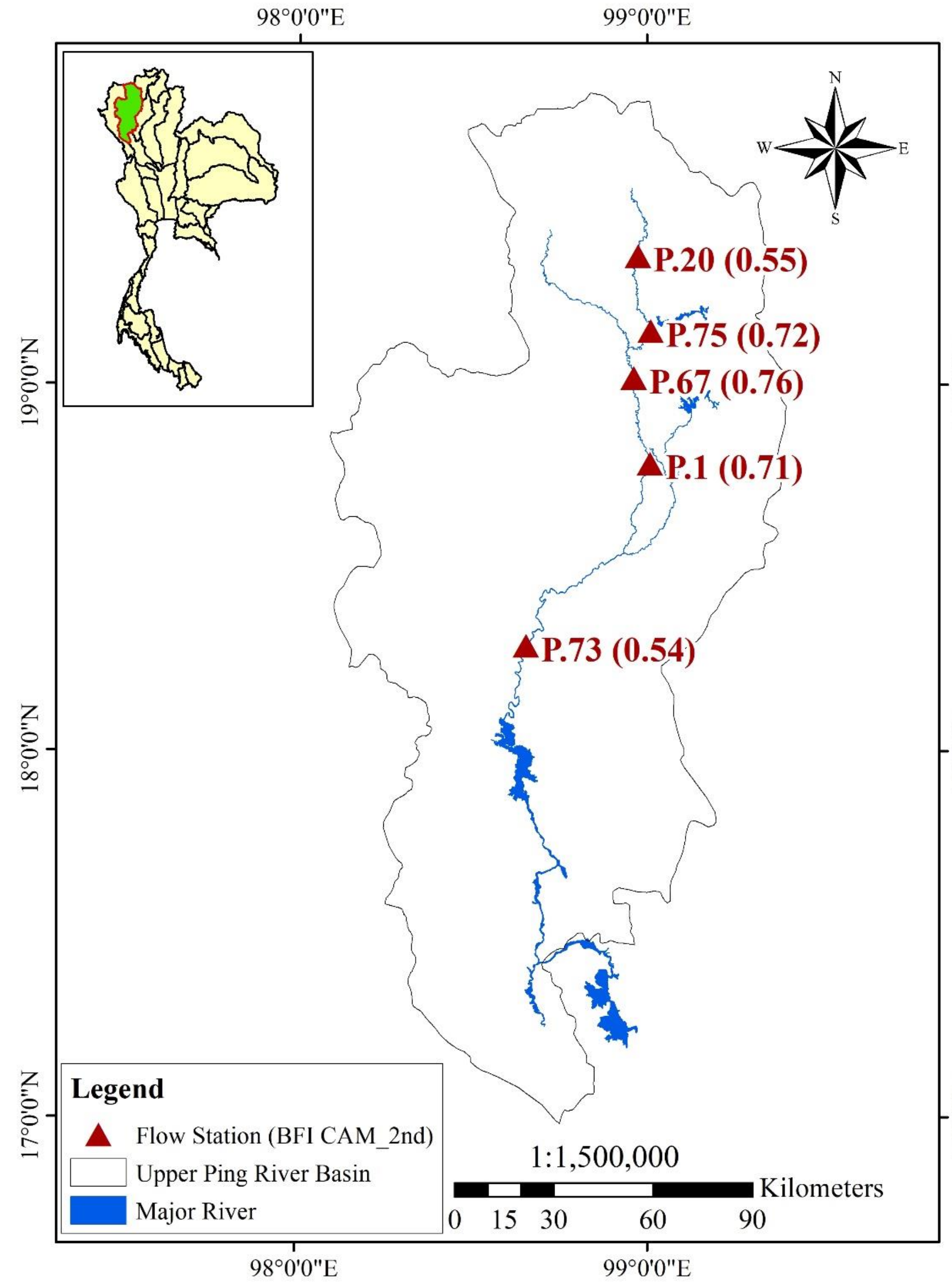
98°0'0"E
99°0'0"E
19°0'0"N
18°0'0"N
17°0'0"N
N
W
E
S
P.20 (0.55)
P.75 (0.72)
P.67 (0.76)
P.1 (0.71)
P.73 (0.54)
Legend
Flow Station (BFI CAM_2nd)
Upper Ping River Basin
Major River
1:1,500,000
Kilometers
0 15 30 60 90

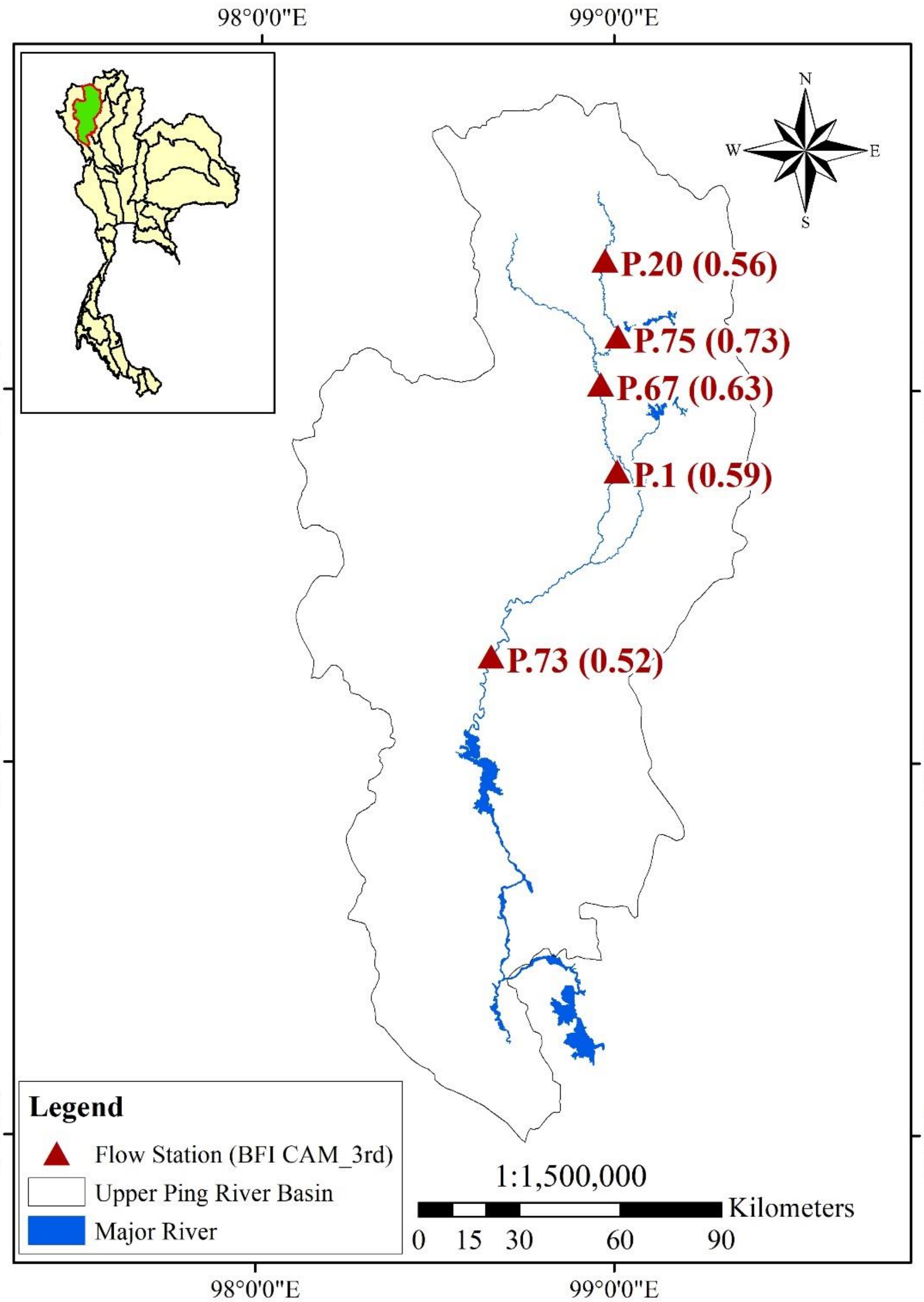

98°0'0"E
99°0'0"E
19°0'0"N
18°0'0"N
17°0'0"N
N
S
W
E
P.20 (0.56)
P.75 (0.73)
P.67 (0.63)
P.1 (0.59)
P.73 (0.52)
Legend
Flow Station (BFI CAM_3rd)
Upper Ping River Basin
Major River
1:1,500,000
Kilometers
0 15 30 60 90

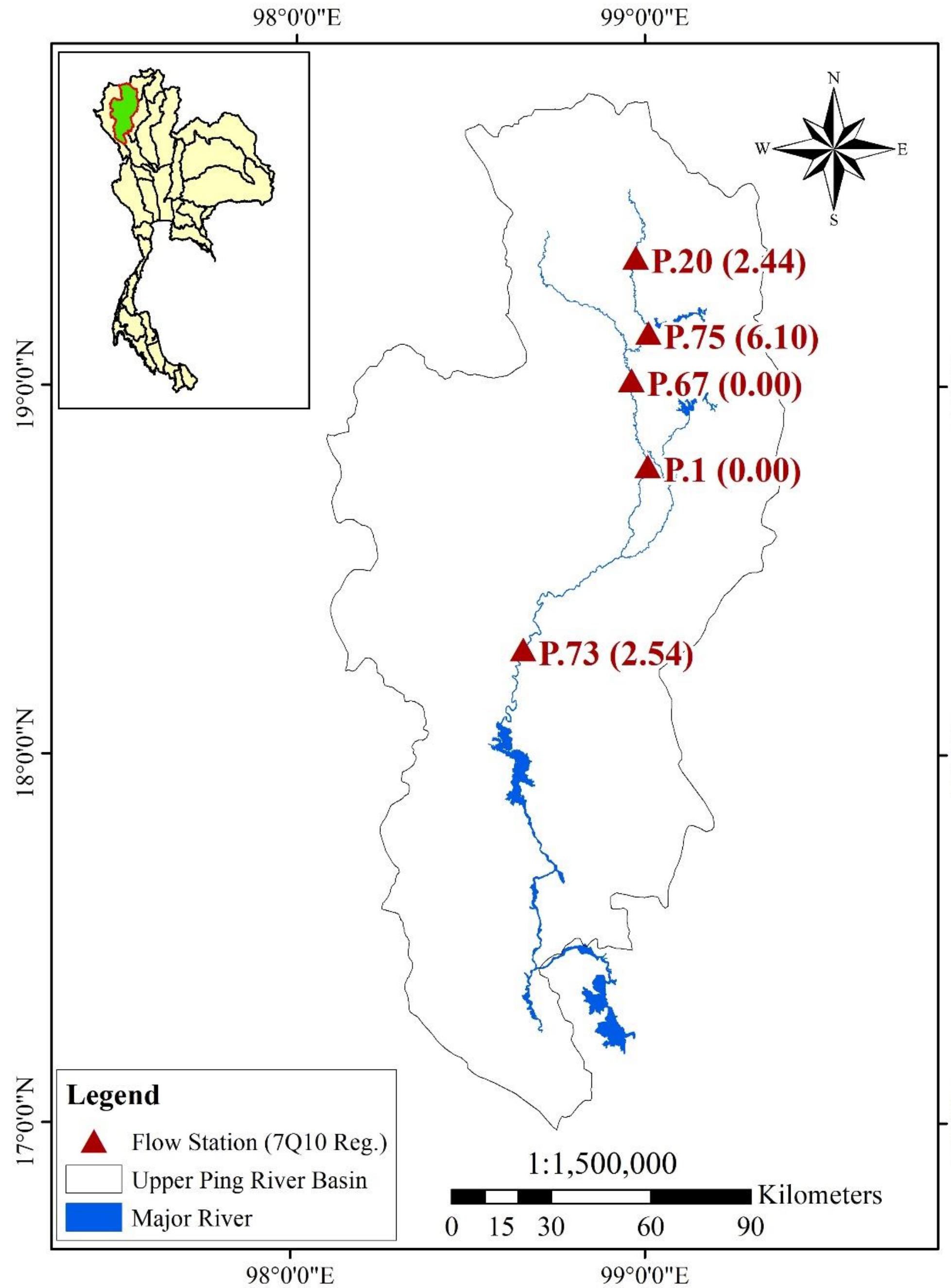
98°0'0"E
99°0'0"E
19°0'0"N
18°0'0"N
17°0'0"N
N
S
W
E
P.20 (2.44)
P.75 (6.10)
P.67 (0.00)
P.1 (0.00)
P.73 (2.54)
Legend
Flow Station (7Q10 Reg.)
Upper Ping River Basin
Major River
1:1,500,000
Kilometers
0 15 30 60 90

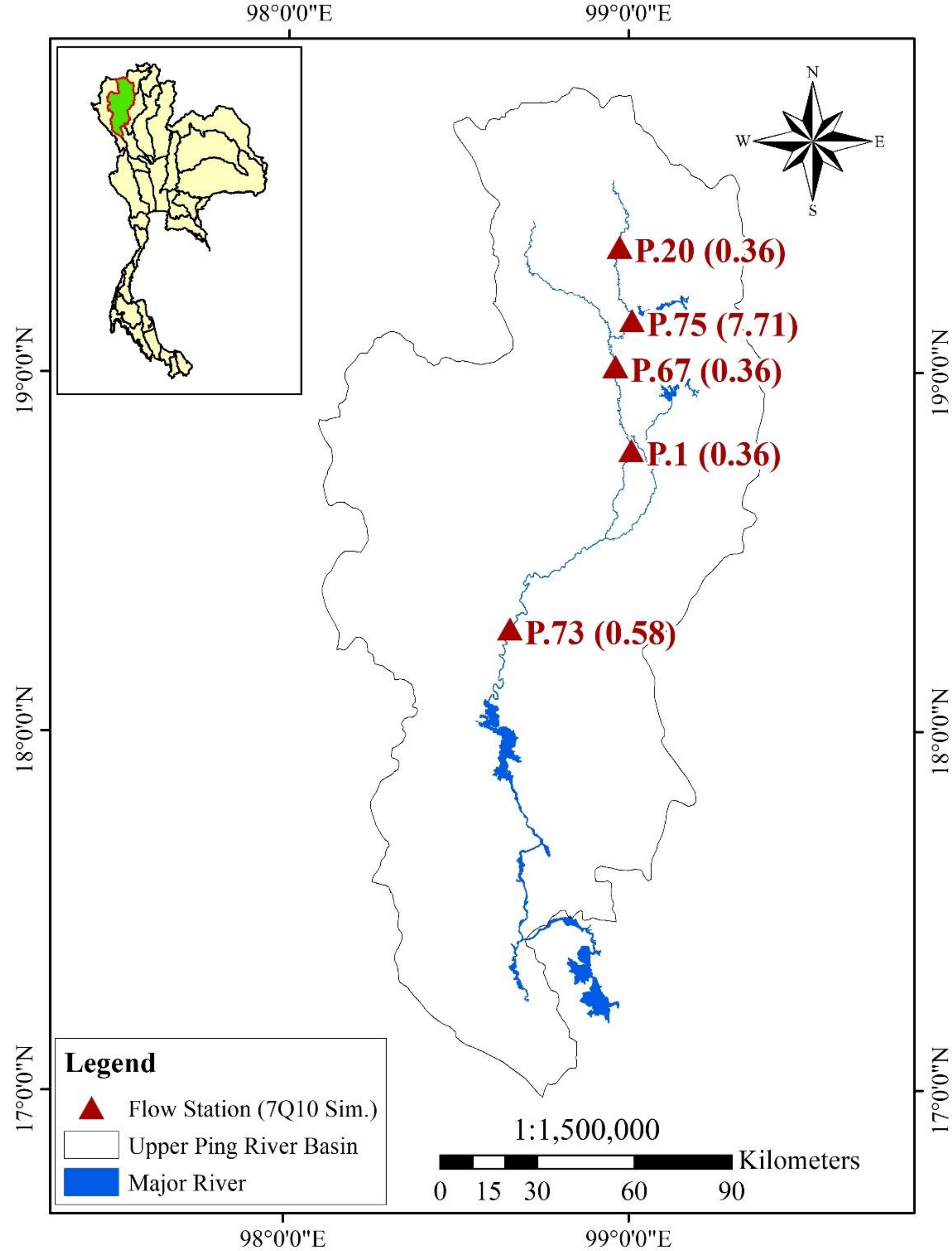
98°0'0"E
99°0'0"E
19°0'0"N
18°0'0"N
17°0'0"N
N
S
W
E
P.20 (0.36)
P.75 (7.71)
P.67 (0.36)
P.1 (0.36)
P.73 (0.58)
Legend
Flow Station (7Q10 Sim.)
Upper Ping River Basin
Major River
1:1,500,000
0 15 30 60 90
Kilometers

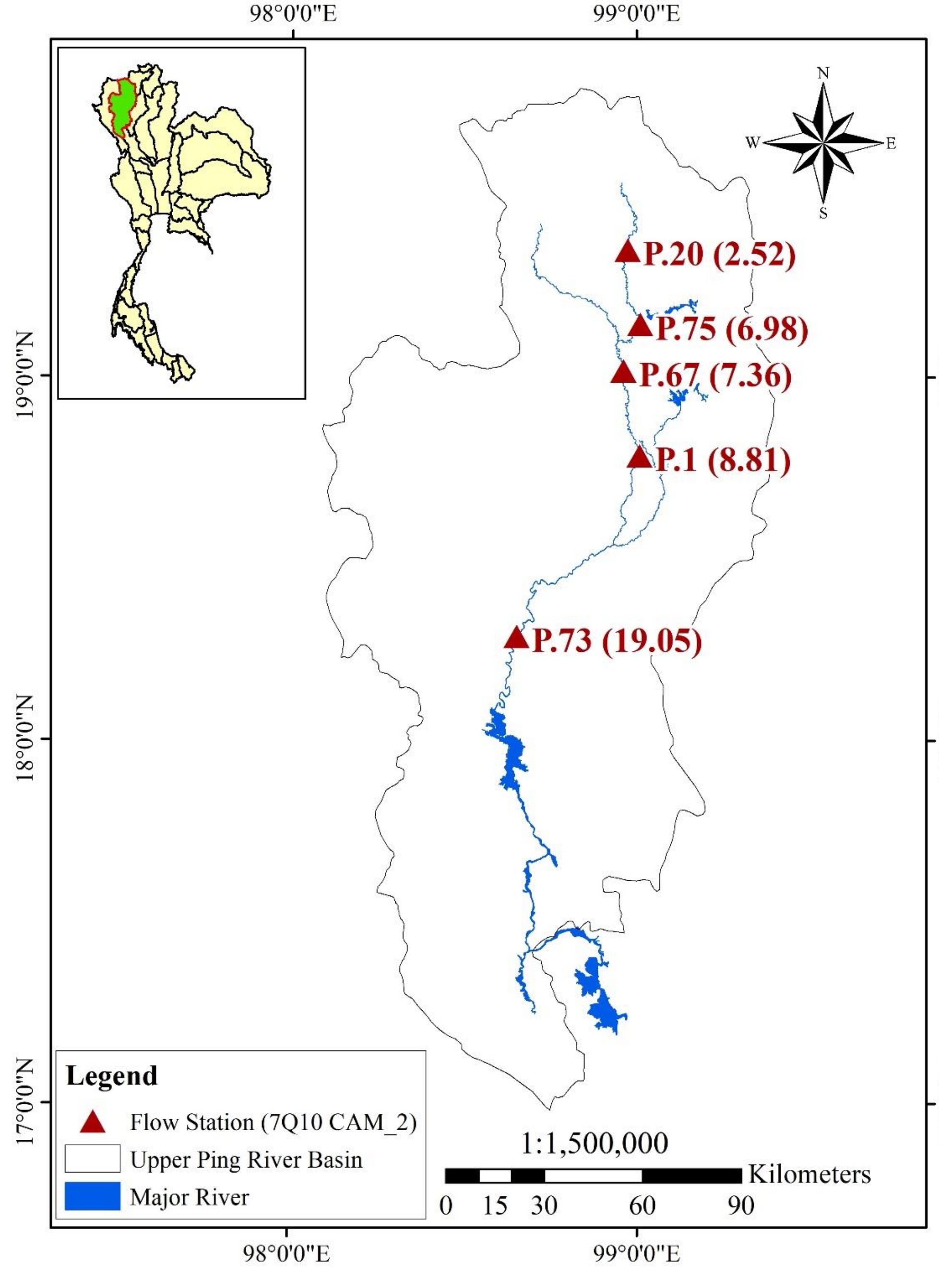
98°0'0"E
99°0'0"E
19°0'0"N
18°0'0"N
17°0'0"N
N
W
E
S
P.20 (2.52)
P.75 (6.98)
P.67 (7.36)
P.1 (8.81)
P.73 (19.05)
Legend
Flow Station (7Q10 CAM_2)
Upper Ping River Basin
Major River
1:1,500,000
Kilometers
0 15 30 60 90

VITA

NAME	Sokseyla Man
DATE OF BIRTH	09 October 1994
PLACE OF BIRTH	Prey Veng province, Cambodia
INSTITUTIONS ATTENDED	Bachelor's Degree in Water Resources Engineering and Rural Infrastructure, Institute of Technology of Cambodia, Cambodia
HOME ADDRESS	Prey Veng province, Cambodia
PUBLICATION	Attending The 5th EIT International Conference on Water Resources Engineering: Title "Low-flow Assessment Methods for Ungauged Subbasin in the Upper Ping River Basin, Thailand".
AWARD RECEIVED	1. Scholarship Program for ASEAN Countries, Chulalongkorn University